

# **A practical implementation of ROMDA,**

*A method for reliability prediction and optimization  
through degradation analysis*

Master thesis graduation project by

**M.A. Damen**

Eindhoven, June 2004

Department of Technology Management  
Technische Universiteit Eindhoven

Graduation committee:

**dr. ir. J.L. Rouvroye**

Department of Technology Management  
Technische Universiteit Eindhoven

**prof. dr. ir. A.C. Brombacher**

Department of Technology Management  
Technische Universiteit Eindhoven

**ir. J.A. van den Bogaard**

Department of Technology Management  
Technische Universiteit Eindhoven

**ing. G. Hulsken**

Flextronics B.V.  
Venray, The Netherlands

---

**Abstract**

This master thesis project attempts to apply the ROMDA reliability concept by ir. Van den Bogaard on a Finisher module of a photocopier. A model is developed that enables Flextronics to predict reliability and make decisions regarding preventive maintenance and re-use of the module based on one performance indicator. Based on this model also an improvement of the design of the Finisher with regard to robust reliability was calculated.

---

## **Acknowledgement**

Nearly every good book I've read had an acknowledgment chapter in some way. This is however not the reason for me to write one. The work in this report could have never been done without the help, efforts and support of many people. Therefore I would like to express my gratitude for their important contribution.

First of all I want to thank my parents, Ad and Agaath, for providing me with the opportunity to study at the Technische Universiteit Eindhoven and for their unconditional support. I also want to thank my brother Robbert for motivating me by telling me "students don't work hard and only go out and drink beer". This encouraged me to prove him wrong and work harder.

At Flextronics I would like to thank all the guys from the MTL department for their efforts. It was only through their help, knowledge and expertise that it was possible to perform the experiments that we did. This graduation project taught me a lot about the technical side of being an industrial engineer. Thanks for your efforts and for the conversations and discussions.

A special thanks goes out to Ilse de Visser. First of all for providing me a way of transportation from Eindhoven to Venray and second for the conversations we had during the ride. I think that these conversations made life a lot easier.

At the university I have another team of people to thank for their efforts, help and discussions. First of all I want to thank my supervisor dr. ir. Jan Rouvroye for always having time to answer my questions and especially for all the help with my Matlab issues. Secondly I want to thank my graduation professor prof. dr. ir. Aarnout Brombacher for his clear, useful and straight to the point advice. I also want to thank dr. Roxana Ion for her help with my mathematical issues.

My main thanks however go out to ir. Johan van den Bogaard for whom and with whom I worked during this project. Thank you for all the advice, discussions and support. I wish you all the luck with the last few months of your PhD. research.

And last and certainly not least I want to thank all my friends, family and especially my girlfriend Manda for cheering me up when I was down and putting up with me when I was cranky.

Mark Damen,  
June 2004

---

## **Management summary**

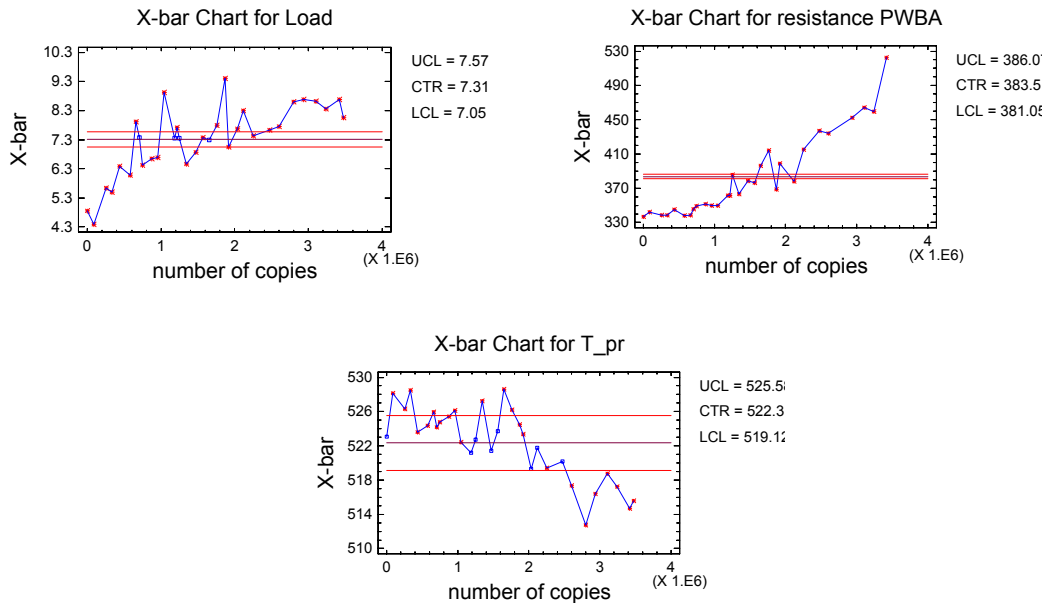
This master thesis performs and evaluates the practical implementation of a method for reliability prediction and optimization through degradation analysis and robust design. ROMDA, as the method is called, attempts to identify the dominant failure mechanism of a complex product in its design stage. The degradation of the design parameters that cause this failure mechanism is modeled as a function of time and subsequently related to a performance characteristic that indicates the degradation of these design parameters. This results in degradation models of the design parameters and a model of the performance characteristic as a function of its (degrading) design parameters. Now reliability can be assessed by predicting when the product's technical specification limits will be exceeded. Relating the performance characteristic to its design parameters provides the additional possibility to optimize product design with respect to robust reliability. Here robust reliability implies finding an optimal balance between Mean Time To Failure (MTTF) and the variance of this MTTF.

The conflict between today's market trends and business drivers requests for the possibility to assess quality and predict reliability earlier in the design stage. Together with Flextronics International Europe B.V., Venray, Océ N.V. Venlo and Eurandom, the Technische Universiteit Eindhoven started a project subsidized by the Dutch government to develop, evaluate and implement a method for reliability prediction and optimization. For this master thesis Flextronics provided its knowledge, experience and products to answer the following research question:

*Is it possible to implement the ROMDA concept as proposed by Van den Bogaard into practice and apply it to design optimization, preventive maintenance and re-use?*

In chapter 2, the reader is introduced to the literature that is relevant for understanding and performing the concept. Subsequently chapter 3 explains how the concept works and chapter four introduces the reader to the Finisher module of the photocopier on which implementation took place. The chapter further discusses the results that were achieved before this project. These include failure mode identification, identification of its dominant design parameters and performance characteristic and an early model for the performance characteristic over life. The identified failure mode was the stagnation of the paper transport function. This function is driven by the nip motor, which was expected to stall as a result of the increasing load on the motor. The performance characteristic current rise time of the nip motor was chosen to measure the performance of this function. Screening of the design parameters and noise factors that could influence the current rise time resulted in the design parameters load and resistance of the PWBA, which is the unit that controls and drives the nip motor.

The next chapter discusses the Accelerated Degradation Test that was performed during this research project. Analysis of the results shows that it is permitted to model the design parameters load and PWBA resistance as a function of time. The observations of the degradation data were supported by literature, which made a strong case for their resulting degradation models. Also the performance characteristic significantly shows to decrease over time, which proves that it can be used to predict performance. The following figures show the degradation that was observed.



The performance characteristic only indicates how it is affected by the design parameters up to the time that it is measured. As the influence or degradation rate of the two design parameters may change with time this may also affect the performance characteristic. Therefore only the design parameters were modeled as a function of time.

$$Load\ increase(t) = 2,0522 + 7,13689 \cdot 10^{-7} \cdot (t - 745.541,5)$$

$$R\ increase(t) = 1,293 \cdot 10^{-11} \cdot t^2$$

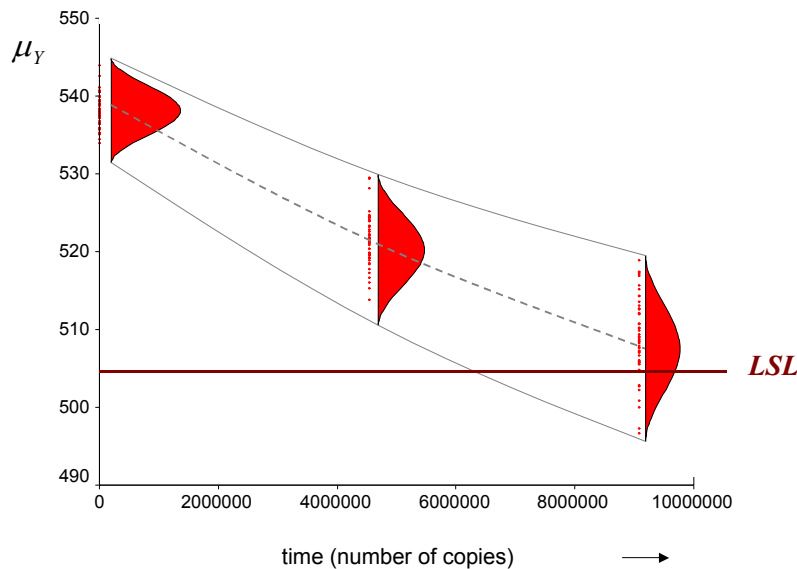
Two of the measured back-up parameters for the stapler, current peaks A and C, also showed to change with use. The test moreover showed that the identified failure mechanism was not the first to fail. The following table indicates the prior failures.

Component	TTF	Units	Cause of failure
Stapler cartridge	26078	Staples M7	Unknown/use
Edge solenoid	69340	Staples M6	Plastic broken
Tamper rail	1188170,5	Movements	Contamination/friction
Moving stapler rail	0,5*212868 = 106434	Movements	Contamination/friction
Metal plate M6	254236	Staples M6	Torn plate
Tamper rail*	2231656*	Movements	Contamination/friction

Especially the rails within the Finisher turn out to be weak spots that fail as a result of wear due to contamination and friction. Therefore the current rise time cannot be used to represent the performance of the entire module.

The obtained information and degradation models are used to conduct an experiment that predicts the influence of the design parameters on the performance characteristic over technical life. Therefore the degradation of the design parameters is superimposed on the performance characteristic, taking into account the initial unit-to-unit variation of the design parameters between the Finisher modules. The design parameters were set at values that they were expected

to have at  $t=0$ , halfway the Finisher's life and just before failure. This resulted in a model of the performance characteristic as a function of time and model of the performance characteristic as a function of its design parameters for the population of Finisher modules. Together with the degradation models of the design parameters and the specification limit of the performance characteristic, this provides the possibility to predict reliability at any moment in time. The following figure shows how the performance characteristic is expected to behave over time.



The resulting models of the performance characteristic over time are as follows:

$$\begin{aligned} \mu_Y(t) &= 538,024 - 3,942 \cdot 10^{-6} \cdot t + 8,289 \cdot 10^{-14} \cdot t^2 \\ \sigma^2_Y(t) &= 3,88 + 3,928 \cdot 10^{-7} \cdot t + 2,252 \cdot 10^{-13} \cdot t^2 \end{aligned}$$

The lower specification limit of 504,28 microseconds was calculated based on the mean failure time of the load for the product population. This time was substituted into the equation above, which resulted in a lower specification limit (LSL) for the current rise time of 504,28 microseconds. As the figure shows, this LSL leads to the rejection of products that still function properly. Therefore this specification limit is not a hard failure limit.

In chapter 7 an optimization step was performed on the design of the Finisher module. Therefore a model of the performance characteristic as a function of its design parameters was needed. This model that also resulted from chapter 6, is as follows:

$$\mu_Y = 504,964 + 6,292\mu_{X_1} + 24,794\mu_{X_2} - 0,692\mu_{X_1}^2$$

First the performance in the present situation was evaluated using simulation. As performance indicators the Mean Time To Failure (MTTF) and the log of the standard deviation of the Time To Failure (SDTTF) were used. This resulted in a MTTF of 11.215.541 copies and a log(SDTTF) of 14,48.

Subsequently functions for the MTTF and the log(SDTTF) are established by means of Design Of Experiments based on simulation. For these functions the optimal balance is calculated for the with respect to robust reliability.

This resulted in optimal design parameter settings of 4,768 Ncm for the load and 989  $m\Omega$  for the PWBA resistance. This leads to an improvement of MTTF of 12,1 % while the SDTT increased with 8,3 %. The calculation method for the optimization step allows the person that performs the calculation to pre-determine if the emphasis should be put on MTTF or on SDTTF.

The calculated MTTF in the optimized situation is possibly higher than this would be in reality. This is due to the fact that not the performance characteristic, current rise time, but the design parameter load causes failure of the paper transport function.

## **Conclusions**

The conclusions that can be drawn from this research are as follows:

Regarding the specific case of the Finisher module:

- The dominant failure mode of the Finisher was not found in the failure mode identification phase.
- The specification limit on the current rise time is not a hard technical failure limit and therefore a Finisher may still be functioning properly although its current rise time has exceeded the limit. This may in extreme cases lead to underestimation of the reliability of used Finishers and therefore to the decision not to re-use reliable systems
- The calculation of the MTTF in the optimization step is possibly higher than this would be in reality due to the fact that not the performance characteristic, current rise time, but the design parameter load causes failure of the paper transport function.

Regarding the method ROMDA:

- Using a failure mechanism that is the result of the failure of one of the design parameters results in a soft specification limit for the performance characteristic and more difficulties with design optimization.
- ROMDA concept should be applied to products with a large development time. These are mainly professional (production) systems.

Finally, it may be concluded that it is possible to implement the ROMDA concept into practice. The resulting time dependent model of the performance characteristic provides the possibility to monitor the performance of the system in the field. This provides the possibility to plan preventive maintenance at moments that lead to lower costs. The models also provide the possibility to estimate the reliability of the system based on the performance characteristic. Reliability predictions may be used to estimate the chance of the system's survival in the field during another economical life. Finally the last phase of the concept led to an improvement of the design with respect to its time-to-failure.

One of the objectives of Flextronics could however not be satisfied. The current rise time of the nip motor is not a performance characteristic that can be used to measure or predict the performance of the entire Finisher module, but only of the paper transport function.

---

## **Recommendations**

The recommendations that follow from the conducted research are the following.

Regarding the method ROMDA:

- It is strongly recommended that failure mode identification on large complex systems be performed with field data, when this is available.
- Failure mode identification: apply more relevant criteria for failure mode identification. These may be “time dependency”, “type of failure” (instantaneous, gradual or rapid) and “measurability”.
- When the specification limit on the performance characteristic is dependent on the failure of a design parameter, the optimization step can possibly be performed more accurately by linking the specification limit of the performance characteristic to this design parameter.

Regarding verification of the results:

- Verify and update the obtained models with field data.

Regarding further research on the Finisher:

- Conduct further research on the Tamper rails to find the dominant failure mode of the Finisher module.
- The current peaks A and C may be used in further research as performance characteristics of the stapler function.

---

## **Frequently used abbreviations**

<b><i>ADT</i></b>	<i>Accelerated Degradation Test</i>
<b><i>ALT</i></b>	<i>Accelerated Life Test</i>
<b><i>ANOVA</i></b>	<i>Analysis of Variance</i>
<b><i>CDF</i></b>	<i>Cumulative Density Function</i>
<b><i>DOE</i></b>	<i>Design of Experiments</i>
<b><i>DP</i></b>	<i>Design Parameter</i>
<b><i>FMEA</i></b>	<i>Failure Mode and Effects Analysis</i>
<b><i>LSE</i></b>	<i>Least Square Estimation</i>
<b><i>LSL</i></b>	<i>Lower Specification Limit</i>
<b><i>MLE</i></b>	<i>Maximum Likelihood Estimation</i>
<b><i>MSA</i></b>	<i>Measurement System Analysis</i>
<b><i>MTTF</i></b>	<i>Mean Time-to-failure</i>
<b><i>PC</i></b>	<i>Performance Characteristic</i>
<b><i>PDF</i></b>	<i>Probability Density Function</i>
<b><i>PWBA</i></b>	<i>Printed Wire Board Assembly</i>
<b><i>ROMDA</i></b>	<i>Reliability Optimization Method through Degradation Analysis</i>
<b><i>TTF</i></b>	<i>Time-to-failure</i>
<b><i>USL</i></b>	<i>Upper Specification Limit</i>

---

## Table of contents

<b>Preface.....</b>	<b>12</b>
<b>Chapter 1 Introduction.....</b>	<b>13</b>
§ 1.1 <i>History of reliability prediction</i> .....	13
§ 1.2 <i>Motivation</i> .....	13
§ 1.3 <i>Purpose of research</i> .....	16
§ 1.4 <i>Structure of this thesis</i> .....	18
<b>Chapter 2 Literature.....</b>	<b>20</b>
§ 2.1 <i>Introduction</i> .....	20
§ 2.2 <i>Reliability problems</i> .....	21
§ 2.3 <i>Predicting reliability</i> .....	23
§ 2.3.1 <i>The Bathtub curve</i> .....	24
§ 2.3.2 <i>The Roller coaster curve</i> .....	26
§ 2.4 <i>Accelerated testing</i> .....	27
§ 2.4.1 <i>Degradation testing</i> .....	28
§ 2.4.2 <i>Degradation models</i> .....	29
§ 2.5 <i>Robust Design</i> .....	30
§ 2.6 <i>Tolerance Design</i> .....	32
§ 2.7 <i>Discussion</i> .....	34
<b>Chapter 3 Concept description .....</b>	<b>36</b>
§ 3.1 <i>Introduction to the concept</i> .....	36
§ 3.2 <i>Profound concept description</i> .....	37
§ 3.3 <i>Summary &amp; discussion</i> .....	40
<b>Chapter 4 Concept Roadmap .....</b>	<b>43</b>
§ 4.1 <i>Introduction</i> .....	43
§ 4.2 <i>Description of the Roadmap</i> .....	43
§ 4.3 <i>Description Finisher Module</i> .....	47
§ 4.3.1 <i>Failure mode</i> .....	48
§ 4.3.2 <i>Performance characteristic</i> .....	49
§ 4.3.3 <i>Dominant design parameters</i> .....	50
§ 4.4 <i>Discussion</i> .....	50

---

<b>Chapter 5 Accelerated Degradation Test .....</b>	<b>52</b>
§ 5.1 Introduction.....	52
§ 5.2 Parameters and expectations.....	53
§ 5.3 Experimental set-up .....	55
§ 5.3.1 Measurement System Analysis .....	58
§ 5.4 Test results .....	59
§ 5.4.1 Paper transport function.....	59
§ 5.4.2 Stapler function.....	63
§ 5.4.3 Tray election function.....	65
§ 5.4.4 Observed failures .....	65
§ 5.5 Degradation models DP's.....	67
§ 5.6 Conclusion and discussion.....	69
§ 5.6.1 Conclusion .....	69
§ 5.6.2 Discussion .....	70
<b>Chapter 6 Relating the PC to the DP's .....</b>	<b>71</b>
§ 6.1 The limit setting experiment.....	71
§ 6.2 Main experiment .....	72
§ 6.2.1 Experimental design.....	73
§ 6.2.2 Time points .....	74
§ 6.2.3 Level settings .....	75
§ 6.2.4 Measurement system analysis.....	77
§ 6.3 Results Main experiment.....	78
§ 6.3.1 Analysis of the results .....	78
§ 6.3.2 Regression model.....	81
§ 6.3.3 Specification limits .....	83
§ 6.4 Discussion.....	84
<b>Chapter 7 Design optimization .....</b>	<b>87</b>
§ 7.1 Performance present situation.....	87
§ 7.2 Optimization of the Finisher module .....	89
§ 7.3 Discussion.....	90
<b>Chapter 8 Conclusions &amp; recommendations.....</b>	<b>92</b>
§ 8.1 Research question .....	92
§ 8.2 Review of this research .....	92
§ 8.3 Final conclusions .....	94
§ 8.3.1 Finisher module .....	94
§ 8.3.2 ROMDA.....	95
§ 8.3.2 Research question .....	95

---

§ 8.4 Recommendations .....	95
§ 8.4.1 ROMDA.....	96
§ 8.4.2 Verification .....	96
§ 8.4.3 Further research .....	96
<b>References.....</b>	<b>97</b>
<b>Appendix A: Degradation test experiment.....</b>	<b>101</b>
<b>Appendix B: Used data degradation test .....</b>	<b>104</b>
<b>Appendix C: Degradation Data PWBA resistance .....</b>	<b>107</b>
<b>Appendix D: Verification experiments .....</b>	<b>108</b>
<b>Appendix E: Degradation analysis back-up parameters .....</b>	<b>109</b>
<b>Appendix F: Main experiment.....</b>	<b>114</b>
<b>Appendix G: Unit-to-Unit variation.....</b>	<b>117</b>
<b>Appendix H: Restoration of the shafts.....</b>	<b>118</b>
<b>Appendix I: The Desirability Technique .....</b>	<b>119</b>
<b>Appendix J: Side study.....</b>	<b>120</b>

---

## **Preface**

In this preface I shortly want to describe the background of the research that was conducted for this master thesis. The project in which I participated during these last nine months is a cooperation between several parties. One of the main participators is the Dutch government, which subsidizes the research. It does this by means of the so-called E.E.T. program, which stands for Economy, Ecology and Technology. By means of this program the government tries to give the nation's companies incentive for technological innovation that leads to environmentally conscious production and lower costs by reducing waste and energy losses. In short, the research should be sensible with regard to the three areas economy, ecology and technology.

The other participators in the project are:

- Flextronics International Europe B.V., Venray, The Netherlands
- Technische Universiteit Eindhoven, Eindhoven, The Netherlands
- Eurandom, Eindhoven, The Netherlands
- Océ-Nederland B.V., Venlo, The Netherlands

The work for this master thesis was conducted at the Mechatronics Laboratory of Flextronics in Venray. Flextronics is the leading Electronics Manufacturing Services (EMS) provider focused on delivering operational services to technology companies. With fiscal year 2004 revenues of USD\$14.5 billion, it is a major global operating company with design, engineering, manufacturing, and logistics operations in 29 countries and five continents. At the location in Venray Flextronics assembles photocopiers and cash dispensers for its customers.

The research and achievements in this report were mainly cooperation between Flextronics and the Technische Universiteit Eindhoven. This work is part of my graduation project to finalize my study of Industrial Engineering and Management Sciences at the department of Technology Management.

---

# Chapter 1 Introduction

## § 1.1 History of reliability prediction

The need to predict reliability has not always existed. It was not until World War II that reliability became of interest. Army weapons, vehicles and equipment needed to be reliable in order to cause as much casualties at the enemy's side while preventing casualties at one's own side. During this war, electronic tubes were by far the most unreliable components used in electronic systems. In the nineteen fifties this observation led to various studies and ad hoc groups whose purpose was to identify ways that their reliability, and the reliability of the systems in which they operated, could be improved [1]. This time period was the advent of the reliability engineering discipline.

In 1962 the US Navy published the first version of the US Military Handbook US MH-217. Quickly MH-217 became the standard by which reliability predictions were performed [2]. Its underlying method is still widely used in engineering.

Until the nineteen seventies reliability engineering mainly focused on technical aspects. In this decade the first ISO standards were introduced as a consequence of the increasing importance of quality and reliability for industry. This protocol was introduced with the objective to standardize the way of producing quality products and making this process more effective.

In the 1980's there was an explosive growth in integrated circuit (IC) technology, which presented unique challenges to reliability modellers. As technology advanced it became every day more difficult to model the complexity of an IC. This resulted to an elevation of the level of reliability modelling, making models more complex but also more accurate.

Much of literature in the nineteen nineties centred around the debate on whether the reliability discipline should focus on physics-of-failure based or on empirically based models (such as MH-217). Meanwhile the role of the customer became more prominent as a result of higher demands and higher warranty claims. This resulted in a drift of focus of reliability to the warranty period, which still remains today [3].

This section has served to provide the reader with an idea of how reliability engineering and prediction originated, which developments there have been and where it stands today. The following section will focuses more profoundly on the reasons why reliability prediction is so important and motivates the need for the conducted research.

## § 1.2 Motivation

The acceleration rate of product development that started during the World War II continued when the war ended. As new technologies were invented and new products came to market, the customer got used to these new possibilities. In contrast to the past, where companies decided the customer's options, the roles have changed. Nowadays customers are telling the companies what they want and expect. This has led to the fact that products are becoming ever more complex and diverse. However, this higher complexity is of no concern to the customer and he or she refuses to accept lower levels of quality and reliability of the products he or she buys.

Meanwhile, the world is getting smaller every day. This means that markets are expanding due to globalisation. Globalisation affects the complexity of information sharing and business itself [4]. A customer is no longer restricted to a limited number of national companies but has the additional possibility to choose between offers from companies from various nations to select the best buy. This extended offer in combination with the faster succession of technologies has led to the increasing importance of time-to-market of new products and technologies. A company that is too late at the market may miss out on a share of the profit, where as being the first to market usually leads to the highest profits. The market trends that are distinguished can be summarized as:

1. More demanding customer
2. Increasing complexity of products
3. Shorter time-to-market
4. Increasing complexity of (global) business processes

On the other hand, launching a product on the market that is not well developed and which still has reliability problems may put a company's image to waste. The best way to make products reliable is to thoroughly test all possible product-customer combinations for an extended period of time before releasing a product to the market. Unfortunately this is too time consuming and expensive. Manufacturers of high volume consumer products are currently under strong (financial and time-) pressure, because they have to deal with four different, but often conflicting, business drivers simultaneously [5]:

1. *Time*: does the product reach the market at the required moment in time?
2. *Profit margin*: is the difference between product cost and product sales price adequate?
3. *Functionality*: is the product able to fulfill its intended functions?
4. *Quality*: does the product fulfill its intended purpose?

In order to make their products more reliable many companies have implemented statistical process control (SPC) to verify the quality level of the batches that are produced. Despite of such SPC programs many companies still deal with reliability problems of products in the field. The reason why these weaknesses are not discovered during quality control is the fact that these quality controls take place at a specific moment in time. A weak product may therefore still pass the specifications of the quality control program, but nevertheless fail after a short period of operation in the field.

The earlier the potential failures or weaknesses are identified, the cheaper the changes are. Therefore it is of great importance to put much effort into the first phases of the product development process. The decision to make changes to a later phase of the product development process leads to exponentially higher costs with time (figure 1.1), because already closed processes need to be re-started.

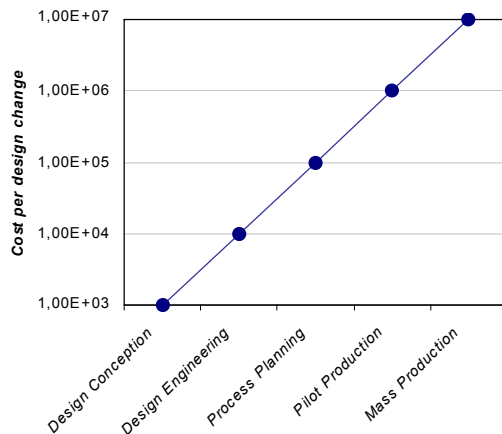


Figure 1.1: Cost of a design change [6]

The early phases of the product development process are also the phases in which the actual costs and price of the end product are largely determined. Wrong decisions in early phases lead to higher costs later on in the product development process or in production. The choice of a designer to use cheap and unreliable components in a product's design may lead to higher production costs as a result of an increase of production waste. The worst case that can be imagined is the necessity to re-call products from the field as a result of reliability issues. Presently, product rejection by customers within the warranty period is a major problem for many companies [7]. Figure 1.2 shows the percentage in which the different phases of the product creation process determine the total costs in relation to the actual costs made.

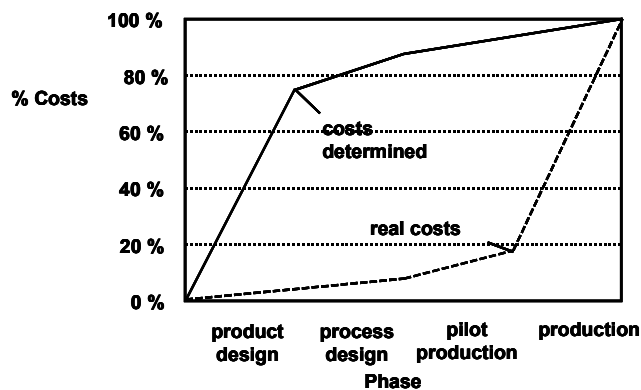


Figure 1.2:  
Real costs vs. determined costs as a result of the phases of the product development process [8]

In order for a company to optimize its business it needs to maximize its benefits over the product's life. This implies optimizing the chain of product development process, product creation process and product utilization process.

When a product is in use by the customer, its technical life can be extended by timely applying preventive maintenance to the parts that are subjected to wear. Applying preventive maintenance may be clearly cheaper than exchanging the product for a new one when the amount of wear can be significantly reduced.

After the product's economical life has ended, because the customer no longer wishes to use the product or because it has lost (some of) its functionality, there may be parts of the product that still function properly and thus have a longer technical life than economical life. In order to save costs it can be very beneficial for companies to re-use these products or product parts during another economical lifetime. This saves the company production costs, costs for processing waste and reduces pollution.

This calls for the need to be able to make correct and profound reliability analysis and predictions as early and fast as possible in the design stage to reduce time-to-market. In classical reliability theory one focuses on system and component reliability. Reliability is assessed based on analysis of failure mechanisms, failure times and hazard rates. Prediction is done by means of Accelerated Life Tests (ALT) to predict the Time-To-Failure (TTF) of a system.

The failure of a system can be caused by a large variety of reasons. These failures can usually be traced back to deterioration (gradual or rapid failure) or catastrophic failure [9]. Literature does however not focus very well on finding the underlying mechanisms, like variability and reliability of components that cause these failures. Failure of a product with respect to a performance characteristic can be traced back to the degradation of these components that influence this performance characteristic [10]. Here the performance characteristic can be defined as a measure of how well a product fulfills its function. The degrading components that influence this performance characteristic can be seen as design parameters. Hitherto there has not been significant work that tries to predict the influence that adjusting these design parameters can have on the reliability of the designed product.

In the next section a new reliability optimization concept is introduced that can be applied in the design stage of the product development process. The concept tries to find the relation between the degrading design parameters and the influence these have on the performance characteristic. Therefore this concept uses accelerated testing in the design stage to reduce time-to-market. Furthermore the purpose of the research for this master thesis regarding the reliability concept is discussed.

### **§ 1.3 Purpose of research**

This thesis evaluates the practical possibility of implementing a concept to design for reliability that is proposed by J.A. van den Bogaard in his PhD. research. In his paper *A Method for Reliability Optimization through Degradation Analysis and Robust Design* [10], he proposes a concept to optimize and improve the design of complex systems. Here the dominant failure mechanism of the system is identified and related to the degradation of the design parameters that influence its performance characteristic. Where design parameters are physical product parameters that can be influenced by the designer. And the performance characteristic is a measure of how well the product fulfills its intended function.

Observation of the product's physical degradation and analysis of this degradation based on engineering knowledge combined with literature provides for a better understanding of the failure mechanisms and higher credibility of reliability predictions.

In his PhD. research Van den Bogaard tries to answer the following question:

---

*Is it possible to predict and design for reliability (with respect to a performance characteristic) through parameterization of the performance characteristic, and by superimposing the degradation profiles of the design parameters on the performance characteristic under study, at the concept design stage itself?*

The concept, which from now on will be referred to as Reliability Optimization Method through Degradation Analysis (ROMDA), was successfully evaluated by Van Hoorn [11] in his master thesis. He proved by means of simulations that it was possible to significantly improve product design. In the last phase of his master thesis he made an initial step to the implementation into practice.

Van Hoorn's work has been the point of departure for this master thesis. However the practical part of his work does not cover the entire ROMDA concept. This concept, for which a roadmap for implementation was elaborated during this master thesis was only partially executed and could therefore not be used for reliability purposes. Moreover, the phases that were executed could be improved as a result of new data and new ideas and research.

The research in this thesis was conducted in cooperation with Flextronics International, Venray. Its objective was to develop a method to improve product design and make optimal re-use and preventive maintenance decisions based on one performance characteristic that represents the quality of an entire product. Therefore the performance characteristic should be assessed on a regular basis to determine the quality of the product. The feedback that is provided can then be used to plan and perform preventive maintenance at financially convenient moments before the product fails.

The products that Flextronics produces usually have a much longer technical life than economical life. This means that the customer decides to replace the product long before it fails even though the product is still in fine technical health. In order to save money and reduce waste Flextronics wants to re-use its products. Therefore it needs to make accurate reliability predictions for another economical life. Therefore the performance characteristic needs to be related to time. Finally the design needs to be improved with regard to this performance characteristic

In this master thesis the ROMDA concept is applied to a Finisher module of a photocopier to verify whether this concept can be used to satisfy these objectives. At the start of this graduation project the phases zero to six of the concept were already performed. The results of these phases were assumed to be correct and valid. During this project the final four phases of the roadmap were executed. These phases are the ones that make the concept unique in its kind.

This work tries to capture and predict the reliability of the Finisher module by means of degradation analysis. Degradation analysis, in contrast to Time-To-Failure analysis, makes it possible to analyze and predict reliability closer to the root of the cause of degradation. Degradation analysis and modeling is not uncommon to literature. Degradation analysis is used here to predict the reliability of components or small simple products. This thesis attempts to analyze, model and predict the reliability of a large complex system through degradation analysis and engineering knowledge. Thereby degradation or performance of several functions of the system is monitored during an accelerated degradation test. Next an experiment is performed to model the behaviour of the performance characteristic over life as a result of the degradation of its design parameters. Therefore the degradation of the design parameters is superimposed on the performance characteristic by means of a time dependent Design of Experiments. The combination of the degradation models of the design parameters and the model for the performance characteristic as a function of these design parameters is finally used to optimize the

design of the Finisher module (population). This thesis additionally contains a side study on estimation of parameters in nonlinear mixed effects degradation models by means of maximum likelihood estimation. This was done to have a better understanding of degradation modeling. The results are presented in appendix J and can be used to increase the accuracy of estimations.

To summarize, this master thesis focuses on the practical implementation of the ROMDA concept as developed by Van den Bogaard. It deals with the practical difficulties, issues and resulting decision making that distinguish practice from theory. The conclusions of this report consist of statements considering the practical applicability of the concept and recommendation on improvements to the concept and to the way this research was conducted. The research question is consequently formulated as follows:

#### **Research question**

*Is it possible to implement the ROMDA concept as proposed by Van den Bogaard into practice and apply it to design optimization, preventive maintenance and re-use?*

The next section discusses the structure of this thesis. It discusses the chapters to come and summarizes their contents.

#### **§ 1.4 Structure of this thesis**

In the next chapter, the reader is introduced to the field of reliability engineering and prediction. The chapter starts by introducing the reader to some essential definitions and reliability prediction methods. The classical reliability concepts and prediction methods are described first [3, 12] subsequently the reader will be presented to the Roller coaster curve [13, 14]. The different phases of the Roller coaster curve are then related to possible types of reliability problems [4]. Subsequently this literature chapter converges to topics that are of specific interest to the ROMDA concept. These are first methods for accelerated testing, degradation testing and degradation analysis. Next the concepts Robust Design [15] and Tolerance Design [16] are explained and discussed. These are concepts that attempt to improve product quality. The specific literature shows a strong relation to the concept of this research that attempts to predict and optimize reliability.

In chapter 3, the proposed concept for reliability prediction and optimization is introduced. The concept that can be used in the design stage attempts to analyse and model the degradation of the design parameters of the dominant failure mechanism of a product. These are then related to the performance characteristic that represents this degradation. The resulting performance characteristic as a function of time can be used for reliability prediction purposes and moreover can be used for optimization through its design parameters.

Chapter 4 makes the first step to practice. It discusses the roadmap that was developed for implementation, the product on which implementation takes place and the results that were achieved hitherto. First the roadmap discusses the order of the phases, subsequently the used product, a Finisher module of a photocopier, is presented. And finally the dominant failure mechanism and the results that were achieved before this master thesis project are discussed.

In order to capture the degradation of the dominant design parameters an accelerated degradation test was conducted. Chapter 5 discusses the set-up of the experiment and analyses the observations. The chapter shows that the design parameters degrade and that the performance characteristic is affected by this degradation. This results in models of the design parameters as a function of time.

In chapter 6, these degradation functions are used for the set-up of an experiment that superimposes the degradation of the design parameters over life on the performance characteristic. For this the obtained degradation models are extrapolated to just before failure. This experiment makes use of unit-to-unit variation of the design parameters of new Finishers to simulate the effect that different design parameter settings would have on the performance characteristic of this product. The experiment resulted in a model of the performance characteristic over time.

The combination of models that was obtained is then used in chapter 7 to optimize product design. This chapter optimizes the product's design with regard to robust reliability. The design parameter settings are identified that maximize time-to-failure, while minimizing the variance.

Finally, chapter 8 will answer the research question that was presented in the previous section. The chapter contemplates the results and conclusions of this work, which will lead to the final conclusions and recommendations to the concept.

## Chapter 2 Literature

*“If you steal from one author, it's plagiarism; if you steal from many, it's research”*

*Wilson Mizner (1876 - 1933)*

The field of reliability engineering is a large and ample one. It consists of many specializations divided over many engineering sectors. Over the years this has led to a huge amount of theories, laws, models and concepts. This chapter starts by providing the reader with an overview of reliability essentials. The first section introduces the definitions of quality and reliability and explains what they may mean to the different players in the market. Subsequently section two shows how business processes and reliability problems may be categorized. This categorization will return later on to specify the area of reliability problems on which the ROMDA concept can be applied and also on what types of products it is relevant to apply the concept. Subsequently it is described how reliability predictions can be made based on time-to-failure, how product populations can be subdivided into categories and which reliability problems can be distinguished within these categories. As of section 2.4 the emphasis will move to topics that are more specific for the practical work that is conducted in this graduation project. Accelerated degradation testing and degradation modeling is used by ROMDA to capture the time aspect for reliability predictions. In chapter five an accelerated degradation test is conducted based on the literature on this subject in section 2.4. The concepts Robust Design and Tolerance Design, which are introduced in section 2.5 and 2.6, are methods that allow for improving quality or reliability. In chapter seven of this thesis design optimization with regard to robustness of reliability is performed. Finally the last section provides a review of the topics in this chapter and leads in the concept description that will take place in the next chapter.

### § 2.1 Introduction

We start by giving the reader some definitions on generally used terms in the field of reliability. First of all a definition of quality is provided for

**Quality:**

*The ability of a product or system to fulfill its intended purpose [12]*

Upon reading this definition it may become clear that quality is strongly related to reliability. The standard definition of reliability as employed by IEEE is as follows

**Reliability:**

*The ability of a system or component to perform its required functions under stated conditions for a specified period of time [17]*

Hence reliability may be seen as time related quality. As a consequence of this definition reliability can be perceived from two points of view. There is the buyer's view and the manufacturer's view [3]. Both have their own independent opinion on what quality and hence reliability means to them. Buyers can be divided into three categories: individuals, businesses and government agencies.

Individuals buy products either for obtaining certain benefits, for pleasure or for both. The performance of the product has a major impact on customer satisfaction.

Businesses on the other hand buy products to use them as equipment or tools. This makes the reliability of equipment, tools and machines critical to the company. The performance of such equipment depends on its reliability as well as on other factors, such as usage intensity and maintenance. When a failure occurs, the impact can be significant, e.g. economic loss, damage to property and damage to persons.

The government as a buyer is one that regularly buys specialized systems (e.g. for military purposes). These often involve new technologies and must meet very demanding performance criteria. Such systems are not only very expensive to purchase, they are also expensive to operate and maintain.

From a manufacturer's point of view, the reliability of a product is influenced by several technical factors like design, materials, manufacturing, distribution and quality control. Product reliability affects sales, warranty costs and profits. Poor reliability implies low customer satisfaction and this in turn affects sales and results in higher warranty costs. This challenges the manufacturer to find an optimal relation between the production aspects and the commercial aspects.

The different interests of the buyer and the manufacturer may lead to conflicting opinions on how products or systems should perform, usually reaching an apogee when a product or system fails.

When a system, product or component ceases to perform its intended function we speak of a failure. Kumar and Crocker use the following definition of the failure of a system [18].

**Failure of a system:**

*Any event or collection of events that causes the system to lose its functionability*

Where functionability is defined as

**Functionability:**

*The inherent characteristic of a product related to its ability to perform a specified function according to the specified requirements under the specified operating conditions*

Now that the reader has become familiar with the meaning of terms like quality and reliability and more importantly what these terms mean to the different players, the next section will discuss how products can be categorized based on their business processes and which reliability problems can be distinguished. In chapter three this will be related to the application area of the ROMDA concept.

## **§ 2.2 Reliability problems**

The question which reliability problems are relevant for a product is strongly dependent on its lifecycle strategy. The strategy that a company pursues usually depends on the developments in technology, developments in the market and the type of product that is being developed (or the type of market). Roughly products can be divided in three groups depending on their business process [4].

These groups are:

- A) Business processes depending on products where the economical lifetime (0-3 years) is much shorter than the technical lifetime (High tech fast innovation products).
- B) Business processes depending on products where the economical lifetime (3-10 years) is comparable to the technical lifetime (Consumer goods such as televisions and cars).
- C) Business processes depending on products where the economical lifetime (10 years and beyond) is much longer than the technical lifetime (Professional (production) systems).

Products that have short economical lives have business processes that generate earlier failing products. Thus technical quality of a product depends on its economical lifetime.

According to [19] reliability problems can be categorized based on three dimensions. These dimensions are:

**Time dependency:**

- failure is time independent and occurs at a random and unexpected moment in time
- failure involves some form of wear and is time or use dependent

**Specifications:**

- the product has broken down and does not meet technical specifications nor customer requirements (hard)
- the product has not broken down but shows lower performance. It does no longer meet technical specifications. (soft)

**Statistics:**

- the difference in users or difference in products affects the reliability of the product
- reliability problems are equal for all products in all situations

Figure 2.1 shows a graphical representation of how reliability problems may be classified according to these three dimensions [19].

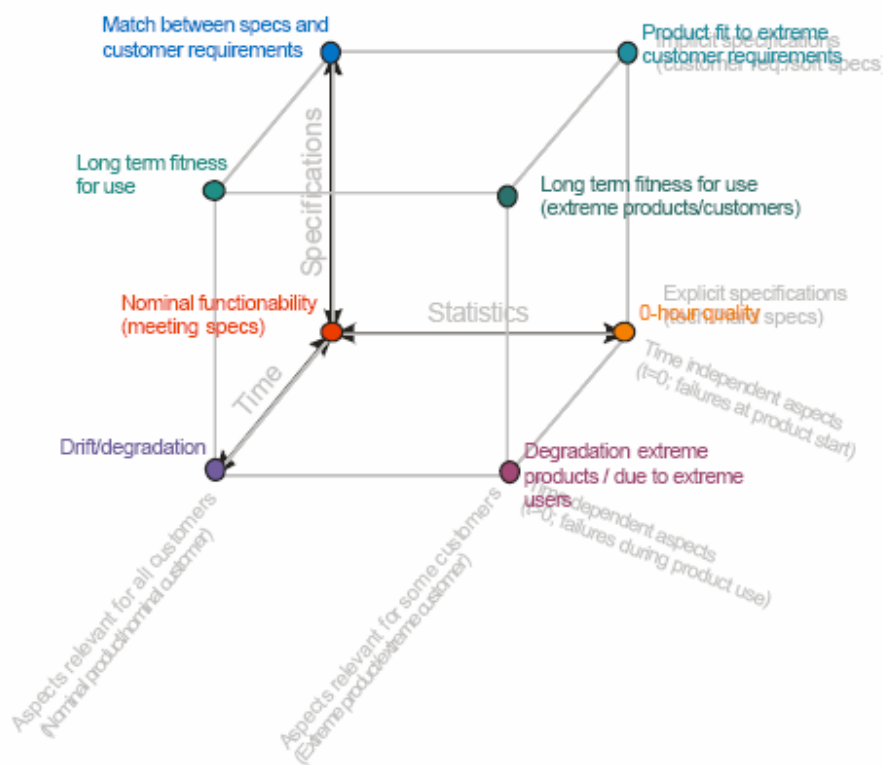


Figure 2.1: Different types of reliability problems

The problems or causes of failure that are presented above will be used in chapter 3 to define the area of reliability problems in which the ROMDA concept can be applied. At the end of this thesis the experience that was gained during the project will be used to more accurately define the types of products and business processes on which application of the ROMDA concept will be most profitable.

The next section introduces the topic of reliability prediction. As reliability prediction is one of the objectives of the ROMDA concept, understanding this topic is also of high importance as a background for the chapters to come. Furthermore the next section introduces the Bathtub curve and Roller coaster curve. The different phases of this second curve will be related to the categorizations of business processes and reliability problems that were introduced in this section.

### **§ 2.3 Predicting reliability**

Basic reliability measures are used to predict the system's ability to operate without maintenance and logistic support. In order to make these predictions, a reliability function and a failure function need to be defined. Mathematically the probability of failure of a system before a certain time can be defined in terms of its Cumulative probability Density Function, abbreviated as CDF. The probability that a system fails before time  $t$  can be stated as  $F(t)$ . Hence the reliability of a system can be stated as

$$R(t) = 1 - F(t) \quad (\text{eq 2.1})$$

and therefore

$$F(t) + R(t) = 1 \quad (\text{eq 2.2})$$

The probability density function of  $t$ ,  $f(t)$ , describes the probability that an item that is functioning properly at time  $t$  fails in the time interval  $[t, t + dt >$  and is defined as

$$f(t) = \frac{dF(t)}{dt} \text{ or just the same as } f(t) = -\frac{dR(t)}{dt} \quad (\text{eq 2.3})$$

The functions presented provide a basis for elementary reliability and failure probability calculations. Using these functions, the expected value of a system's time to first failure can be calculated. This is called the Mean Time To Failure (MTTF) and is generally used as a measure of reliability for non-repairable items [18]. Mathematically, MTTF can be defined as

$$MTTF = E(T) = \int_{-\infty}^{\infty} tf(t)dt = \int_{-\infty}^{\infty} R(t)dt \quad (\text{eq 2.4})$$

MTTF is often confused with Mean Time Between Failures (MTBF). Although the two seem to be the same thing, MTBF is only equal to MTTF in case a system is brought back to an as-good-as-new state after repair. Otherwise it is smaller. MTBF can, in this case, only be predicted when the quality of the repair is known (or when assumptions are made).

Another frequently used function is the hazard rate function, also called failure rate function. This function is defined as follows.

#### **Hazard rate:**

*The hazard rate at time  $t$  is defined as the probability that a system fails instantaneously given that it has survived up to time  $t$ .*

This is mathematically described by

$$h(t) = \frac{f(t)}{1 - F(t)} \quad (\text{eq 2.5})$$

What this function implies is that the probability of instantaneous failure of a system may change with time. Some product populations are more susceptible to failures when they get older; other populations have a higher instantaneous failure probability when they are new.

The explicit form of the hazard rate function is quite distinct for different classes of systems [12]. Electronic devices tend to have a short and inconspicuous wear-in period after which the failure rate is essentially constant for a long period of time (fig 2.2 a). Mechanical devices on the other hand usually have a hazard rate curve that shows a short but clear wear-in period followed by a long span of time with a monotonically increasing failure rate (fig 2.2 b).

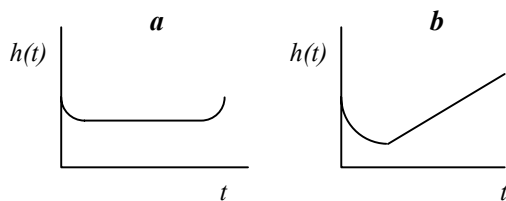


Figure 2.2: Hazard rate function of  
 a) Electronic devices  
 b) Mechanical devices

Literature distinguishes between two types of hazard rate curves with which it classifies the susceptibility of a product population to failure over time. These are the so-called Bathtub curve and Roller coaster curve. The following sub-sections will go into further detail on these two specific failure rate curves.

### § 2.3.1 The Bathtub curve

The Bathtub curve is used to describe the failure rate for many engineering components. Not only the failure rates of electrical components but also of mechanical components can be described by using the Bathtub curve. It can be mathematically modeled by three Weibull distributions [3, 12]. This probability distribution has the following properties:

When shape parameter  $0 \leq \beta < 1$  the failure rate will be decreasing, when it is 1, it will be constant and when  $\beta > 1$  it will be increasing.

The Bathtub curve may be divided into three phases:

1. Infant mortality or early failure period ( $0 \leq \beta < 1$ )
2. Useful life period ( $\beta = 1$ )
3. Wear-out period ( $\beta > 1$ )

This leads to the following failure rate or hazard rate curve of figure 2.3.

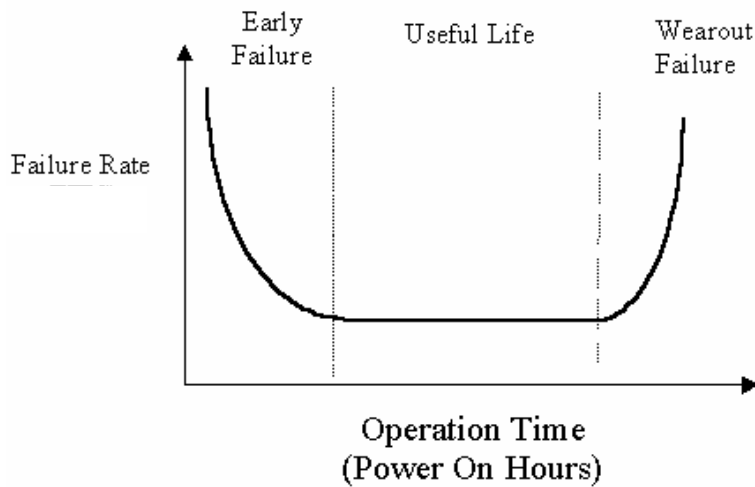


Figure 2.3: Bathtub failure rate function [12]

For each of these three periods different reasons exist why failures occur.

#### 1. *Infant mortality period*

Missing parts, sub-standard material batches, components that are out of tolerance and damage in shipping are some of the quality weaknesses that may cause excessive failure rates near the beginning of design life. The preferred method for eliminating such failures is through design and product quality control measures that will reduce variability and hence susceptibility to infant mortality failures.

#### 2. *Useful life period*

This middle section of the bathtub curve contains the smallest and close to constant failure rates and is referred to as the useful life. These failures are caused by random events and are normally not an inherent defect in the system or device.

#### 3. *Wear-out period*

The right side of the bathtub curve is a region of increasing failure rates. During this period of time ageing factors become dominant. The failures tend to be dominant by cumulative effects such as corrosion, embrittlement, fatigue cracking and diffusion of materials.

With regard to electronic devices it was discovered that a failure rate curve in the form of a bathtub did not always accurately represent reality. This failure rate had quite a distinct curve, which as a result of its form, was to be known as the Roller coaster curve.

### § 2.3.2. The Roller coaster curve

Research by Wong [13] and Brombacher [14] has shown that in several branches of electronics industry, especially in the areas with a high degree of technological innovation a Roller coaster curve can be used to replace the constant failure rate model to generally model the product behaviour in the field. Wong already discovered this phenomenon as soon as 1988. The form of the bathtub is said to be rather exception than rule in this area of industry.

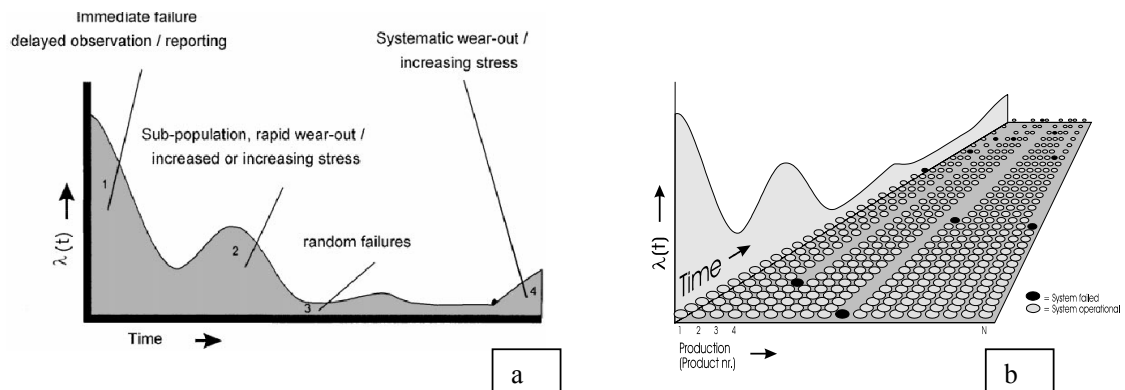


Figure 2.4: The Roller coaster curve

Figure 2.4 a) shows the categories that can be distinguished within the Roller coaster curve. This curve is the result of a translation from failures in the field on a time-axis as is shown in figure b). The white dots indicate that a product is still functioning, while the black dots indicate a product's moment of failure.

The Roller coaster curve may be subdivided into four classes of failures. *Hidden 0-hour failures, Early wear-out, Random Failures and Systematic wear-out.* [20]

#### 1. Hidden 0-hours failures

These are products that arrive out of customer specification at the customer. They have either slipped through final tests, have been damaged during transport or are used in an unanticipated manner. Although, theoretically, these failures should all be observed at the moment of commissioning of the product, complex functionality or delay in customer reporting can cause delay in observing and reporting a failure.

#### 2. Early wear-out

Regarding high-volume consumer goods it is quite likely that there are considerable differences between products. The same is true with regard to how different customers use a certain product. In this case it is possible that there exist distinct sub-populations of products that show different reliability behaviour than the main population with regard to wear-out. In the failure rate curve these sub-populations can appear as one or more humps. These sub-populations are quite difficult to test during production because on product level they initially perform according to specifications.

#### 3. Random failures

Companies produce products to operate in normal user operating conditions. It is, however, impossible to design a product in such a way that it can cope with all possible occurrences. External events with a strong "random" character, such as lightning and mechanical shocks can produce failure at any moment in time. In these cases where the likelihood of occurrence

for these events is constant in time and constant over the product population, the effect will be a constant failure rate.

#### *4. Systematic wear-out*

Particularly mechanical products and also categories of electronic products show some form of degradation over time. Well-known time effects are corrosion of metals and increased brittleness of plastics. At the moment in time where this wear-out starts to dominate the failure rate curve it will lead to an increasing failure rate.

The bathtub curve and the roller coaster curve allow for classification of failures over time. A failure however can be the result of several causes or problems. First the phases of failure of the roller coaster curve will be related to the three distinguished business processes of the previous section. Or better said a relation will be made between the three types of business processes and the types of failures that they generate. Products by group A (economical life  $\ll$  technical life) usually are subjected to failure in the phases one and two of the Roller coaster curve. For group B (economical life  $\approx$  technical life) these are phases one, two and three, while failures for groups C (economical life  $\gg$  technical life) usually occur in phase three and four. Note that companies that create products with short economic lifetimes have business processes that produce earlier failing products with different failure characteristics.

The same relation can be made regarding the types of reliability problems that are distinguished in section 2.2. Reliability problems that are time dependent usually occur in the phases 2 and 4 of the roller coaster curve. Problems regarding statistics (user and/ or product dependent) can be related to the phases 1 and 2 of this curve. And specification problems will often occur in the phases 1, 2 and 3. This cube, together with the Roller coaster curve, will be used again in chapter 3 to define the application area of the ROMDA concept.

The roller coaster curve, just as the bathtub curve, is a result of failure times of a product population. Information on failure times can be obtained in two ways. The first is by means of feedback on failed products in the field. However, obtaining field data from service centers often proves to be a slow process. Reliability engineers often face field data with a small number of failures and a large number of suspensions. This leads to the fact that in engineering practice, problems regarding field data reliability analysis occur frequently [21]. The other way is by accelerating the ageing process of the product. This is called accelerated testing and can be applied as soon as in the design phase of the product. Hereby it is possible to obtain information on weaknesses, Time-To-Failure (TTF) and reliability before the product is introduced to the market. The following section discusses this tool in more detail. Special attention is paid to degradation testing and degradation modeling. These topics are of paramount importance for the concept of chapter three, because it uses accelerated degradation testing in order to model and predict system reliability. Chapter five will put the theory on this topic into practice.

### **§ 2.4 Accelerated testing**

In order to compete in the market, companies have to produce the right products with a shorter time to market and at lower costs than before. Shorter time to market requires the product development process to change the way of working from the classical “wait and react” to anticipating and preventing problems as early as possible in the development process. While in a classical product development process products could be tested when available from (pilot) production, a modern, time-driven development process requires optimization long before larger series of products are available [20]. In these types of environment applying accelerated testing in the design phase can be paramount.

However, data obtained from accelerated tests in a laboratory may differ from that what is obtained in the field. Laboratory data are likely to provide more information per sample unit, both in the precise time to failure and in the mechanism by which failures occur. Conversely, the sample size for field data is likely to be much larger, allowing for more precise statistical estimates to be made. Equally important, laboratory experiments may not adequately represent the environmental condition of the field, even though attempts are made to do so. The exposure to dirt, temperature, humidity and other environmental loading encountered in practice may be difficult to predict and simulate in the laboratory [12]. Therefore irrelevant failure mechanisms are sometimes found.

Accelerated tests are traditionally used to find flaws or weaknesses in the product design. But they can also be employed to assess and predict reliability. Generally there are two types of accelerated tests: the compressed time test and the advanced stress test.

### **Compressed-time testing**

Compressed-time testing is a way of testing in which the product is used more steadily or frequently during the test than in normal use, but the loads and environmental stresses are maintained at the level expected in normal use [12]. An example could be a television set that is turned on and off very frequently and which channels are changed more often than during normal operating life. Precaution should be taken. If the cycle is accelerated too much, a situation can be established in which the conditions of operation change and no longer reflect the actual product life. A television set in real life is turned off; then it has time to cool down. When it is turned on again it makes a cool start. If an accelerated cycle is run too fast, capacitors within the television set may still be charged. This leads to different operating conditions and possibly earlier failure.

### **Advanced-stress testing**

Some systems are in continuous operation during their life cycles. Other systems are constantly exposed to deterioration whether they are active or not. For these types of systems, compressed-time testing does not accelerated the failure mechanism. In these cases advanced-stress testing may be applied. The test uses an increase in load or a harsher environment to accelerate the failure mechanism. This only works if a decrease in reliability can be quantitatively related to an increase in stress level.

According to Meeker and Hamada [22] accelerated life tests are mainly fit for detecting two types of failure modes: Unavoidable degradation failure and known infant mortality.

The following sections will discuss in more detail how accelerated life tests are conducted and will especially focus on a special kind of accelerated testing, degradation testing.

#### **§ 2.4.1 Degradation testing**

Accelerated life testing of products, components and materials is used to get information quickly on specific lives, life distributions, failure rates, mean lives and reliabilities. Accelerated testing is achieved by subjecting the test units to application and operation stress levels that are more severe than normal or use stress levels, to shorten their lives or their times to failure. If the results can be extrapolated to the use stress levels, they yield estimates of the lives and reliabilities under use stress [23]. This section focuses in more detail on a specific kind of accelerated testing; degradation testing.

For some products or devices it is difficult to obtain failure time data fast, because their Time-to-Failure is quite long. For these kinds of devices it may be possible to obtain degradation

measurements over time. These measurements may contain useful information about product reliability [24]. Sometimes it is possible to measure physical degradation as a function of time. In other applications actual physical degradation cannot be observed directly, but measures of product performance degradation may be available. Modeling performance degradation may be useful, but could be complicated because performance may be affected by more than one underlying degradation process [25]. Nevertheless the advantages of degradation data over TTF data are quite strong, because [23]

- Degradation is a natural response for some tests
- It provides useful reliability inferences even with zero failures
- It provides more justification and credibility for extrapolative acceleration models (Modeling closer to physics-of-failure)
- It can be more informative than failure-time data. (Reduction to failure time data loses information)

In literature, various degradation tests are described, modeled and analyzed [24 - 31]. Meeker and Lu [24, 25, 26] describe how degradation data can be used to estimate parameters of a degradation model and use this for the prediction of Time-to-Failure. Section 2.4.2 discusses characteristics that are inherent to degradation models and gives some examples of degradation models.

In their article Yang and Yang [31] propose a method for estimation of a life distribution by using data from degradation measurements. Meeker, Lu and Escobar [25, 26] introduce an adapted form of Maximum Likelihood Estimation to estimate model parameters based on degradation measurements. The resulting model is used to estimate the life distribution.

#### **§ 2.4.2 Degradation models**

In chapter thirteen of their book [25], Meeker, and Escobar give examples of degradation models with three sorts of forms: *Linear* degradation, *Convex* degradation and *Concave* degradation. He states there are two sorts of variation that cause variation in degradation and failure times:

- Unit-to-unit variability
- Variability due to operating and environmental conditions

Variability due to operating and environmental conditions speaks for itself. The more stress that is applied during operation or in the product's operating environment, the faster it is due to deteriorate and fail.

Unit-to-unit variability however can have several causes:

- 1) *Initial conditions*. Individual units will vary with respect to the amount of material available to wear, initial level of degradation, amount of harmful degradation causing material, etc.
- 2) *Material properties*. The specific properties of degrading materials may vary from unit to unit, leading to variation in degradation speeds.
- 3) *Component geometry or dimensions*.
- 4) *Within-unit variability*. The units itself will have different properties, e.g. defects.

When the underlying degradation mechanisms and the degradation causing factors are known, it is possible to make time-dependent models of degradation (or performance). Chiao and Hamada [27] use such a model to describe the degradation of the intensity of light emitted by a LED. Meeker, Lu and Escobar [24] use the Paris-rule model to describe fatigue crack growth of a certain alloy.

Degradation testing in contrast to testing for failure times provides much more information on the underlying mechanisms and reasons for failure. Especially when a product's TTF is much larger than its economic lifetime or when time to market is short it is very costly to test until failure without influencing the TTF. In these cases degradation testing provides useful information about degradation paths, which can be extrapolated with higher certainty. The ROMDA concept also uses degradation testing to capture the degradation paths of certain so-called design parameters. This provides the possibility to make estimations of degradation at any moment in time. The next section discusses a concept called Robust Design. This method reduces the sensitivity of a product to the factors that cause variance by adjusting the settings of certain product parameters. The basic idea behind this method is used by the ROMDA concept to improve product reliability with regard to robust reliability. In chapter seven this is applied to the design of a Finisher of a photocopier.

### § 2.5 Robust Design

This section deals with a certain design optimization technique called Robust Design. Its principles and way of working will be explained in the first part. Robust Design is basically a method for making a product's quality insensitive to noise factors. However it can also be applied for achieving robust reliability. The second part of this section explains how this can be achieved.

In quality engineering there exist three methods for reducing the variance in product quality [15].

1. Screening out bad products
2. Discovering the cause of malfunction and eliminating it
3. Application of the Robust Design method

Especially screening out the bad products is a very intensive and expensive method for improving the quality of the product population. It does not only lead to higher costs as a result of scrap, but also the quality inspections and rework cost the company money. Eliminating the cause of malfunction is usually applied by setting higher tolerances on specific components. Even though this method is cheaper than the first, it does lead to higher rejection rates.

The third method of reducing the variance, called Robust Design, accepts the presence of certain noise factors and tries to make the product's performance insensitive to these noise factors.

Now how does Robust Design exactly work? The method uses two steps. The first step consists of reducing the variance of the product's performance. The second step is taken to undo a possible shift of the mean of the product's performance. Figure 2.5 [15] explains these steps graphically.

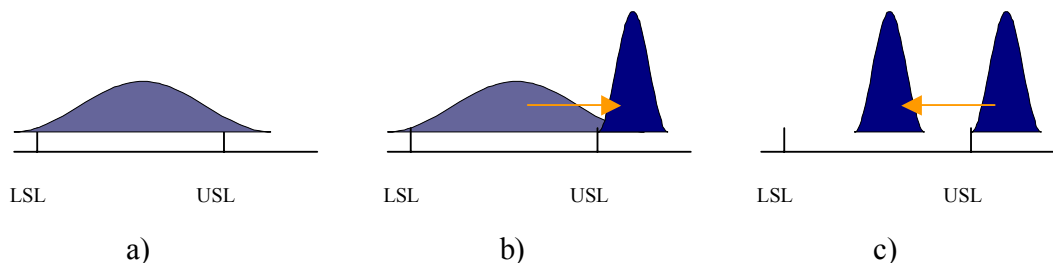
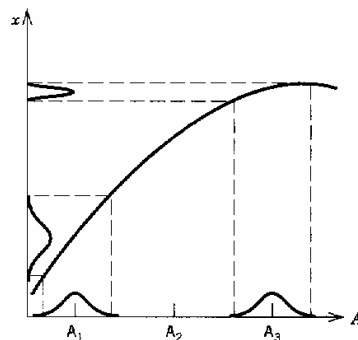


Figure 2.5: Distribution of the performance characteristic

- a) nominal situation
- b) step 1: reducing the variance
- c) step 2: shifting the mean

At first the mean of the performance characteristic is on target, but its variance is too large. In order to reduce this variance a design parameter is changed in such a way that the variance of the performance characteristic is reduced or minimized. This may however affect the mean of the performance characteristic in such a way that it is off target. In this case a second step has to be taken. In that step another design parameter is changed to adjust the mean of the performance characteristic back on target without this having affect on its variance.

What robust design actually does is exploiting the inherent nonlinear relationship among the product or process parameters, the noise factors and the quality characteristics. In figure 2.6 such a nonlinear relationship is presented [15].



*Figure 2.6: Performance characteristic 'x' versus design parameter 'A'.*

An increase of design parameter  $A$  will result in a higher performance characteristic  $x$ , but also in a lower variance of this performance characteristic. Therefore the designer may choose to reduce the variability in the performance of the product by increasing design parameter  $A$ . If this leads to an offset of the mean value of the performance characteristic as in figure 2.5 b) the designer needs to re-adjust the mean of performance by making changes to a second design parameter (figure 2.5 c) without affecting (or affecting less) the variance of the performance characteristic  $x$  (figure 2.6).

In case a product has several performance characteristics with the same design parameters the so-called Desirability Technique [32] can be applied. This technique optimizes a linear programming problem with multiple response variables by translating the value of each response variable to a desirability factor based on its optimal value. When one chooses the TTF as one response variable and its standard deviation as another, the Desirability Technique can be used to achieve robust reliability. Then desirability can be optimized by setting the design parameters in a way that leads to the highest desirability and therefore to optimal robust reliability.

The explanation of Robust Design in this section concerned the quality characteristic of a product or product population. Similarly we may have a description of a performance characteristic over time, which may be seen as a characteristic that describes the degradation of a product or product population. In order to achieve robust reliability design parameter settings need to be identified that minimize the variance of the performance characteristic over time while maintaining the mean value over time (degradation path) the same or better as before. This implies that these parameter settings reduce unit-to-unit variability over time to a minimum.

Literature describes various ways of improving reliability and to make it robust. Condra [33] describes how one can design for robust reliability. He describes a degradation experiment for a fluorescent lamp by Tseng, Hamada and Chiao [28, 29]. In this experiment the effect of three factors or design parameters on the performance characteristic Light Intensity is evaluated. Design Of Experiments [33] is used for this purpose. The experimenters use four runs with a different combination of level settings at each run. For each run (or combination of level setting) five lamps are used in order to compensate for lamp production variability. Each of the twenty lamps is subjected to the same degradation test. The results of the degradation tests indicated that only two out of three factors were of influence on the TTF and they were set at the level that maximized their life span. The other factor was set at the level at which it was before the experiment.

In another experiment using LEDs, Chiao and Hamada [27] also take into account a noise factor. They estimate the parameters of a degradation model and the probability density function per run. Based on the PDF they calculate the reliability during the warranty period per run. The factor settings for the run that lead to the highest warranty reliability are selected. This way of design also takes into account the variance in TTF.

Robust Design is a relatively cheap and effective way to reduce the variability between products. This section also demonstrates how Robust Design may be applied to reliability. When Robust Design does not lead to the wanted results a following step can be taken. This is called Tolerance Design. The next section explains the Tolerance Design concept and shows its relation and application to reliability purposes.

## **§ 2.6 Tolerance Design**

In this section the Tolerance Design concept is discussed. This concept makes use of the relationship between the performance characteristic and its design parameters in order to graphically demonstrate product quality acceptance. It also demonstrates that product rejection is not necessarily a result of the performance characteristic that exceeds its specifications, but also of one of the design parameters that exceeds its specifications. In the first part of this section the Tolerance Design concept is briefly explained. In the second part it is applied to reliability purposes.

In order for a product or component to be accepted as qualitatively satisfactory it has to comply with some constraints or specifications. When a product does not have these properties it is rejected. In this chapter it is discussed how a certain design method proposed by Spence and Singh Soin [16] can be applied to our goal of achieving robust reliability. In their book they describe an electric circuit for which the quality characteristic or performance characteristic is the voltage over a certain resistor. This voltage depends on the two resistors in the circuit. Here the resistors may be seen as design parameters and the output voltage as the performance characteristic. Each of these three parameters has its specifications. When one of the three parameters does not conform to its specifications the product, which is the electric circuit, is rejected.

When the mathematical relationship between the design parameters and the performance characteristic is known a so-called *Region of Acceptability*, in which the product conforms to specifications, can be made as in figure 2.7 [16]. The black rectangle in figure 2.7 b) shows the output of the production process.

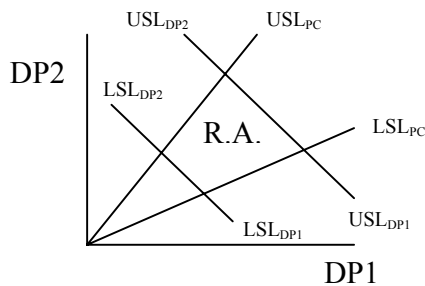


Figure 2.7 a) Region of acceptability

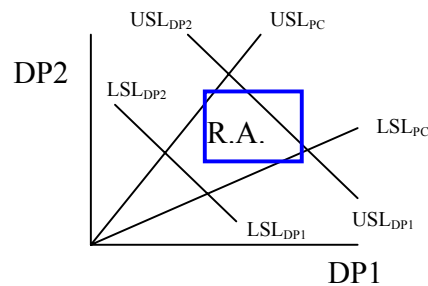
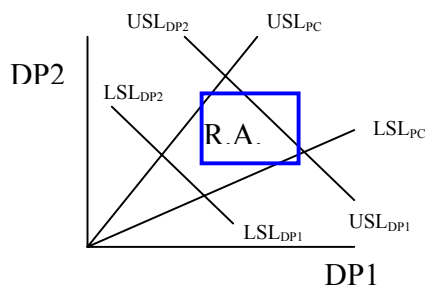
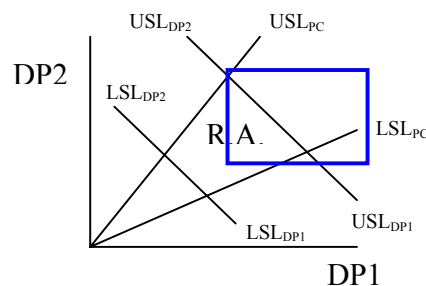


Figure 2.7 b) Process output

In this study the same concept is used in a different way; namely to describe degradation of the performance characteristic with time. When the design parameters degrade, they affect the performance characteristic of the product. Hence the value of the performance characteristic moves out of the region of acceptability. As not every product deteriorates equally fast, the differences between the products and hence their performance characteristic may become larger when time passes.



Time = zero hours



Time = 1 economical life

Figure 2.8: Degradation of the performance characteristic

Tolerance Design proposes three methods of design improvement for a production process. These should be applied after Robust Design, because they are more expensive.

- *Design centring*: changing the nominal values of the parameters so that the black rectangle moves inside the R.A.
- *Tolerance assignment*: after centering the region of tolerance it is obvious that tightening tolerance, which leads to a smaller rectangle, will lead to a higher yield.
- *Variability reduction*: reducing variability leads to a more constant performance. This performs well when the process is well centered.

In conclusion Tolerance Design is a method for parameter design that is best applied after Robust Design. This topic is the last subject of this literature chapter. The final section of this chapter is a discussion on the treated topics and serves as an introduction to the next chapter in which the ROMDA concept will be enlightened.

---

## **§ 2.7 Discussion**

This chapter introduces the reader to the field of reliability engineering. It starts by providing the reader with some definitions on basic reliability terms. Here expressions like quality and reliability are explained from the point of view of the manufacturer, the customer and the government. In section 2.2 reliability problems are categorized based on the three dimensions time, statistics and specifications. Based on these dimensions the reliability problems on which the ROMDA concept focuses can be distinguished. This will follow in chapter three.

In section 2.3 the reader is introduced to reliability prediction. The section starts with simple prediction methods for reliability and failure probability. Subsequently the term failure rate or hazard rate is introduced, which consequently leads to the categorization of failures based on the bathtub curve in section 2.3.1 and the roller coaster curve in section 2.3.2. The different failures and phases of these curves are then related to the categorizations made in section 2.2. These problems are then related to the four different phases of the roller coaster curve.

In order to be able to make predictions on system performance one has to know its degradation or behaviour over time. A fast way of obtaining this information when no field data is present is by means of accelerated testing. Section 2.4 elaborates extensively on the subject of accelerated testing. Special attention is paid to degradation testing as this has been performed during a fair part of this master thesis. During this master thesis project a special case of a Maximum Likelihood function for fitting degradation data and functions was evaluated as a side study. This was done to enrich the possibilities of the concept with regard to degradation modeling. The results of this study can be found in appendix J.

Section 2.5 deals with Robust Design. First it is explained what Robust Design means. Subsequently it is explained how the method can be applied in practice. And finally the step is made to robust reliability. For several examples in literature it is described how one can design for robust reliability. Achieving robust reliability is one of the objectives of the ROMDA concept. This means that design parameter settings must be found that lead to a TTF that is as high as possible while minimizing variance. Robust Design is a powerful method for reducing variance.

When Robust Design does not have the wanted effect on the rejection percentage of the production process, the design can be further adjusted by means of Tolerance Design, which is discussed in section 2.6. This section makes an adjustment to the Tolerance Design concept in order to make it applicable to reliability purposes. Optimizing reliability in this situation is done by designing the system so that it stays within the region of acceptability as long as possible while the increase of variance is as small as possible. Reliability optimization is a prominent point in the ROMDA concept.

Despite of the enormous amount of literature on reliability there exists a gap that the concept of the next chapter tries to fill. This concept makes the step of applying reliability prediction based on degradation data to a large complex product or sub-system. Hereby it relates the Performance Characteristic of the dominant failure mode to its dominant design parameters. This yields the possibility of reliability optimization by means of optimal design parameters settings. It also provides the possibility for optimal re-use decisions and optimal replacement time decisions for preventive maintenance. The nearest concept of reliability modeling and optimization know to us in literature is an article by Tseng, Hamada and Chiao [29].

The literature introduction that is given above is necessary to understand the introduction of the ROMDA concept by Van den Bogaard, which is presented in chapter three. The chapter starts

---

with a simple introduction of the concept. The second section however goes into more detail on the calculative aspects of the concept. Finally the last section of the chapter provides the basic elements that must be obtained from practice in order be able to apply the possibilities of the concept. These elements serve as input for the chapter thereafter. Finally the chapter is concluded with a short discussion.

---

## Chapter 3 Concept description

### § 3.1 Introduction to the concept

After the introduction to the relevant literature for this master thesis, this chapter will explain what the concept called Reliability Optimization Method through Degradation Analysis (ROMDA) does and how it works. The purpose behind the research for the ROMDA concept is to develop a method for reliability prediction of complex products that allows for optimization of the product's design for robust reliability. Optimization for robust reliability here implies finding the desired balance between a large time-to-failure and a small variance of this time-to-failure.

The concept attempts to do this by capturing degradation information of the design parameters and linking this to a performance characteristic. Here the terms performance characteristic and design parameter can be defined as follows:

**Design parameter (DP):**

*Physical product parameter that can be changed by the designer*

**Performance characteristic (PC):**

*A measure expressing how good a product fulfills one or more of its intended functions*

What the ROMDA concept targets to do is identify the most dominant failure mechanism for a certain product (population) and find a performance characteristic that represents its functioning. The concept then assumes that this performance characteristic, and thus the failure mechanism, is affected by the degradation of its design parameters. Figure 3.1 shows how the performance characteristic of the product population is affected by the degradation of its design parameters. The depth in the figure represents the time axis. Note that a product fails when the PC or one of the DP's exceeds its specification limits (section 2.6 Tolerance Design). Specification limits can be defined as follows.

**Specification limits:**

*Certain chosen values (upper and lower limits) defining the boundaries of an interval for the performance characteristic under study outside which the product is not able to fulfill the related intended function(s) properly anymore*

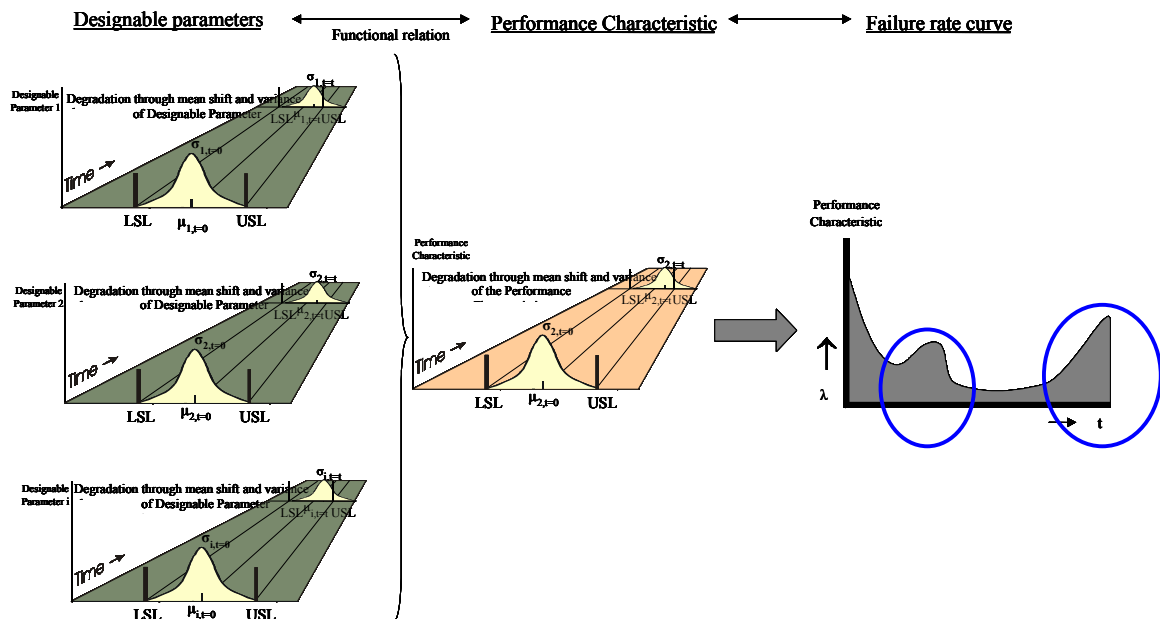


Figure 3.1: Concept Visualization

The figure shows how the degradation of the design parameters affects the performance characteristic over time. As this theory only applies to products that fail due to wear or degradation, the ROMDA concept only focuses on the phases two and four of the roller coaster curve (section 2.3.2).

Decrease in performance over time is affected by the degradation of the design parameters. Hence in order to make sound predictions of performance over time, the degradation of the design parameters needs to be captured.

The way in which the degradation of the design parameters affects the performance characteristic is supposed to be established by a functional relationship. The ROMDA concept attempts to predict the behaviour of the performance characteristic over time by superimposing the degradation of the design parameters on the performance characteristic. This results in the underlying functional relationship and the expectation of the behaviour of the performance characteristic over time.

The resulting functions enable the possibility to predict reliability and TTF based on the specification limits. Moreover the use of design parameters make it possible to find the optimal design parameter settings that minimize product variance and maximize Time-To-Failure.

The next section, called Profound concept description, will go into more detail on how the concept is executed and what mathematical relationships need to be established before the results can be used for reliability prediction and optimization.

### § 3.2 Profound concept description

The previous section stated that the first step in the concept is to find the most dominant failure mode for a product population. The best way of doing this is by means of support from field data. Field data can not only tell us which failure mode occurs most, but just as important, proves that a

certain part of the product can fail or deteriorate. In case it is impossible to find sufficient and reliable field data, the most dominant failure mechanism can be estimated by means of Failure Mode and Effects Analysis (FMEA) [34]. FMEA makes use of information such as field data (if possible), knowledge and experience of engineers and experiences with past products and models. In order to make FMEA applicable to the objective that it has in this concept, the way of performing FMEA should be adjusted with some extra criteria. Section 4.2 will elaborate on how this should be done.

When the most dominant failure mode is found, the performance characteristic for this failure mode should be identified. Subsequently, the design parameters and noise factors that could possibly cause or affect the degradation or value of the performance characteristic should be identified.

The next step in the concept is to verify whether these identified design parameters and noise factors actually do have effect on the performance characteristic. This can be achieved by means of Design Of Experiments (DOE.) [33], where it is verified if a variation in level setting of the DP's has effect on the value of the PC. This type of rough DOE is also referred to as Response Surface Method.

For the remaining design parameters an accelerated degradation test needs to be set-up to describe the degradation of the DP's and to see whether the value of the PC changes consequently. The concept uses accelerated degradation testing in order to reduce time-to-market. The DP's of a product population can deteriorate over time in three different ways (see fig 3.2). The first possibility is that only the mean of a design parameter changes (a), the second is that only the variance of the design parameter changes (b) and the third possibility is that both the mean and the variance change.

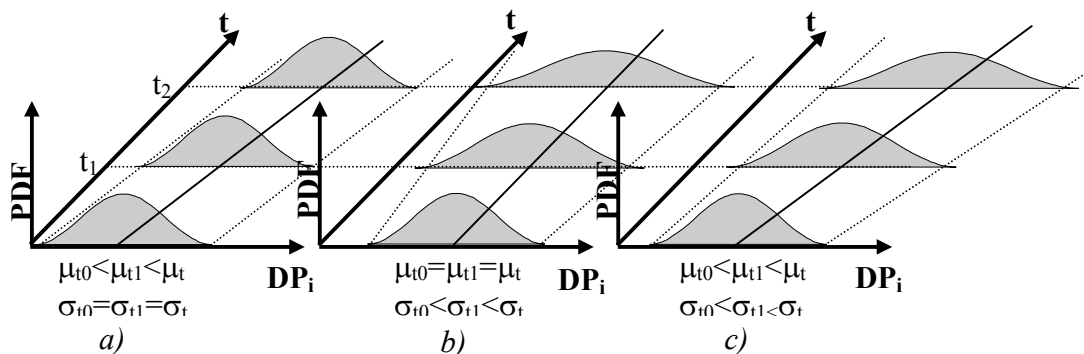


Figure 3.2: Three possible degradation profiles of the design parameters  $DP_i$

- a) Shift in mean
- b) Variance change
- c) Both shift in mean and variance change

In order to verify to which degradation profile the subjected product population belongs unit-to-unit information must not only be available on new products, but also on aged products. This information can be obtained through the use of reliable field data or by degradation testing multiple units.

This phase will result in the description of the degradation of the design parameters with time. As mentioned degradation can be perceived by a change in the mean of the DP and a change of the variance of the DP.

$$\mu_{DP}(t) = f(\mu_{DP(0)}, t) \quad (eq.3.1)$$

$$\sigma_{DP}^2(t) = f(\sigma_{DP(0)}^2, t) \quad (eq.3.2)$$

The next step is to describe a functional relation between the PC and its dominant DP's. When no physical functional relationship is known in literature, this can be done by means of Design Of Experiments. Here the design parameters are manipulated to represent the degradation of a product population over time. This results in the behaviour of the performance characteristic for the product population. The mathematical relationship that can be derived from this is a description of the performance characteristic as a function of its design parameters.

$$PC(t) = g(DP_1(t), DP_2(t), \dots, DP_n(t)) \quad (eq.3.3)$$

where n is the number of different dominant design parameters that the value of the PC depends on.

The performance characteristic at time t=0 has a functional relationship with its design parameters at t=0. In mathematical form this looks as in equation 3.4 and 3.6. Note that there may be more than one performance characteristic for the product (population).

$$\mu_{PC_j} = h_{1j}(\mu_{DP_{10}}, \mu_{DP_{20}}, \dots, \mu_{DP_{n0}}, \sigma_{DP_{10}}^2, \dots, \sigma_{DP_{n0}}^2) \quad (eq.3.4)$$

$$\sigma_{PC_j}^2 = h_{2j}(\sigma_{DP_{10}}^2, \sigma_{DP_{20}}^2, \dots, \sigma_{DP_{n0}}^2, \mu_{DP_{10}}, \dots, \mu_{DP_{n0}}) \quad (eq.3.5)$$

This functional relationship in combination with the degradation of the dominant design parameters over time result in the description of the performance characteristic over time. When the substitution of equation 3.1 in equation 3.4 and equation 3.2 in equation 3.5 is made, one obtains the function for the performance characteristic over time:

$$\begin{aligned} \mu_{PC_j}(t) &= h_{1j}(\mu_{DP_1}(t), \mu_{DP_2}(t), \dots, \mu_{DP_n}(t)) \\ &= h_{1j}[g_{11}(\mu_{DP_{10}}, t), g_{12}(\mu_{DP_{20}}, t), \dots, g_{1n}(\mu_{DP_{n0}}, t)] \quad (eq.3.6) \end{aligned}$$

$$\begin{aligned} \sigma_{PC_j}^2(t) &= h_{2j}(\sigma_{DP_1}^2(t), \sigma_{DP_2}^2(t), \dots, \sigma_{DP_n}^2(t)) \\ &= h_{2j}[g_{21}(\sigma_{DP_{10}}^2, t), g_{22}(\sigma_{DP_{20}}^2, t), \dots, g_{2n}(\sigma_{DP_{n0}}^2, t)] \quad (eq.3.7) \end{aligned}$$

With this combination of functions, it is possible to predict the value of the performance characteristic and hence at any time determine the system's performance regarding this PC. When the specification limits of all the identified performance characteristics are known we can calculate and predict the product's reliability by the following function [33]:

$$R(t) = \prod_{j=1}^m \Pr[LSL_j \leq PC_j(t) \leq USL_j] \quad (eq.3.8)$$

where  $LSL_j$  and  $USL_j$  are the lower and upper specification limit for performance characteristic j.

In case the performance characteristic is determined (or assumed) to be normally distributed, reliability can be estimated as follows [35]. First, estimate reliability if the product fails when  $PC_j \leq LSL_j$ , then

$$R(t) = 1 - \Pr[PC_j(t) \leq LSL_j] = 1 - \Phi_{norm} \left[ \frac{LSL_j - \mu_{PC_j}(t)}{\sigma_{PC_j}(t)} \right] \quad (eq.3.9)$$

Subsequently, reliability is estimated if the product fails when  $PC_j \geq USL_j$ , then

$$R(t) = 1 - \Pr[PC_j(t) \geq USL_j] = \Phi_{norm} \left[ \frac{USL_j - \mu_{PC_j}(t)}{\sigma_{PC_j}(t)} \right] \quad (eq.3.10)$$

Taking both specification limits into consideration, reliability becomes:

$$\begin{aligned} R(t) &= \Pr[LSL_j \leq PC_j \leq USL_j] \\ &= \Phi_{norm} \left[ \frac{USL_j - \mu_{PC_j}(t)}{\sigma_{PC_j}(t)} \right] - \Phi_{norm} \left[ \frac{LSL_j - \mu_{PC_j}(t)}{\sigma_{PC_j}(t)} \right] \quad (eq.3.11) \end{aligned}$$

Mean Time To Failure can now be estimated by means of equation 3.12.

$$MTTF = \int_0^{\infty} R(t) dt \quad (eq.3.12)$$

A final step in the ROMDA concept is to optimize the product population with regard to robust reliability. This may be done by means of a combination of parameter design and Robust Design as performed by Van Hoorn [11] on the Thermostat example in [15]. This resulted in a significant improvement of reliability and robustness.

### § 3.3 Summary & discussion

In summary the concept is focused on obtaining five concept elements before optimization can take place. First of all it seeks to find the dominant failure mode of a product population. Second, it needs to determine the factor that represents this failure mode, the performance characteristic. Subsequently the dominant design parameters need to be identified. These are the most important parameters for which their degradation affect the value of the Performance Characteristic and hence are cause of the failure mode. Next to the design parameters also noise factors that affect the PC need to be identified. The fourth element is the description of the degradation behaviour of the design parameters. And the final element is the description of how the design parameters influence the performance characteristic.

In summary:

- ⇒ **Dominant failure mode of a product population**
- ⇒ **Performance Characteristic that represents the failure mode**
- ⇒ **Dominant design parameters + noise factors that influence the Performance Characteristic**

⇒ **Description of the degradation behaviour of the Design Parameters**

$$\mu_{DP}(t) = f(\mu_{DP}, t)$$

$$\sigma_{DP}^2(t) = f(\sigma_{DP}^2, t)$$

⇒ **Description of the influence of the Design Parameters on the Performance Characteristic**

$$\mu_{PC} = f(\mu_{DP_1}, \mu_{DP_2}, \dots, \mu_{D_n})$$

$$\sigma_{PC}^2 = f(\sigma_{DP_1}^2, \sigma_{DP_2}^2, \dots, \sigma_{DP_n}^2)$$

**Discussion**

The concept that is described above provides the possibility to model and predict the lifetime and reliability of products. In contrast with conventional reliability prediction methods that use failure time data, it uses observation of physical degradation. Therefore it focuses on the subpopulations that fail as a result of wear out. These are the phases two and four of the roller coaster curve. Relating this back to the discussed reliability problems of section 2.2 the problems to which the concept applies may be categorized by means of the three dimensions ‘time’, ‘specifications’ and ‘statistics’ [19]. The ROMDA concept, as mentioned only applies to products that fail as a result of degradation, therefore the factor ‘time’ is relevant. With regard to the dimension ‘specifications’ it can be said that the concept applies to both hard and soft failures as defined in section 2.2. For the dimension ‘statistics’ it can be said that the concept has the ability to distinguish between products and users.

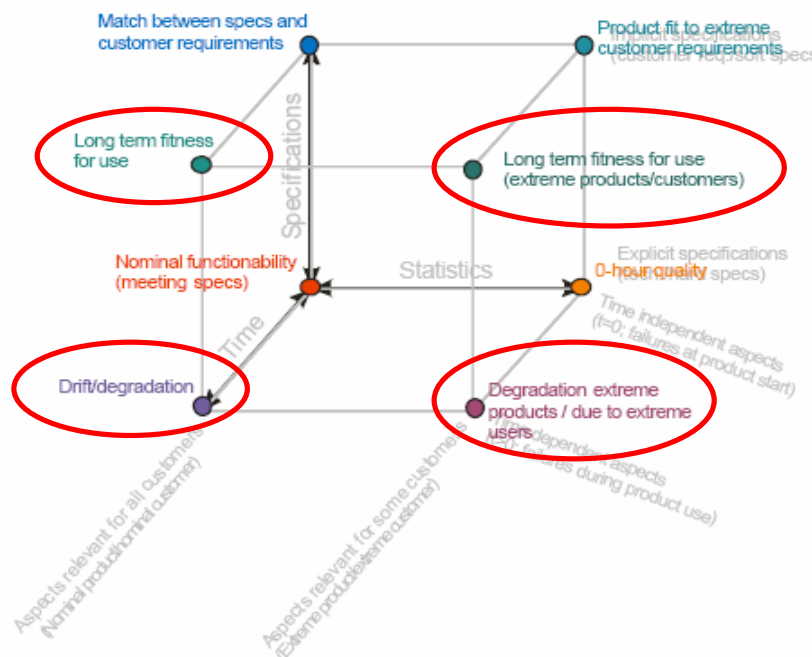


Figure 3.3: Application of the ROMDA concept to reliability problems

Figure 3.3 shows that this combination for three dimensions indicates that the ROMDA concept may be applied to all categories of reliability problems that are affected by time. Note that it does not apply to reliability problems where the technical specification limits are not exceeded.

The concept provides the possibility to model the degradation of sub-systems or even entire products as a result of the identification and modeling of its dominant failure mechanism and the factors that influence this failure mechanism. Contemporary literature only goes as far as providing degradation estimations on components or non-complex products. Modeling reliability by means of degradation of components provides a better understanding of the failure mechanisms and allows for direct application of engineering knowledge. As reliability is modeled as close to the source as possible it provides more credible and accurate estimations than failure time data.

Modeling performance degradation can be complex because it may be influenced by more than one underlying degradation process [25]. In the ROMDA concept these underlying degradation processes are the design parameters. Overlooking one of the design parameter can have great consequences for the validity of future experiments and predictions.

Another strong point of the concept is that it provides a way to obviate a possible lack of field data. This makes the concept especially useful in the product development phase or in situations where the product has just recently been introduced to the market.

The idea of relating a performance characteristic to its design parameters creates the opportunity for optimization of product reliability by means of the identification of the optimal design parameter settings. The possibility of reliability prediction also makes the concept applicable for making optimal re-use decision. Thirdly, because the value of the performance characteristic is related to the degradation of its design parameters, it provides us with the opportunity to make optimal decisions for preventive maintenance of the design parameters.

The results that were achieved by Van Hoorn in his master thesis prove the theoretical functioning and possibilities of the concept in a simulated environment. The next chapter discusses the Roadmap that was developed to put the concept into practice. It provides for a predefined plan of action that should lead to the most efficient and accurate implementation of the ROMDA concept. Furthermore the chapter describes the product module on which implementation has taken place and the first phases of the concept that had already been performed before the research described in this thesis.

---

## Chapter 4 Concept Roadmap

### § 4.1 Introduction

After these first three chapters of introduction and theory, it is time to put the concept to the test. The theory sounds promising and so do the results from the simulation experiments by Van Hoorn. But can the concept be successfully implemented for a real product or system that does not necessarily obey the laws of statistics and reliability theory. Or to refer to the research question of this thesis:

*Is it possible to implement the concept as proposed by Van den Bogaard into practice and apply it to design optimization, preventive maintenance and re-use?*

In order to test and possibly prove the potential of this concept, the translation to a real product environment needed to be made. This project was started in cooperation with Flextronics, Venray, Eurandom, Eindhoven and later also Océ, Venlo. The work that was done in this thesis was mainly collaboration between the Technische Universiteit Eindhoven and Flextronics. Flextronics provided the products and engineering knowledge on these products, while the Technische Universiteit Eindhoven provided the theoretical concept and the roadmap for implementation.

Past work on the Finisher module resulted in a prediction model for the stagnation of a stepper motor as result of the increase of mechanical system load. Here time was simulated by means of parameter setting in a Design of Experiments.

During this thesis improvements were made with regard to the set-up of Van Hoorn's experiments. Changing the order in which certain experiments should be conducted leads to better results regarding reliability and Time To Failure prediction. This accumulated in a Roadmap or protocol that, when followed, should lead to a logical and efficient structure that facilitates the implementation of this project and future projects. The roadmap focuses mainly on the practical work that has to be done regarding the product or product module on which the concept is applied.

In the remainder of this chapter the Roadmap will be described and explained, indicating the reasons for conducting certain phases and elucidating the chosen order of execution. The next section will focus on the product under study, the Finisher module of a photocopier. Its function, functioning and physics of failure shall be described in detail. From here the performance characteristic and design parameters are derived and the chapter will conclude with a discussion.

### § 4.2 Description of the Roadmap

This section provides the roadmap for the execution of the ROMDA concept that was applied during this master thesis project. The roadmap serves as a protocol that needs to be followed during implementation. It is constructed in such a way that it leads to a logical and efficient foundation and structure that maximizes the possibilities of the concept.

First the necessary concept elements (section 3.3) that need to be obtained before it is possible to make predictions on reliability, predictions on TTF and optimize the design are repeated. These were as follows:

- ⇒ **Dominant failure mode of a product population**
- ⇒ **Performance Characteristic that represents the failure mode**
- ⇒ **Dominant design parameters that influence the Performance Characteristic**
- ⇒ **Description of the degradation behaviour of the Design Parameters**

$$\mu_{DP}(t) = f(\mu_{DP(0)}, t)$$

$$\sigma_{DP}^2(t) = f(\sigma_{DP(0)}^2, t)$$

- ⇒ **Description of the influence of the Design Parameters on the Performance Characteristic**

$$\mu_{PC} = f(\mu_{DP_1}, \mu_{DP_2}, \dots, \mu_{DP_n})$$

$$\sigma_{PC}^2 = f(\sigma_{DP_1}^2, \sigma_{DP_2}^2, \dots, \sigma_{DP_n}^2)$$

In the follow-up of this section all the phases of the Roadmap will be mentioned. Nevertheless, this report shall only elaborate on the essential elements that the concept wishes to obtain. The complete Roadmap will thus not be presented in this chapter.

The Roadmap for the reliability concept consists of eleven phases. Figure 4.1 shows the outline of the roadmap, which will be related to the elements described above. Subsequently they shall be discussed and explained.

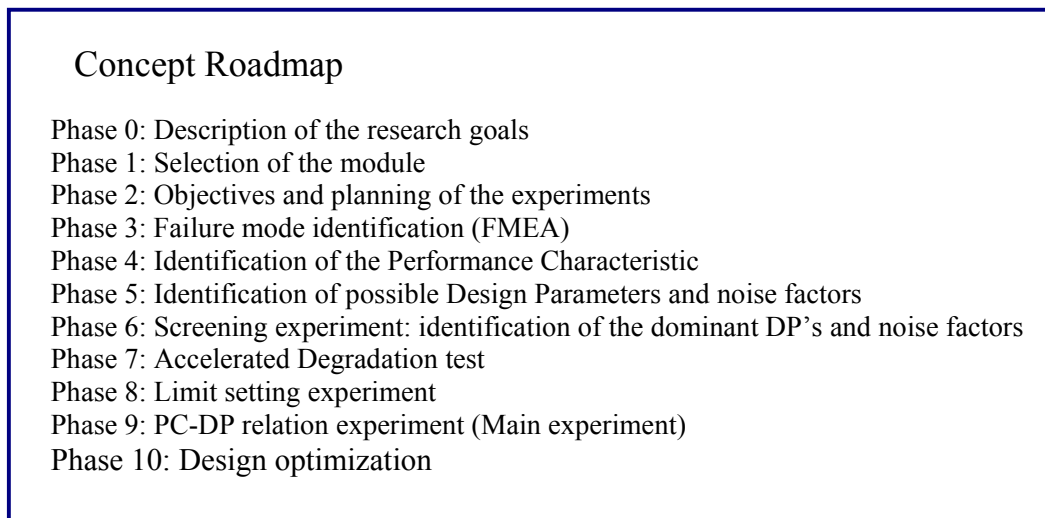


*Figure 4.1: Concept Roadmap*

Now the phases of the Roadmap are related to the coinciding elements that are necessary for the concept. In other words, these phases describe which activities need to be performed in order to successfully obtain or achieve the elements described above. Minor attention will be given to phases zero to three, as these phases were all performed in past times in the project and do not apply to this thesis.

In the first three phases (zero to two) the foundation for the remains of the project is laid. As probably every Roadmap, this one starts with the description of the goals of the concept and the research (**phase one**). Naturally every step that is taken should be made with the achievement of these research goals in mind. The **second phase** considers the selection of the module or system

that will be studied during the project. This may be done by means of FMEA, where the following four factors may be the criteria:

- *Economical aspects for now and the future*
- *Diversity in failure-mechanisms in the module.*  
The more different failure mechanisms the system has, the more complex it will be to understand and study. The choice of a too complex system should be prevented.
- *Frequency/Intensity of failures per module*  
This factor serves in order to prevent the selection of a module that is not or hardly subject to failure.
- *Re-cycling/Re-use/Preventive Maintenance/New-build possibilities*

### **Dominant failure mode of a product population [phase 3]**

**Phase three** was also performed in a previous period in the project. This is a paramount phase, because forgetting a failure mechanism may have consequences for future experiments. This master thesis proposes an alteration to the standard method for conducting Failure Mode and Effects Analysis (FMEA). First of all it needs to be made time-dependent. Therefore a column needs to be added that questions if a factor degrades and thus is *time-dependent*. A column that questions if this occurs *gradual, rapid* or *catastrophic* [9] and a column that questions if a factor is *measurable* may also be added. During this thesis it is assumed that the FMEA was conducted in an appropriate way and that the outcomes were correct. Section 4.3.1 contains the outcome of this phase.

### **Performance Characteristic that represents the failure mode [phase 4]**

As a result of the FMEA the performance characteristic may be deduced in **phase four**. The performance characteristic is a parameter that describes how well the function related to the dominant failure mode performs. Section 4.3.2 presents the results of this phase for the product module of section 4.2.

### **Dominant design parameters that influence the Performance Characteristic [phase 5 & 6]**

The parameters that possibly influence the value of the performance characteristics and whose degradation cause the failure of the product's function, can be derived from the FMEA. This coincides with **phase five**. However, these parameters that are provided by the FMEA are not necessarily of influence. On the contrary; the FMEA is performed in order not to accidentally forget any possible influence. Therefore a simple Screening experiment needs to be performed in **phase six** that identifies the design parameters and possible noise factors that affect the performance characteristic. This is done by means of the Response Surface Method. More details on how it is performed are provided in [11]. The outcomes of phase five and six for this thesis are presented in section 4.3.3.

A more detailed description of the phases zero to six can be found in [36].

### **Description of the degradation behaviour of the Design Parameters [phase 7]**

Description of the degradation behaviour of the dominant design parameters will be obtained by means of an Accelerated Degradation Test. The reasons for conducting the degradation test in this phase are the following:

#### *1) Check for degradation*

As the failure modes are identified by means of a qualitative tool as FMEA, it cannot simply be assumed that the identified failure mode does occur. Therefore it should be checked to see if degradation actually does take place.

2) *Determination of the shape of the curves*

A degradation test cannot always be conducted until product failure. Sometimes it takes a lot of time for the product to fail, or the product's life cannot easily be accelerated. Therefore it may be necessary to determine the curve's shape (linear, concave, convex) in order to be able to extrapolate its function till it exceeds specification limits.

3) *Description of the degradation paths*

The most important function of the life test experiment is the description of the degradation paths of the factors as a function of time. These functions are paramount in order to implement the concept. The results of this phase are the following functions:

$$\mu_{DP}(t) = f(\mu_{DP(0)}, t)$$

$$\sigma_{DP}^2(t) = f(\sigma_{DP(0)}^2, t)$$

4) *Input for further experiments*

The final reason for conducting the life test is, that it serves as an input for the PC-DP relation experiment or main experiment. The parameter settings that are used for the DOE in the main experiment should be derived from the life test. The reason for this is the following. The influence that the design parameters have on the performance characteristic may differ or change over time [11]. In order for the main experiment to result in a proper description that relates the design parameters to the performance characteristic, the settings for its DOE should be made corresponding with time in order to equally spread the influences over time.

The number of units that are tested should be as many as is economically, resource wise and time wise possible. Using more than one unit provides the possibility of taking unit-to-unit variability into account in the main experiment (phase 9). The set-up and performance of the Accelerated Degradation Test has been the subject of a fair part of this thesis. The test and its results will therefore be extensively described in chapter five.

### **Description of the influence of the Design Parameters on the Performance Characteristic [phase 8 &9]**

Proper execution of the phases eight and nine should lead to the description of the Performance Characteristic as a function of its Design Parameters.

$$\mu_{PC} = f(\mu_{DP_1}, \mu_{DP_2}, \dots, \mu_{DP_n})$$

$$\sigma_{PC}^2 = f(\sigma_{DP_1}^2, \sigma_{DP_2}^2, \dots, \sigma_{DP_n}^2)$$

In order to obtain these relationships a Design of Experiments will be conducted in **phase 9**. Here the influence of the DP's on the PC is determined by setting the values of the DP's. Therefore it was decided to take the average of these influences over product life. This will be achieved by performing three DOEs. One with the Design Parameter levels at  $t=0$ , one with DP levels just before the failure mode occurs and one with DP levels of halfway the module's life.

In order to get to know the maximum settings of the DP levels just before the failure mode occurs, a Limit setting experiment (**phase 8**) needs to be performed first. Here the failure mode is simulated as a result of a change of the DP's.

The values of the DP's halfway the degradation process are obtained through the degradation functions that result from phase seven. For this the limits of at least one DP needs to be known.

During Van Hoorn's master thesis the experiments of phase 8 and 9 were already performed. However, for the PC-DP relation experiment the input of a Degradation Test was not used. Therefore the influence of the DP's on the PC is not in concordance with time, which may possibly affect the design parameter settings and hence accuracy of the experiments.

This Roadmap plans the ADT before the PC-DP relation experiment and thus makes it possible to use degradation information as input for this second experiment. Thereby probably increasing the accuracy of estimation of the PC as a result of the values of its DP's.

When these elements have been obtained, phase 10, the Concept application phase, may commence. This phase is concerned with optimization of the design. Therefore the “optimal” values for the design parameters need to be identified. Optimal in this case means that the MTTF should be as large as possible while minimizing the variance of this MTTF.

The following sections of this chapter deal with the implementation of the Roadmap up to the start of this master thesis.

### **§ 4.3 Description Finisher Module**

This entire section will go into depth on the object of study, on which the research for this thesis was conducted, the so-called Finisher module (with High Capacity Feeder). We start by giving the reader an idea of what this module actually does. After which we describe the results of the FMEA that was conducted, leading to an explanation of the *physics of failure* of this failure mechanism. From this the performance characteristic and design parameters for this PC are described respectively. Finally the last section will lead out this chapter by presenting the results of Van Hoorn. These will be discussed, giving motivation for conducting the new experiments in order to fulfill and improve this model.

The Finisher module that is used is part of a photocopier or printer. It is, as a matter, the last part of the photocopier through which the paper is transported. In figure 4.2 one can see more clearly what the module looks like.



*Figure 4.2: The Finisher module*

The Finisher module has basically four functions. It makes sure that the paper is transported out of the photocopier. When the paper nears the end, there is the possibility of the paper coming out of the top tray or main tray, depending on the customer's wishes. When the main tray is chosen, a Tamper makes sure that the paper is accumulated in neatly piled stacks. This main tray needs a Tamper for A4 size paper, because its exit is wider than that of the top tray. This is because of its capability to process A3 size paper. A second stack of paper can be moved further than the first stack in order to distinguish between sets. The main tray also has the possibility to move up and down in order to neatly collect the next sheet of paper. The fourth function the Finisher has is the possibility to staple. This can be done at the top corner of the paper stack; this is done by the fixed stapler and at various other places along the length of the sheets, done by the moving stapler. During the measurements, a so-called High Capacity Feeder (HCF) was fixated to the Finisher in order to feed the Finisher with sheets of 80 grams A4 paper that it could process.

### Failure Mode

As very few failures of the Finisher module have been observed in the field, the identifications of the failure modes for this module were dominantly based on engineering knowledge and intuition. Based on a FMEA and on past experiments conducted at Flextronics the paper transport within the Finisher module was selected as the function of the system that would be studied with regard to failure. Paper transport, which is provided for by the nip motor, is one of the main functions of the Finisher module. In the following section the *physics of failure* of this paper transport system shall be discussed in more detail.

#### § 4.3.1 Failure mode

As mentioned in the previous section, the paper transport in the Finisher module is provided for by the so-called nip motor, which is controlled by the Printed Wire Board Assembly (PWBA.). The NIP motor is a stepper motor that drives the shafts in the system that facilitates the paper transport. The nip motor is connected to these shafts by a belt. Each shaft has rubber rolls on it that has friction with the paper and hence gives thrust to a sheet of paper. Figure 4.3 shows the rolls-mechanism system of the paper transport. The nip motor connects to all the shafts by means of two belts. The lower belt provides for the transportation to the main tray and the upper belt does this for the top tray.

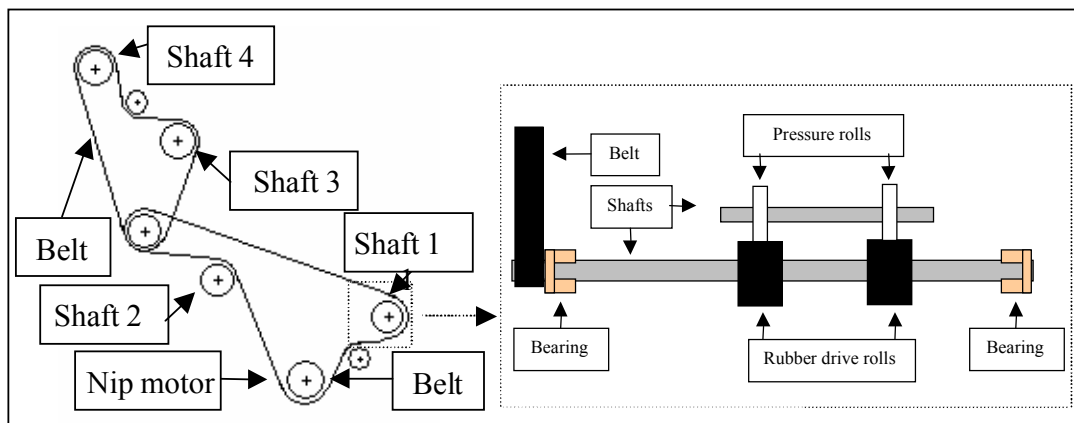


Figure 4.3: Rolls mechanism driven by nip motor

Previous experiments and research [37] has shown that certain components within this transportation system do not or hardly deteriorate with time. A conducted degradation test on the deterioration of the rubber rolls showed no significant deterioration. Likewise, degradation tests subjected to the stepper motor did not result in degradation. Neither were there any known failures in the field regarding this stepper motor. These two components were therefore assumed to not degrade.

The factor that was presumed to lead to failure of the system was increasing friction between shafts and bearings, leading to a higher mechanical load. This friction is caused by contamination and deterioration of the bearings.

#### Mechanical load on the system

The purpose of bearings is to support revolving shafts or axles in space, enabling them to rotate or oscillate freely and to carry the loads applied to them. With respect to the type of friction in them, bearings are classified as sleeve bearings or bushings (sliding friction) and antifriction, or ball and roller bearings (rolling friction) [38]. The types of bearings that are used in the paper transport

system of the Finisher are *sleeve bearings*. Sleeve bearings are supports of revolving components operating under conditions of relative sliding motion of the journal surface over the bearing surface. Friction within these bearings can increase due to loss of lubrication, a change in the properties of the lubricant, corrosion or a change in the mechanical properties of the bearing itself as a result of fatigue [38].

Experiments have shown that it is possible to provoke the failure of the paper transport function by artificially increasing the load on the nip motor. This increase in load eventually leads to a stagnation of the motor and thus of the paper transport.

#### § 4.3.2 Performance characteristic

A first gut feeling could tell us that an increase in load on the system's shafts and bearings would lead to a reduction of the paper speed. Results of the *Main tray experiment* however showed that this variable remained constant as the load on the system was increased. This was due to the way that a stepper motor works which keeps its speed at a constant level. Therefore another indicator had to be found that changed as a result of the system load. Hence the factor to measure is the factor that changes in order to keep the nip motor speed at the same level.

When the load on the stepper motor is increased, a change occurs in the current profile of the nip motor. The so-called *current rise time* ( $T_{pr}$ ) (figure 4.4) decreases when the load on the stepper motor increases.

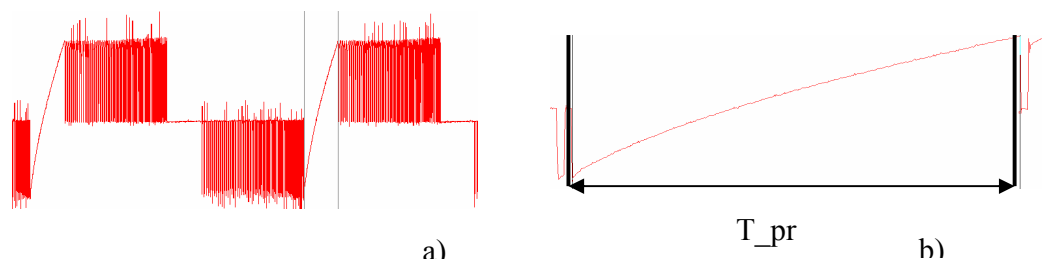


Figure 4.4: Signal of the nip motor current (a) and current rise time (b)

The physics behind this phenomenon is as follows. The nip motor is driven with a constant pulse frequency. When the load on the motor increases the speed with which the motor 'steps' from pole to pole decreases. However, this reduction in speed leads to less self-inductance and therefore to less electromagnetic force. Hence there is less force that opposes the current and this will therefore reach faster the current limit setting on the PWBA. The reduction in current rise time compensates for the slower steps of the motor, which will altogether lead to the preservation of the nominal speed.

When the value of the load on the motor gets to high, the stepper motor will no longer be able to make the next step, resulting in a stagnation of the motor and hence the stagnation of the paper transport. In the degradation experiment that is discussed in chapter five, the  $T_{pr}$  of only one of the four coils is measured. This is done because it reduces the variance of the measurements. The current rise time will from now on serve as the performance characteristic as described in chapter 3. The next section will identify the dominant design parameters that influence the value of the performance characteristic.

### § 4.3.3 Dominant design parameters

Now that the performance characteristic is defined the factors or design parameters that influence this performance characteristic need to be found. There are two criteria that these design parameters have to meet. First they have to have dominant influence on the performance characteristic and secondly they have to deteriorate over time, as a change of the design parameters causes the failure of the transport function.

This identification of the dominant design parameters was done in the Main tray experiments [39]. This resulted in three dominant influences on the  $T_{pr}$ , namely:

- Input Voltage 24V
- Mechanical load on the shafts
- Electric resistance of the Printed Wire Board Assembly (PWBA)

The 24V power supply is a factor that is kept constant by the system, unless the electric resistance of the PWBA increases. Therefore the factor Input Voltage 24V is eliminated as a design parameter.

#### ***Electric resistance of the PWBA***

The PWBA is a printed circuit board that controls practically all the sub-systems of the Finisher module. When its electric resistance increases, the PWBA “absorbs” more of the input voltage, resulting in a lower rest-voltage that is submitted to its adjusted devices. This influences the current pulse to the nip motor and hence its current rise time ( $T_{pr}$ ). The PWBA resistance is expected to increase as a result of an increase of the resistance of its contacts. The resistance of these contacts degrades as a result of fretting corrosion [40].

### § 4.4 Discussion

This chapter presented a brief description and explanation of the Roadmap in the first section. In this section it is proposed to add some extra columns to the standard way of conducting FMEA in order to make the failure mode identification process better applicable to the objectives of the ROMDA concept. As from the second section on the chapter discusses the object of study for the implementation of the concept, followed by the results of the implementation of the phases three to six of the Roadmap in section three. This resulted in the Performance Characteristic (Y) and dominant Design Parameters (X1 and X2) as presented below in figure 4.5.

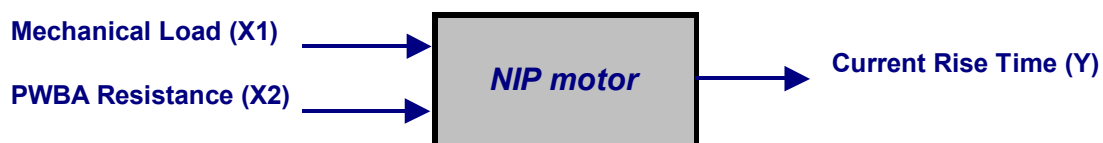


Figure 4.5: Black box representation of the design parameters of influence

Van Hoorn already came as far as performing a limit setting experiment and a PC-DP relation experiment. However in the new Roadmap that was introduced in this chapter it was decided to perform these phases after an Accelerated Degradation Test. The reason for this is that this order leads to correct time-related factor settings and hence a more accurate PC-DP relation function. Nevertheless the results of his experiment have served and may serve as a good guide for what to observe in the Degradation Test of phase 7. Therefore this model is presented here nonetheless.

$$\mu_Y = 595.58 - 2.68\mu_{X_1}(t) + 31.76\mu_{X_2}(t) - 0.79\mu_{X_1}^2(t)$$

This model shows that the expected increase of the PWBA resistance will result in a higher current rise time, while the expected increase of the Load will result in a lower value. The design parameter settings of this experiment were made based on two assumptions. The first was that degradation over time would be linear for both Design Parameters and the second was the amount of increase of the PWBA resistance over life. Naturally it may not be said that these assumptions represent reality. Therefore an Accelerated Degradation Test (ADT) had to be performed in order to verify if the assumptions were correct or not. In case these turn out not to be correct, the ADT will be used to estimate the proper design parameter settings for a possible improvement to the model above.

The next chapter deals with the set-up and the results of the ADT. Chapter five is probably the most important chapter of this thesis as it captures the time aspect that is of vital importance for reliability predictions and therefore also to the ROMDA concept. Moreover it was the most time consuming experiment that had to be conducted. The results of the chapter are degradation models of the design parameters and back-up parameters.

---

## Chapter 5 Accelerated Degradation Test

### § 5.1 Introduction

In this section the accelerated degradation test (ADT) that was conducted on the Finisher module will be described. In the following section the studied functions of the Finisher will be discussed one at a time. The assumed failure mechanisms of these functions shall be explained and from there the deduced parameters for measurement will be discussed. As a consequence of their failure mechanism there were expectancies regarding their degradation, which will also be discussed in section two. The set-up and necessary decisions before the test could be started are specified in section three. Then in the fourth section the final tests results are presented. Subsequently the degradation paths of the factors are modeled. And finally the chapter is concluded with a discussion on the results and the execution of the test.

In order to refresh the reader's memory the reasons of section 4.2 for conducting this experiment are briefly repeated.

- 1) *Check for degradation*
- 2) *Determination of the shape of the curves*
- 3) *Description of the degradation paths*
- 4) *Input for further experiments*

Not only the selected parameters of the paper transport function were measured during this ADT. Besides this paper transport function it was also chosen to measure parameters of the *stapler function* and the *tray election function*. The reasons for this choice are explained in the following section.

During the test only one module was used. Naturally it would have been better from a statistical point of view to use more than one module. Unfortunately the capacity of the research laboratory was not large enough to cope with the simultaneous execution of more than one of such a diverse module. In comparison to the simple systems that were usually subjected to such tests in literature, such as certain light sources, small components or metal parts, the Finisher module is an extensive and complex system that consists of conflicting and interacting parts. This same complexity is what makes the degradation test and the reliability concept so unique for their kind. Another argument that partly justifies the use of only one module is the experience from literature that performance characteristics for a product population usually deteriorate following more or less the same degradation path.

The third argument that partly justifies the use of only one module is the fact that following experiments for relating the performance characteristic to its design parameters provide the possibility to obviate the lack of field data, even though they do not compensate for a possible increase of unit-to-unit variation.

The fourth and final argument concerns the research question. The first part questions whether it is possible to implement the concept into practice. Therefore dealing with one unit or multiple units has no effect on the answer to this question. This could only affect the settings of the main experiment.

Before moving on to the following section one very important assumption needs to be made. It is assumed that the shapes of the degradation models of the parameters for this module are of the same shape for these parameters in any other Finisher module.

---

## **§ 5.2 Parameters and expectations**

This section first describes and explains the factors that were measured. Thereby the reader is presented with expectations of the time dependent behaviour of these factors. The three sub-systems that were measured are for the paper transport, the stapler function and the tray election (see section 4.3). The reason for choosing these sub-systems is the fact that previous experiments (December 2002 experiments) have resulted in unit-to-unit data on new and field returned Finishers. Moreover this provided the possibility to underpin our expectations on the degradation of these systems. But the most important reason for this choice was the possibility of having back-up systems that could be modeled when the ADT did not result in degradation of the main parameters. For each of these systems the parameters that should represent their degradation were measured. We start by describing the paper transport, then we turn to the stapler function and we end this section with the description and expectations for the tray election function.

### **Paper transport**

The factors that were measured for the paper transport function are the ones that are described in section 4.3. These are the Performance Characteristic current rise time ( $T_{pr}$ ) and its design parameters, PWBA Resistance and Load. The load on the system is expected to increase with time and use as a consequence of contamination and the friction between the sleeve bearings and the shafts (see section 4.3.1). The resistance of the PWBA is expected to increase due to fretting corrosion of its connectors (see section 4.3.3). In his article Malucci [41] shows a graph of the increase of corrosion of connectors as a result of the number of deformation cycles. This graph shows a convex increase of corrosion and hence of connector resistance. In other words, resistance should increase slowly in the first part of life and then increase faster and faster due to fretting. However, in this experiment not the resistance of one connector is measured, but the total resistance of many connectors on the PWBA.

### **Stapler function**

The stapler function of the Finisher module consists of two staplers, a fixed stapler and a moving stapler. These are also referred to as M6 for the moving stapler and M7 for the fixed stapler. The fixed stapler (M7) has the possibility to staple the corner of a package of sheets and the moving stapler (M6) does the same along the length of the package of sheets. For both staplers the current profile and stapling time were measured.

The stapling time is the time it takes for a stapler to put a staple in a package of fifty sheets of paper. The number of fifty sheets is taken because this is the maximum number of sheets that can be stapled with the used stapler. Hence failure of the stapling function will be defined as the situation in which the stapler is no longer able to staple this amount of staples correctly. The stapling time is measured two times for the moving stapler M6 at different stapling locations. In the current profile three current peaks are measured. These are peaks a, b and c in figure 5.1a)

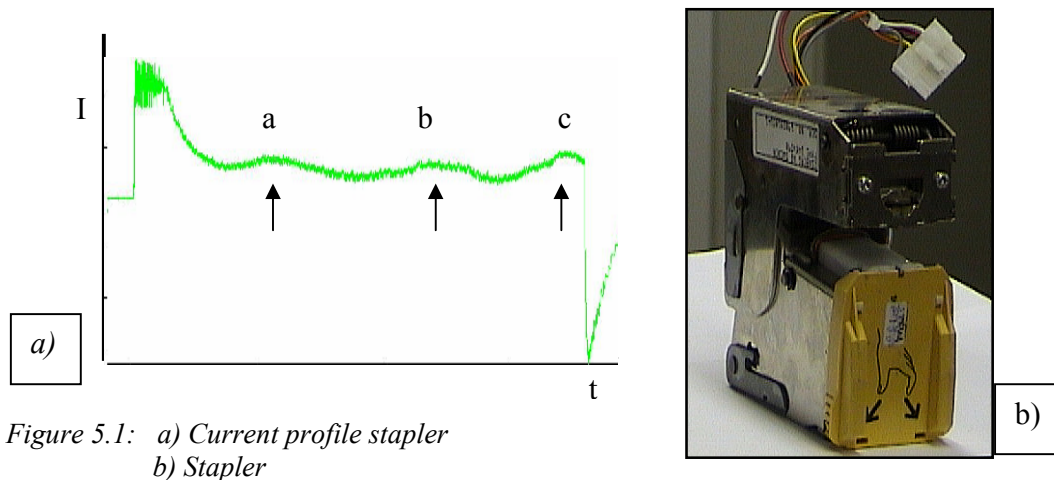


Figure 5.1: a) Current profile stapler  
b) Stapler

- ⇒ Peak a represents the current consumption of the stapler when the stapler anvil is lifted.
- ⇒ Peak b is the current consumption when the stapler stitches the staple.
- ⇒ Peak c is the current consumption when the stapler is reset to its initial position.

This curve is smoothed in order to reduce the rather large variation that occurs within the peaks.

The stapling time of the stapler depends on the number of sheets that are stapled. More sheets logically leads to a higher stapling time. Therefore it is expected that when the stapler deteriorates, it will have more trouble stapling. Hence the stapling time is expected to increase with use. This expectation seems to be supported by the data of the December 2002 experiments at first glance. However, later on during the project it was discovered that the new Finishers that were used in this experiment were different from the field returned ones. One of the main changes to the new design was a faster stapler. This made it impossible to compare the stapler factors for the new and field returned Finishers.

Regarding the current consumption of the stapler it is expected that when the stapler ages, that it will consume more energy to execute its function. This is because the so-called 'eccentric', along which movement is followed or conducted within the stapler, will deteriorate and therefore does not function as well as before. This holds for all three movements of the stapler.

### Tray election

The possibility to switch between trays is performed by the *diverter gate solenoid* also referred to as L3. A solenoid is a magnetic system that can be in only two states. When turned off it finds itself in its normal position and when it is turned on it switches to the other. The diverter gate solenoid is attached to a mechanism that makes the sheet of paper leave through the top tray or main tray. Deterioration of this system occurs through internal friction and contamination within the solenoid, caused by a diminished coating and through friction of the attached system with its surroundings. It is therefore expected that the time needed to initiate the solenoid will increase with its use. This time is the part of its current profile that is indicated by the arrows in the adjacent figure (figure 5.2).

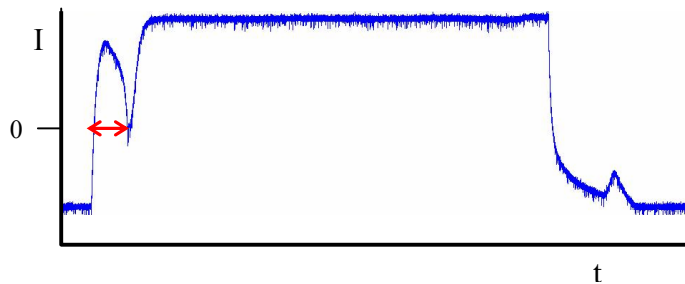


Figure 5.2: Current profile L3

Increase of friction within solenoids occurs faster when the magnetic field of the system is not homogeneous. In the succeeding section it will be explained how the degradation test for these factors was established and which important decisions had to be made before its commence.

### § 5.3 Experimental set-up

A test is only as good as its preparation. With this in mind some crucial decisions had to be made. The objective of the degradation test was to obtain degradation data that represents actual customer use. In other words we wanted to be able to relate the obtained degradation to real time, or number of device activations in this case, as this would be the time factor in the field. In total four decisions were made regarding the following features:

- Cool down time of the bearing at the motor
- Use of paper during acceleration
- Replacement of the Stapler during acceleration
- Times of measurement

In order to simulate the use of the Finisher module by a customer, the Finisher module was controlled by a computer program that made it execute its four basic functions. During actual customer use, the module would be used of and on, but not constantly. Therefore two types of intermissions were included in the cycle. The first was a very short intermission after every nineteen copies. This was done to make the motor start from standstill, having to thrust the shafts of the system when they are in rest. The second intermission was a longer one to make the module, and especially the nip motor and the paper transport shafts cool down to room temperature every now and then. The time that was needed to cool down the Finisher module at the bearings of the motor was therefore determined when it was cooled with a fan. The cool down profile is shown in figure 5.3.

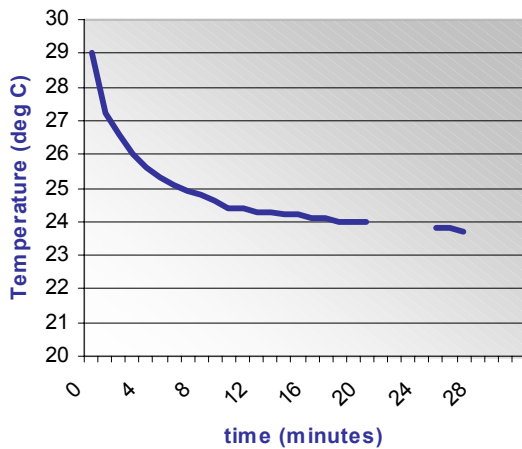


Figure 5.3: Cool down profile at motor bearing

Based on this figure it was chosen to set this second intermission at 30 minutes.

A second decision was made not to let the Finisher process paper while its degradation was accelerated. Degradation of the paper transport function was presumed to occur due to contamination and the friction between the sleeve bearings and the shafts. It was however assumed that the weight of paper had negligible influence on the sleeve bearings in comparison to the shafts themselves and that the use of paper would not lead to more contamination as a result of dust. Moreover it would have been impossible to process the enormous amounts of paper that would be produced.

As a result of the absence of paper, it was impossible to make the stapler function perform on real paper. When the stapler does not have anything to staple, its deterioration does not take place as in a customer use situation. This difficulty in combination with the possibility of internal contamination as a result of accumulating staples, led to the decision to replace the stapler cartridge by a sponge that was to represent the missing paper (figure 5.4). Hence there would be a difference between the amount of force needed to staple a staple and the amount of force needed to 'staple' the sponge. This alteration would only affect the degradation speed of peak b of the stapler. Nevertheless the shape of its degradation path will probably be the same.

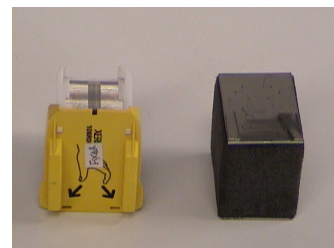


Figure 5.4 Stapler cartridge and sponge

The final decision that had to be made concerned the times or moments at which measurement would take place. As the Finisher is large system, it has various functions and components that may be active at a certain moment. These components may have interactions that affect their performance. Previous experiments on the Finisher resulted in a measurement routine that presents the active functions at five measurement times. Based on the December 2002 experiments it was investigated which functions had interactions and would hence lead to deviations of the measurements. The following table (table 5.1) shows the p-values for the interactions obtained from a Sample Mean Test. These compare the situation when a factor is measured solely and when it is measured while one or more other functions are active. A p-value larger than 0,1 indicates that there is *no* statistical difference between two samples.

Table 5.1 P-values for interactions

	T_pr (M1)	Tcusp (L3)	I peak A (M6)	I peak B (M6)	I peak C (M6)
M1+L3	0,212	0,0			
M1+M6+L3	1,37 E-10	0,0	0,165	0,923	0,138

This table implies, that Tcusp (L3) has to be measured when the L3 solenoid is the only active function. It also clearly shows that measurements on factors of the stapler are not affected by the activity of the nip motor M1 and the diverter solenoid L3. But the stapler does affect the value of the T\_pr. This has led to the following measurement scheme:

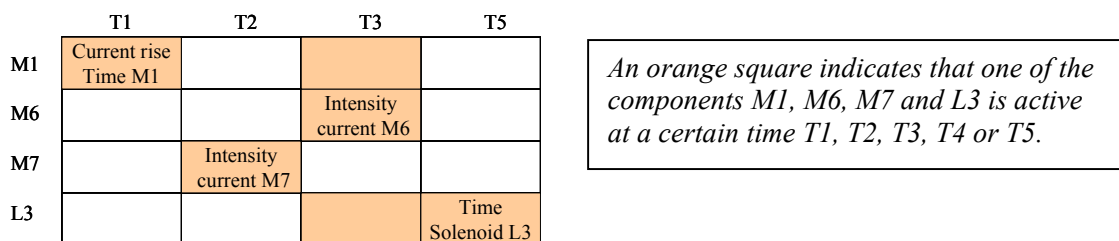


Figure 5.5: Measurement scheme

Based on these four decisions together with the objective of realizing one million copies in one month (or fifty thousand per day assuming twenty work days per month), the following measurement routine was elaborated (see figure 5.6). In practice, the measurements were conducted every two days. When measured the Finisher was loaded with A4 paper (80 grams). The produced paper sets were stapled with the normal stapler. After a test evaluation at approximately one million copies, it was decided to proceed with the test until a minimum of two million was reached. At each measurement time the Finisher was measured five times for all the factors.

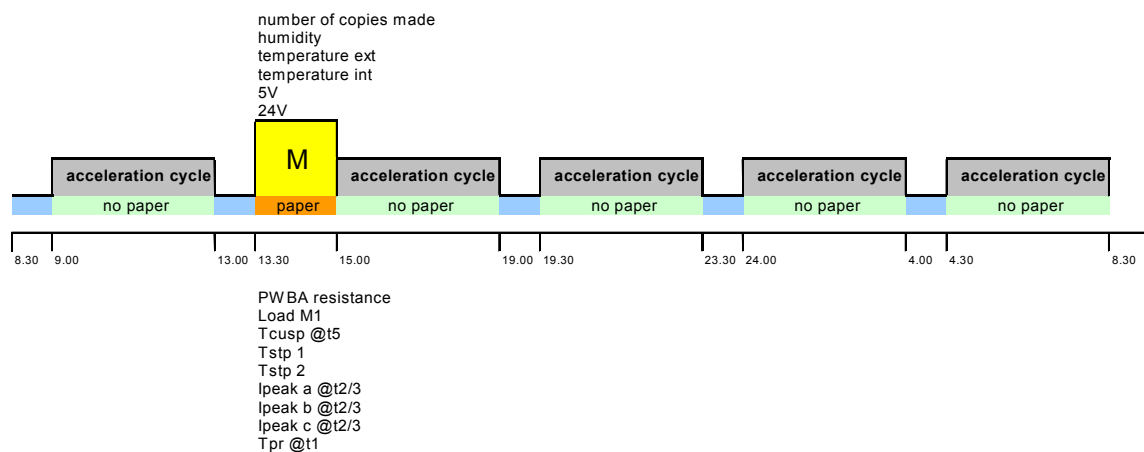


Figure 5.6: Measurement routine

### § 5.3.1 Measurement System Analysis

The vast majority of the factors that were measured had already been subject of measurement various times. These measurement systems were thus previously tested and used on test-retest variability. In order not to lose any valuable time examining all these factors, it was therefore assumed that these measurement systems were stable and predictable. Although this is unexpected, instabilities between measurements could be detected in the beginning of the degradation test when the module does not yet show wear.

Concerning the measurement of the PWBA resistance a new measurement system needed to be used. Measurements for the new PWBA for the degradation test turned out to be stable from the first measurements. However, measurements for field returned PWBAs turned out to be somewhat variable. Therefore the measurement system was fixated in some parts in order to decrease the influence of external factors. This resulted in the following stable system.

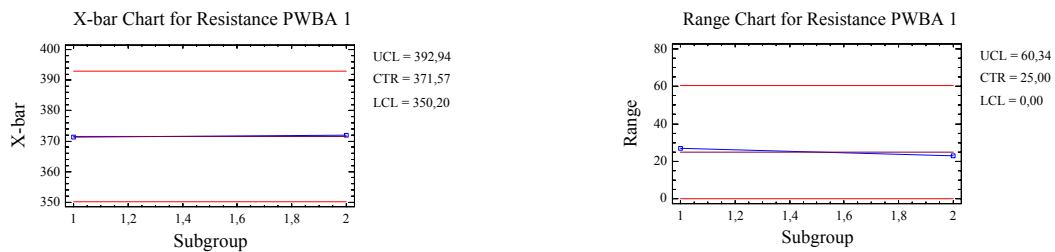


Figure 5.7: Test re-test variation for PWBA 1

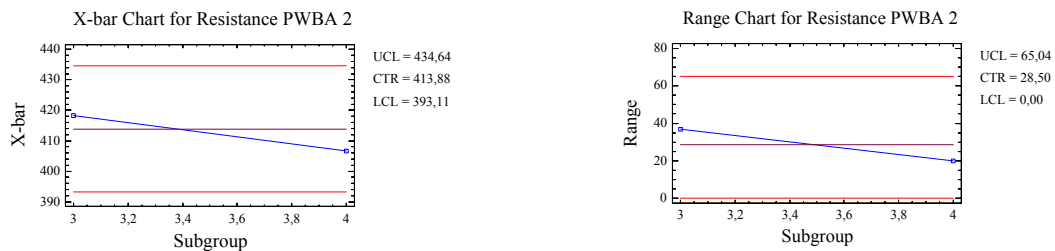


Figure 5.8: Test re-test variation for PWBA 2

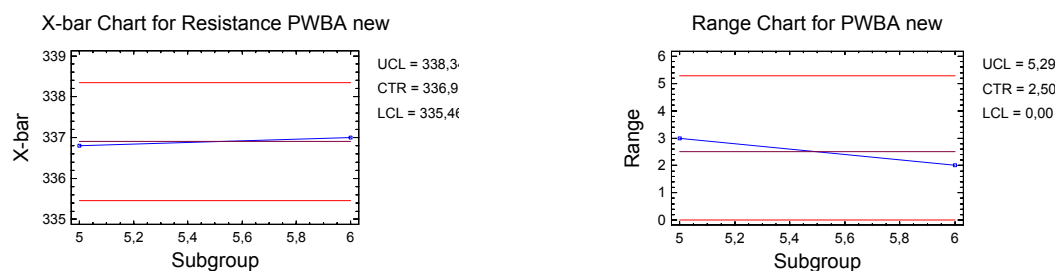


Figure 5.9: Test re-test variation for the new PWBA

The charts still show a rather large variance for the measurements of the field returned PWBA's in comparison to value the variance of the new PWBA, which is almost negligible. It is therefore assumed that this characteristic is inherent to older PWBA's. This is also supported by the values of the resistances of the two field returned PWBAs. The one with the higher value is assumed to be older and also has a higher variance.

This stable system cleared the path to start the degradation test. In the next section the results so far are presented for the measured factors. By means of X-bar charts and Range charts it will be decided whether or not to model the degradation of the measured factors.

## **§ 5.4 Test results**

As the previous section already mentioned, the Finisher was measured approximately every two days. Five measurements were then conducted in order to deal with measurement variability. In this section the results of the test are presented for all the measured factors. The dataset for the test can be found in appendix A. During the degradation test 33 measurements were performed on the several factors. The passed lifetimes for the factors are as follows:

Measurement 33:

Number of copies made by the nip motor M1:	3.475.089,5
Number of staples stapled by stapler M6:	309.750
Number of staples stapled by stapler M7:	154.875
Number of activations by solenoid L3:	504.241

Control charts are used for the analysis of the degradation data of the various factors. One advantage of control charts is that they easily detect peculiarities during measurement routines. This usually expresses itself first in an out-of-control situation of the range chart. High and low peaks in the x-bar chart usually also point to inferences during measurements. The other advantage is that they are fast and easy to obtain with every statistical analysis program.

The following sub-sections each discuss the results of the measured factors for one of the Finisher's functions. The more profound analysis of the back-up parameters of the stapler function and tray election function can be found in Appendix E. Section 5.5 presents the fitted degradation functions for the different factors where it was possible to construct one.

### **§ 5.4.1 Paper transport function**

The measured factors that are critical to the Paper transport function were measured on a time scale of "*number of copies processed*" by the nip motor. Each factor will now be discussed separately.

#### **Mechanical Load on the nip motor**

The load on the nip motor caused by the increase of friction and contamination between the shafts and bearings of the paper transport system turned out to be a variable factor. The properties or state of the lubricant of the sleeve bearings can continuously be affected by movement of the system itself or by movement by the measurement operator. This sometimes led to unexpected increases or drops of the load on the motor. Nevertheless the load turned out to have quite a significant increase. Figure 5.10 shows the X-bar and Range chart for this factor.

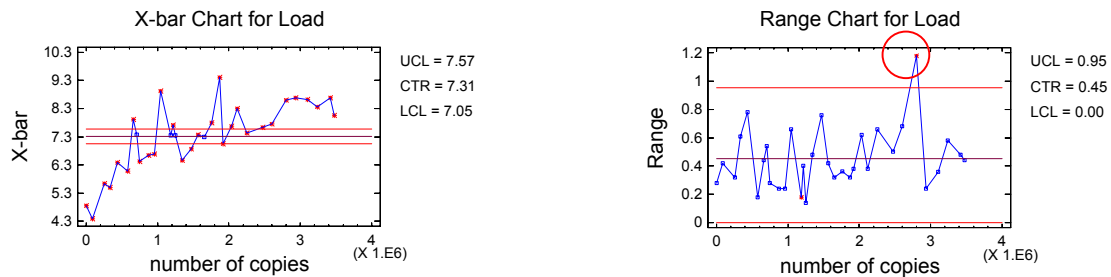


Figure 5.10: X-bar chart and Range chart for the Load

The X-bar chart is significantly out of control. This implies that we have as a matter of fact observed degradation. The range chart is out of control once. This out-of-control situation was due to shaft number one (figure 4.3), which experienced a lot of friction. This friction was resolved during the five measurements and therefore led to higher differences between the obtained values. This measurement was not taken out of the dataset because its mean value corresponded to expectations. Note that even though such a measurement may give rise to the expectation of observing an increasing variance over time, this cannot be deducted from the range chart. As a result of these two charts it may be concluded that it is permitted to model the change of the Mechanical load on the nip motor as a function of *number of copies processed*.

### Electric resistance of the PWBA

Measurement of the resistance of the PWBA suffered from many complications during the ADT. Therefore first the actual observations are presented. Subsequently the out-of-control situations are explained and removed from the data set. This leads to a second control chart with the new purified data. The control charts that are shown in the next figure (figure 5.11) are obtained with two measurement systems. The range chart clearly shows from which point (measurement day 26) the second measurement system is used. The two systems unfortunately lead to other measurement values as a result of a difference in equipment. In the figure below this difference is not yet compensated for. To the measurement data that resulted from the new system 31 mili Ohms need to be added. This calculation is however based on the somewhat dubious last measurement with the first system. This last measurement was however conducted with extra caution.

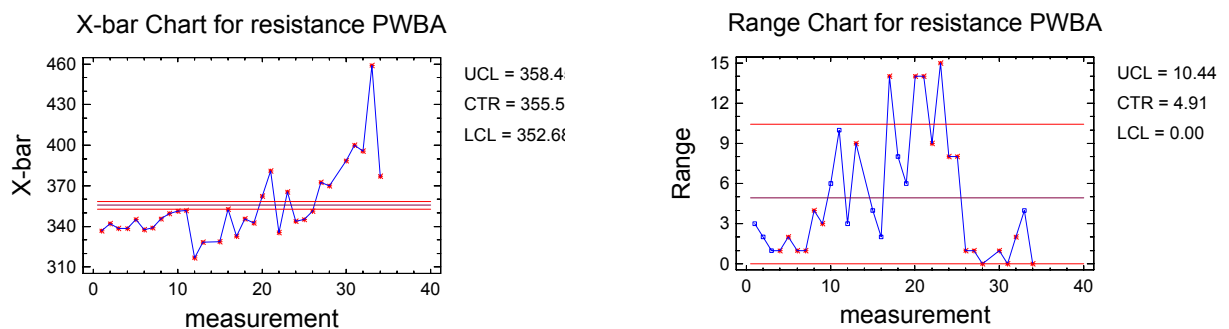


Figure 5.11: X-bar chart and Range chart for the PWBA resistance

The reason why the measurement system was changed during the ADT was the increase of the range. Although at first hand it was expected that this increase was a result of the product's ageing as was observed in the measurement system analysis, it was later found out that two of the connectors on the measurement tool (not PWBA) had aged and become unstable. The measurements that were out-of-control due to ageing of these connectors were removed from the data.

Other important observations are:

- A fuse change on the PWBA between measurements 2 and 3. This seems to have a negligible effect.
- At measurement day 11 the orange wire on the PWBA was soldered before the fifth measurement, which led to an out-of-control range. This fifth measurement was removed.
- A fuse change on the PWBA between measurements 11 and 12. This leads to a drop of 33 mili Ohms between measurement 11 and 12. In the following figures 33 mili Ohms will be added to all the data after measurement 11. Therefore it is assumed that the PWBA did not degrade between measurements 11 and 12. When looking at the trend until measurement 11 this seems to be a good assumption that leads to a negligible error especially when taking into account the higher increases later on.
- At measurement day 17 the operator altered one of the measurements in the set on purpose to see how this would affect the measurement. This measurement was removed.
- At measurement day 19 the orange wire caused variations in the two last observations in the set. These were removed.
- The high variation at measurement day 20 was reduced by removing the most influential measurement in the set.
- The module connector (also called interlock connector) was unplugged twice before the measurement took place. This may explain the extreme drop in resistance of the PWBA. Therefore the last measurement was removed entirely.
- The variation in sets that was observed with the new measurement system was so small that a relatively high range (4 mili Ohms) is devoted to the way of observing by the operator. This range is almost equal to the range at the start of using measurement system one.

After applying these changes the results for the PWBA resistance over time are as in figure 5.12. The used data degradation data for the PWBA resistance can be found in appendix C.

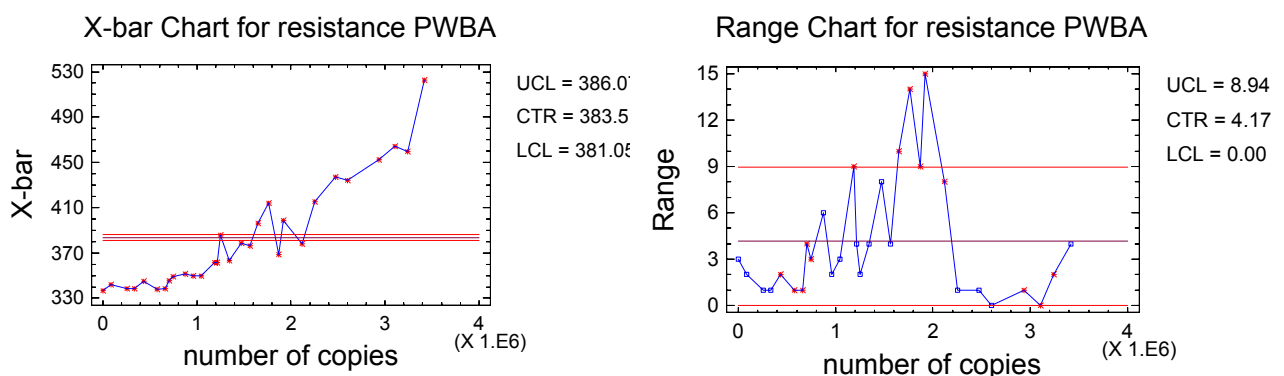


Figure 5.12: New X-bar chart and Range chart for the PWBA resistance

Note that the range chart is still out of control for a number of measurements, but that the upper control limit for the range is lower. Given the degradation that is observed for the measurements that are in control, the ones that are out-of-control do not lead to strange values in the x-bar chart. Therefore it is decided to model the resistance of the PWBA as a function of time.

A remark should however be made regarding the uncertainties whether these observations reflect degradation in an actual customer environment. First of all connector resistance is not only expected to increase with use, but also with actual (calendar) time. This time-factor is only partially present in the measured data. Second, the main connector of the module needed to be disconnected and reconnected after every measurement because of the use of one measurement set-up and one acceleration set-up.

When a connector is disconnected and reconnected a part of the corrosion may be cleaned off. This is another reason why the observed resistance increase may be higher in reality. This also explains the light variability in the x-chart. The third uncertainty lies in the translation that was made from the first measurement system to the second. The offset that is added is calculated based on the last measurement with the first system. Even though this measurement was made with extreme caution the measurement system was still unstable.

### Current rise time of the nip motor

The current rise time of the nip motor is the factor that one expected to change as a result of the change of the two previously described factors. The ‘Maintray experiments’ [39], ‘Screening experiments’ [42] and Van Hoon’s thesis [11] substantiate these expectations. The following X-bar chart and Range chart demonstrate the behaviour of the current rise time.

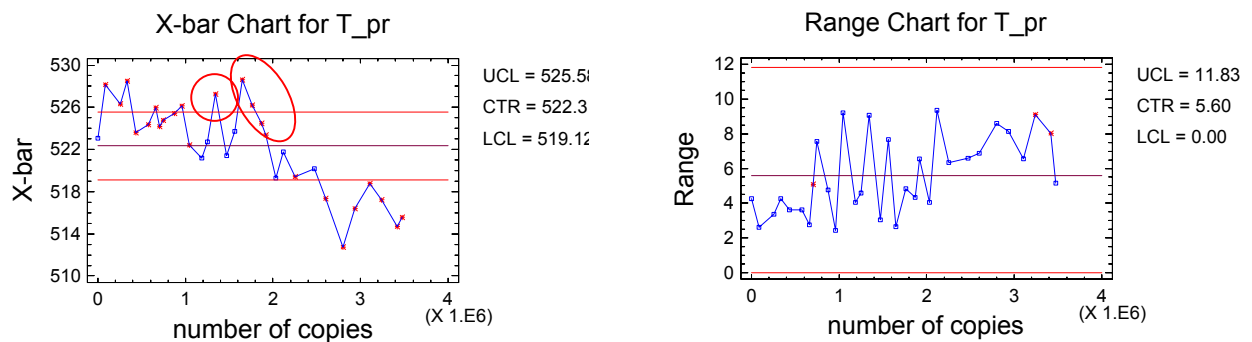


Figure 5.13: X-bar chart and Range chart for the Current rise time (T<sub>pr</sub>)

The figure clearly demonstrates that the range chart is in control. The range seems to be slowly increasing with time. This was also observed in the main experiment in 2002 [11]. The out-of-control x-bar chart shows that the current rise time (T<sub>pr</sub>) decreases with time.

The observations that are circled with a red line in figure 5.12 are unexpected high values that disturb the decreasing trend. After the first circled measurement it was found that the 5V power supply was badly regulated. Therefore an experiment based on [43] was conducted to reproduce this high value. From this Power Source experiment that can be found in appendix D it cannot be concluded that the power supply regulation influenced this measurement.

The second circle involves four observations. These measurements coincide with an out-of-control situation of the solenoid. Here it was found that its cover was not fixated to the system of the solenoid. This led to very high values for the solenoid time and an out-of-control for its range chart. Hence another small experiment (appendix D) was conducted to test if copying this

situation would lead to a higher current rise time for the nip motor. Again it cannot be concluded that loosening the solenoid cover affects the current rise time.

In conclusion it may be said that the current rise time of the nip motor changes with time. According to the screening experiment its behaviour is the result of the increase of the load on the motor and the increase of the resistance of the PWBA, which drives and controls the motor.

### § 5.4.2 Stapler function

In this section it is establish whether there is any degrading behaviour to be observed for the stapler function of the Finisher. The outcomes of its degradation are unfortunately less reliable than those for the paper transport function or for the tray election function, because the stapler was not aged with its normal stapler cartridge and paper, but with a sponge. Another prominent notation should be made with regard to the two staplers. The initially new staplers that were used for the test rapidly failed due to the use of a too large sponge that made the stapler fail at a point at which it would normally be very unlikely to fail. The replacement staplers were unfortunately of unknown age, but were nevertheless used in order to keep the test running. This made it still possible to determine the shape of the degradation models of the staplers.

The first factor of discussion is the stapling time for stapler M6. This time was measured at each of the two positions that it stapled the package of paper. The stapler time was expected to increase with use, as was discussed in section 5.2. All measurements that are presented are for the second set of staplers.

#### Stapling time M6 at position 1 and 2.

With regard to the stapling time it can be concluded that no degradation pattern can be distinguished. Although the x-bar chart in appendix E shows to be out-of-control, there is no indication of a clear form of wear. This indicates that the observations were probably within the variation that is caused by the stapler itself and the used paper. A more profound analysis of this factor can be found in appendix E.

#### Current peaks of stapler M7

The current peaks of stapler M6 are analysed by means of control charts. The x-bar and range charts for M7 show the following for current peak A.

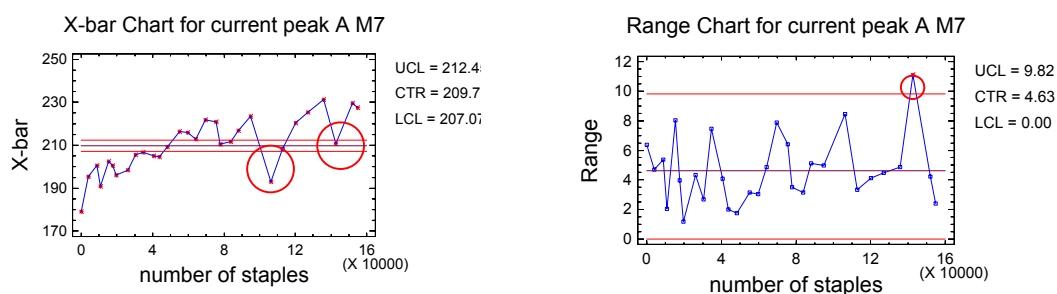


Figure 5.14: X-bar chart and Range chart for current intensity peak A of M7

It may be concluded that the x-bar chart is clearly out-of-control and shows a clear trend of degradation. The same can be concluded for current peak C of stapler M7, which is presented in figure 5.15.

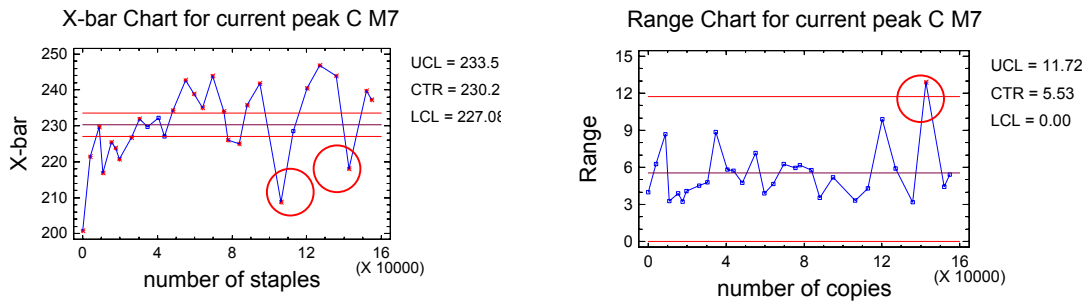


Figure 5.15: X-bar chart and Range chart for current intensity peak C of M7

Appendix E provides a more profound analysis of these factors and explains the circled observations in the figures above. For current peak B no degradation pattern could be distinguished. The analysis of this factor can also be found in the same appendix.

### Current peaks of stapler M6

For the moving stapler (M6) holds the same as for the fixed stapler. This stapler however made twice the number of staples as the fixed stapler made during the degradation test. This factor also shows clear degradation for the current peaks A and C. The following figures show that the x-bar charts of peaks A and C are out-of-control and show a clear trend.

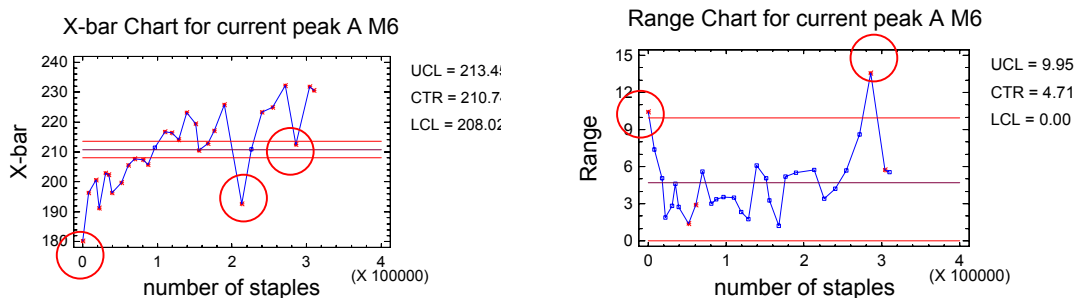


Figure 5.16: X-bar chart and Range chart for current intensity peak A of M6

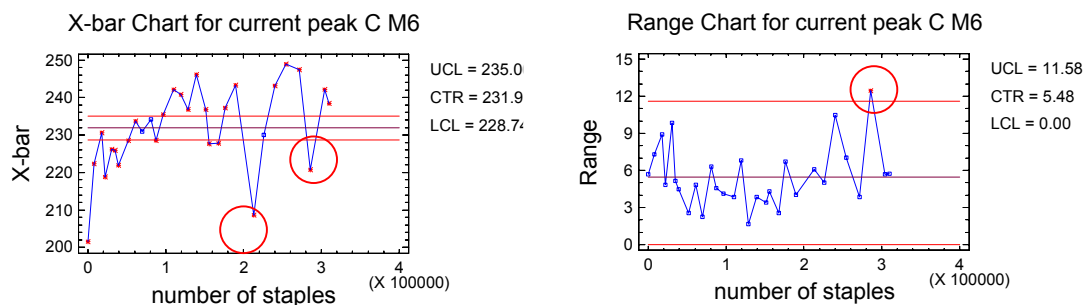


Figure 5.17: X-bar chart and Range chart for current intensity peak C of M6

In appendix E a more profound analysis of these parameters can be found. This appendix also explains the conspicuous observations that are circled in figure 5.15 and 5.16. For current peak B no trend could be recognised even though its x-bar chart was out-of-control (appendix E).

The final conclusion for the stapler function is that it that current peaks A and C show degradation for both staplers.

### § 5.4.3 Tray election function

The tray election function that is performed by the diverter solenoid L3 ages with its number of activations. As described in section 5.2 the solenoid is expected to deteriorate as a result of internal friction and friction of its attached system. As a consequence of this friction the time that is needed for its activation is expected to increase.

The solenoid time is profoundly analysed in appendix E. Based on this analysis it cannot be concluded that the solenoid time shows a clear degradation trend. It is peculiar how it first shows an increasing trend after which it decreases again later on. Therefore it was checked if the iron plunger within the solenoid had become permanently magnetic. The amount of magnetism of the plunger was however so little ( $5,5 \cdot 10^{-4}$  Tesla) that this could not be the cause.

Although it was expected that the solenoid time would increase with time, it cannot be said that this is supported by the data. Therefore it is decided not to model the solenoid time as a function of time.

### § 5.4.4 Observed failures

During the degradation test several components of the Finisher module failed. Table 5.2 below shows the name of the failed component and its TTF that was observed.

Table 5.2: observed failures during ADT

Component	TTF	Units	Cause of failure
Stapler cartridge	26078	Staples M7	Unknown/use
Edge solenoid	69340	Staples M6	Plastic broken
Tamper rail	1188170,5	Movements	Contamination/friction
Moving stapler rail	$0,5 \cdot 212868 = 106434$	Movements	Contamination/friction
Metal plate M6	254236	Staples M6	Torn plate
Tamper rail *	2231656 *	Movements	Contamination/friction

\* TTF is based on use after first failure

Regarding these Time-to-failures it must be noted that the components were replaced with components from field returned Finishers after they failed. These observations can be used for further research or for adjusting the conducted FMEA.

As a consequence of the analysis of the factors in this section it may be concluded, that only five factors significantly show degradation, where time may be expressed in use of a function. These are the following factors:

#### Paper transport function:

- Mechanical Load on the nip motor
- Electric resistance of the PWBA

- Current rise time of the nip motor

**Stapler function:**

- Expected value of the Current consumption peaks A and C of both staplers M6 and M7

### § 5.5 Degradation models DP's

In this section the degradation models for the design parameters are established. For each factor it is described separately how the degradation models were obtained. The first factor to be modeled is the load of the system on the nip motor.

#### Mechanical Load

Literature [44] states that for the increase of the mechanical load on a system two phases can be distinguished. The first phase is a phase of rapid increase until a point after which the mechanical load will increase linearly. This rapid increase at first followed by a slower increasing load is also what can be distinguished for our data.

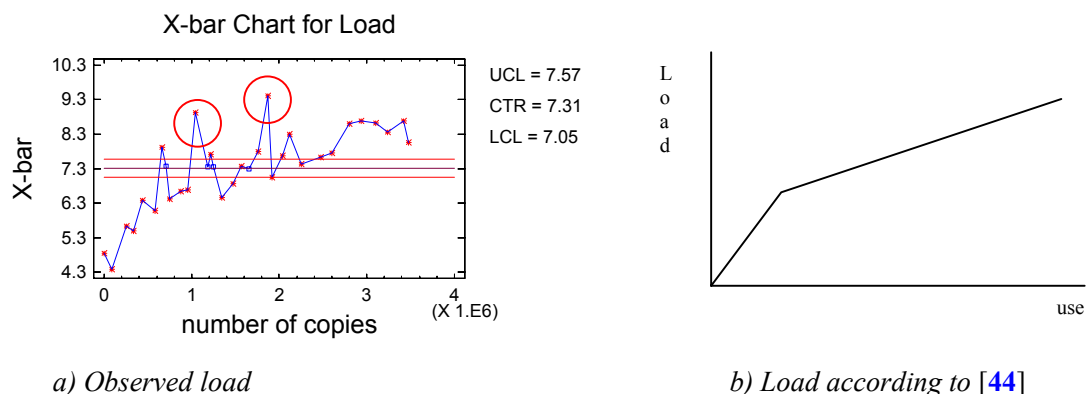


Figure 5.18: Load: reality vs theory

When one compares the observed load is to the theory it is conspicuous that the observed load shows quite some variability. This is due to the fact that the paper transport system is a dynamic system. The properties of the lubricant in the system change with time, rotation and temperature leading temporary deviations in the state of the system. The two red-circled peaks in the x-bar chart are standalone observations of the load that stand out. Removing these two observations lead to a much better fit and moreover to a behaviour that is more consistent to literature. Therefore these two data points are removed for modeling purposes.

The most difficult part of modeling was to find the time point from where on the load shows the slow but steady linear increase. First an ample estimate for this point was made based on the graph of figure 5.18 a). It was chosen to evaluate the measurements 5 to 13 on the performance indicators **standard deviation from estimate** and **R<sup>2</sup> adjusted for degrees of freedom**. Having an as small as possible error for the estimate toward the data is especially important for the second part of the model, because this is the part that will be extrapolated to predict failure time. The choice for the adjusted R<sup>2</sup> for d.f. instead of the normal R<sup>2</sup> has no influence on the outcome of the evaluation because models with the same number of estimation parameters are compared. The first part of the curve was assumed to be linear as well. The table below shows the results of the evaluation.

Table 5.3: Evaluation of the point for linear increase

Part 1	Stdev	R <sup>2</sup> d.f.	Part 2	Stdev	R <sup>2</sup> d.f.
1-4	0,350	57,49	5-rest	0,487	60,00
1-5	0,369	74,06	6-rest	0,490	56,48
1-6	0,384	71,18	7-rest	0,480	53,76
1-7	0,517	77,53	8-rest	0,433	63,32
1-8	0,487	82,38	9-rest	0,418	67,22
1-9	0,560	73,43	10-rest	0,423	63,31
1-10	0,600	67,10	11-rest	0,430	59,65
1-11	0,620	62,36	12-rest	0,437	55,72
1-12	0,609	64,37	13-rest	0,444	55,70

Based on this table it is chosen to model the load as a linear function from measurement 9. This leads to the lowest standard deviation from the estimate for curve part two and to the highest R<sup>2</sup> d.f for both parts. Hence the model from point 9 is:

$$Load_{9-\infty}(t) = 6,9002 + 7,13689 \cdot 10^{-7} \cdot t \quad (eq. 5.1)$$

At this point the nip motor had already processed 745.541,5 copies. Therefore the entire model will be:

$$Load(t) = 6,9002 + 7,13689 \cdot 10^{-7} \cdot (t - 745.541,5) \quad \text{for } t \geq 745.541,5 \text{ copies.} \quad (eq. 5.2)$$

We are however interested in the load increase, because this can be used for every system. The initial load on the motor was 4,848 Ncm. Therefore the expected growth model for the load will be:

$$Load \text{ increase}(t) = 2,0522 + 7,13689 \cdot 10^{-7} \cdot (t - 745.541,5) \quad (eq. 5.3)$$

Where  $t$  is the number of copies processed by the nip motor.

### Electric resistance PWBA

The electric resistance of the PWBA was expected to degrade as a result of fretting and corrosion of the connectors on the PWBA and the main Finisher connector (also called interlock switch). Literature was found on resistance increase of single connectors. Malucci [41] states that the increase *rate* of resistance at a certain point in time is a linear function. Therefore the actual increase is a second order function of time with no first order term. However it cannot be simply assumed that this implies that the increase of resistance on a PWBA with multiple connectors also takes place according to this model. Therefore the second order model was tested using Statgraphics. Statgraphics accepted the second order term in the model and rejected the first order term with a statistical fit of R<sup>2</sup> adjusted for degrees of freedom of 93,34 %, which is high for degradation data.

$$R(t) = 339 + 1,293 \cdot 10^{-11} \cdot t^2 \quad (eq. 5.4)$$

and

$$R \text{ increase}(t) = 1,293 \cdot 10^{-11} \cdot t^2 \quad (eq. 5.5)$$

Where  $t$  is the number of copies processed by the nip motor and the resistance is in milli Ohm.

For the current rise time no degradation model will be made. This parameter is dependent on the degradation of its two design parameters. Both degradation paths show not to be linear over time. Modeling the current rise time may therefore lead to wrong estimations when it is extrapolated beyond the time interval of the degradation test.

## **§ 5.6 Conclusion and discussion**

### **§ 5.6.1 Conclusion**

The accelerated degradation test was performed in order to capture the degradation of the design parameters and to prove that the performance characteristic changes as a result of this degradation. The stapler function and the tray election function were added to the degradation test to be used as back-up functions for in case the design parameters or the performance characteristic would not deteriorate. For all measured factors changes in their performance were observed.

Analysis resulted in the conclusion that only five factors show degradation. These are the mechanical load on the nip motor ( $DP_1$ ), the electric resistance of the PWBA ( $DP_2$ ), the current rise time of the nip motor (PC) and the two back-up factors current peak A and C of both stapler units. For the two design parameters it was possible to find specific literature that indicated the mathematical form of the degradation paths. These forms were supported by the data for these DP's, which resulted in a strong case for their degradation models. Considering the stapler current peaks no relevant literature could be found. The stapler current peaks should however not be seen as a direct measurement of degradation, but as a performance characteristic that is probably affected by more than one degrading design parameter. One of these design parameters is the deterioration of the eccentric along which the stapler performs its function. Another design parameter that affects these current peaks is the resistance of the PWBA, which also drives and controls the staplers. Consequently these stapler factors were not modelled. The degradation test proves however that these parameters are significantly influenced by time or use.

The degradation test was conducted during a considerable period of time (approximately 3,5 months) during which the paper transport function processed almost 3,5 million copies. In this time the Finisher module was subjected to several issues and failures regarding other functions than the identified dominant failure mode. This complicated the measurements and affected testing speed. Especially the rails in the Finisher that are used for the movement of the Tamper and the Moving stapler (M6) turned out to be weak spots. Based on the observed failures (table 5.2) it can be concluded that the phase to identify the dominant failure mode did not result in the identification of the correct failure mode.

The size and complexity of the Finisher also made it difficult to perform measurements. The module has several functions that interact and consequently influence these measurements. This experiment profited from the presence of past data, which made it possible to determine these measurement interactions before the test was started.

The degradation of the design parameters load and PWBA resistance in combination with the observed decrease of the performance characteristic underpins the expectations of the ROMDA concept and the Flextronics engineers. This allows for the continuation with the next experiment, which is an experiment to predict the Finisher's degradation over its technical life. Here the degradation models that resulted from this chapter will be used to superimpose the degradation of the paper transport function over life on its performance characteristic.

---

### **§ 5.6.2 Discussion**

This discussion section serves as a critical note towards the execution of this experiment and to the results that are obtained.

The size and complexity of the system made it time consuming to perform a set of measurements. This in combination with the restricted number of man-hours (due to other activities) led to the decision to test only one Finisher unit. This made it impossible to incorporate the variance in degradation speeds of multiple units in the models. Therefore it is assumed that all Finisher units degrade according the degradation profile of the tested unit. This assumption is disputable but for the time being cannot be proven wrong.

During this ADT it was assumed, based on engineering knowledge, that not using paper during life acceleration would not or negligibly influence the degradation rate of the paper transport function. This seems a good assumption considering the relatively low mass of paper in relation to the mass of the shafts. However, it is possible that the use of paper would entail contamination of the shafts and sleeve bearings, which would increase the degradation of the load on the system.

A few remarks need to be made with regard to the resistance of the PWBA. Section 5.4.1 clearly shows that there have been some complications during the measurement of this resistance. Based on observations during the test some measurements have been removed or adjusted. The ageing of the connectors of the measurement system led to the use of a new measurement system, without these connectors. Therefore a translation had to be made from the measured value with the old system to the measured value with the new system. Even though this translation was made as accurate as possible, it involved the assumption that the last measurement with the old system was correct. Another question mark can be placed with regard to the main connector (or interlock switch). This connector was disconnected and re-connected after the resistance measurement in order to measure the other parameters of the module on another set-up. Every time it is disconnected or re-connected some of the corrosion that is accumulated in this connector may be scraped off, which may result in a decrease of resistance. Electric resistance increase due to corrosion of connectors may not only occur as a result of use, but also as a result of time factors like temperature and humidity [40]. Despite of this literature usually measures contact resistance increase as a result of ‘number of (fretting) cycles’ [41]. The accelerated customer use during the ADT made the contribution of actual time factors smaller than this would be in a customer environment. These arguments all imply that the actual resistance increase may in fact be higher than was observed during this test.

## Chapter 6 Relating the PC to the DP's

The previous chapter proves that the design parameters and the performance characteristics change with time as a result of degradation of the system. The degradation data show that degradation of both parameters is not linear with time as was assumed in the work of Van Hoorn. This made it necessary to adjust and improve the model in order to make it consistent with actual system degradation. Moreover, the increase in load obtained during the degradation test does not lead to the same amount of decrease of the current rise time as that was found in Van Hoorn's model. A possible explanation for this may be that the Finisher that was used during those tests had a different kind of stepper motor or a different software version of the PWBA. The initial current rise time of this nip motor is rather high in comparison to the rise time in the system that was used during the degradation test in chapter five. This gives rise to the suspicion that the experiments in [11] are conducted with a Finisher that possibly has a different version stepper motor or a different version PWBA.

Therefore the same stepper motor and the same PWBA were used as in the degradation test. This chapter continues with the phases eight and nine of the roadmap.

### § 6.1 The limit setting experiment

The objective of the limit setting experiment (phase 8) is to determine the conditions of the design parameters for which the paper transport function still works properly. In order to determine the characteristics of the nip motor, load was added with a mechanical break until the motor stalled. For this the belt that connects the motor to the shafts was removed.



*Figure 6.1: Mechanical break*

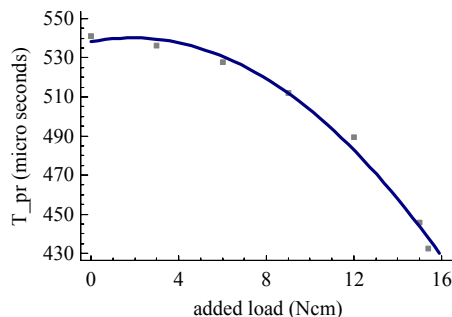
The extra load that the motor could support was measured to be 15,048 Ncm. The same was done for the resistance of the PWBA. Therefore extra resistors were connected in series until the system failed. This was measured to be a maximum of 1,9  $\Omega$ . The nominal load (X1) and nominal resistance (X2) of the PWBA were 5,568 Ncm and 789 m $\Omega$  respectively. Remember that both the load and the resistance were proven to increase with use. And it is thus of no interest to determine the lower boundaries of functioning because a system with these specs would never have functioned in the first place.

A degradation profile for this Finisher was made by systematically adding load to the motor. The resistance was kept at its nominal level. This led to the observations presented in table 6.1.

Table 6.1 The influence of DP load (X1) on the PC current rise time (Y)

Added load (Ncm)	Rise time ( $\mu$ s)
0	541,12
3	536,06
6	527,93
9	512,10
12	489,21
15	445,84
15,4	432,58

Figure 6.2 shows graphically the relation between the load on the nip motor and the effect that this has on the rise time. This effect shows to be a second order quadratic relationship, where the performance characteristic becomes increasingly sensitive to the load when the load becomes higher.



*The current rise time decreases slowly with the first few added Ncm's of load. Then the decrease occurs more rapidly when a higher load is added. This implies that the rise time becomes more sensitive to load when the load increases.*

Figure 6.2: The influence of DP load (X1) on the PC current rise time (Y)

The limits that are obtained in this experiment serve as the expected degradation values of the paper transport function of the Finisher. If one can predict the 'time' or 'age' at which the performance characteristic or one of the design parameters reaches its limit value it is thus possible to predict when the paper transport function fails.

### § 6.2 Main experiment

The main experiment is conducted to construct a mathematical model for the entire product population of Finishers of the performance characteristic as a function of the increase of its design parameters. As the first line already states, the model should represent the entire product population. This implies that at every point in time the performance characteristic has a probability density function with a mean value and a variance. Design Of Experiments [33] is used in order to generate this PDF at a specific point in time. In this research the objective is to predict reliability, which is quality over time. Therefore the factor time needed to be added to the experiments. In order to do this three DOE's are performed at different 'points in time'. These points in time are created by artificially adding degradation to the two design parameters load (X1) and PWBA resistance (X2). Load is added by means of the mechanical break in figure 6.1 and resistance is added by putting resistance in series with the PWBA and the main connector. Figure 6.3 shows a photo of this set-up.

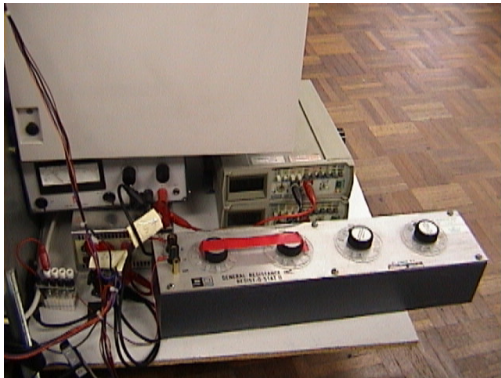


Figure 6.3: Application of extra resistance (X2)

The reason for performing three DOE's and not two is the fact that with three points it is possible to determine whether the response variable ( $T_{pr}$ ) is linear, concave or convex. Moreover it was suspected that the current rise time would be decreasing convex as a result of the limit setting experiment and the experiments by Van Hoorn.

Note that in the first line of the previous paragraph the word increase is used, because the added amount of load and resistance is used.

### § 6.2.1 Experimental design

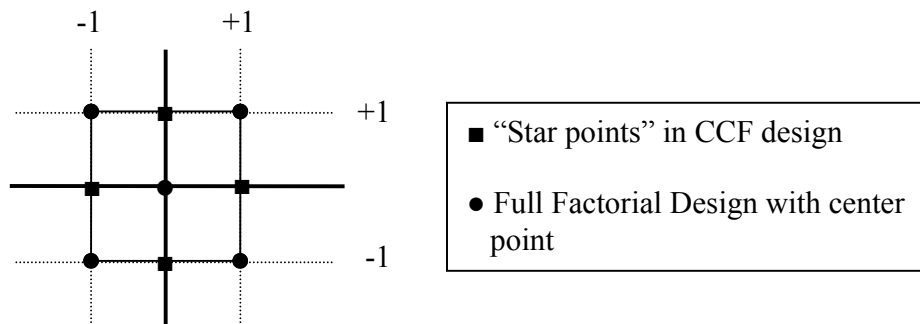


Figure 6.4: Central Composite Face Centered (CCF) design

The design that was used for the experiments is Central Composite Design. This design uses + and – levels settings around a center point. By varying the values of the design parameters around these center point values it is possible to determine the influence of both design parameters on the performance characteristic at each point of time. Besides this it also provides information about how variation in the design parameters, which can be seen as product-to-product variation, influence the variation in the performance characteristic over time. This type of design is augmented with a group of ‘star points’. This allows for estimation of curvature. The type of CCD that is used is called Central Composite Face Centered design. This design only requires three levels, while other CCD's require more [11]. The proposed design consisting of two parameters that will be set on three levels results in  $3^2 = 9$  possible combinations. Each run is performed once per DOE except for the center points for which two replicates will be conducted. This results in a design with eleven runs per DOE. During the experiments these combinations of

settings are randomised in order to prevent that conditions in a previous situation influence the results in a following (appendix F).

### § 6.2.2 Time points

In this section the ‘times’ and settings of the center points are determined for each of the three DOE’s. The objective was to predict performance over life with three DOE’s. Therefore a DOE needed to be performed at  $t=0$  (DOE<sub>0</sub>), in order to know the nominal values of the performance characteristic and at its end of life (DOE<sub>2</sub>) to be able to make good predictions of the TTF. The other DOE, DOE<sub>1</sub>, was consequently chosen at halfway the ‘age’ the Finisher has in DOE<sub>2</sub> (near its end of life) to make the predictions over life as good as possible (with a limited amount of three DOE’s). At each of these times the corresponding settings for the center points of the design parameters are determined. In the following section the + and – levels for the DOE’s are determined. The calculations are presented counter clockwise, starting with the DOE at the highest number of copies, then the DOE halfway its life and finally the DOE around the nominal settings..

#### DOE<sub>2</sub>

For practical reasons it was chosen to use an added break force of 8 Ncm as the highest center point for the load (X<sub>1</sub>). According to the degradation model for the load (eq. 5.3) this amount of load increase would be observed at:

$$time_{DOE2} = 745.541,5 + \frac{8 - (6,9002 - 4,848)}{7,13689 \cdot 10^{-7}} = 9.079.423,625 \text{ copies.}$$

The amount of 745.541,5 copies is the number of copies made at the beginning of the second part of the degradation function for the load and 6,9002 Ncm is the expected load at this same point. During these 745.541,5 copies the load is expected to increase with the amount of  $6,9002 - 4,848 = 2,0522 \text{ Ncm}$ .

The settings for the resistance need to be made at the same number of copies as that that was expected for the load. Using equation (eq. 5.5) this leads to the following added resistance:

$$R(time_{DOE2}) = 1,293 \cdot 10^{-11} \cdot (time_{DOE2})^2 = 1.065,9 \text{ m}\Omega$$

So the level settings for DOE<sub>2</sub> are around 9 Ncm and 1.065,9 mΩ for the added load (X<sub>1</sub>) and added resistance (X<sub>2</sub>) respectively. Based on the calculated number of copies the levels for DOE<sub>1</sub> can now be set.

#### DOE<sub>1</sub>

For DOE<sub>1</sub> the design parameters are set at the levels that they are expected to have halfway the ‘time’ of DOE<sub>2</sub>. This is done to make the best possible predictions over life with three DOE’s. Hence the expected added load and added resistance at  $time_{DOE1} = \frac{1}{2} \cdot time_{DOE2} = 4539711,81$  copies are calculated.

Hence using equation 5.3 the added load will be:

$$\text{Load}(\text{time}_{\text{DOE}_1}) = 6,9002 - 4,848 + 7,13689 \cdot 10^{-7} \cdot (\text{time}_{\text{DOE}_1} - 745541,5) = 4,76 \text{ Ncm}$$

And the using equation 5.5 the added resistance will be:

$$R(\text{time}_{\text{DOE}_1}) = 1,293 \cdot 10^{-11} \cdot (\text{time}_{\text{DOE}_1})^2 = 266,47 \text{ m}\Omega$$

Concluding, the level settings for  $\text{DOE}_1$  are around the 4,76 Ncm and 266,47 m $\Omega$  for the added load and added resistance respectively.

### ***DOE<sub>0</sub>***

The center point settings for the first DOE, which will be called  $\text{DOE}_0$ , are set around the nominal values of the design parameters. This returns the nominal value of the performance characteristic. Therefore the added load and added resistance are chosen as close to zero as possible for both factors.

Now that the work points of  $\text{DOE}_0$ ,  $\text{DOE}_1$  and  $\text{DOE}_2$  are decided, the + and – settings will be determined.

### **§ 6.2.3 Level settings**

In this section the + and – level settings are determined for the DOE's. Each DOE should generate a probability distribution that represents the actual product population at that specific moment in time. Therefore a + or a – setting for a design parameter should represent the value of this design parameter for a randomly chosen other product. This is the expected deviance from the mean value, or standard deviation.

The 'Part-to-Part Experiments' that were conducted at Flextronics on the 4<sup>th</sup> and 6<sup>th</sup> of December 2002 [45] resulted in unit-to-unit data on new, refurbished and field returned Finishers. This data was obtained from five new, five field returned and five refurbished Finishers. The data on the refurbished Finishers was not used because it was not documented what types of repairs or alterations were made to these products. Appendix G shows the obtained measurements for the design parameters in six new Finishers modules. The standard deviations of the design parameters of the population of new Finishers were calculated to be 0,39 Ncm for the load ( $X_1$ ) and 12,9 m $\Omega$  for the resistance of the PWBA.

For the PWBA resistance this standard deviation is larger than the highest standard deviation of variation within sets that was observed during the measurements in the degradation test. This is a minimum requirement in order to be able to measure unit-to-unit variation and draw conclusions from the DOE's. A remark should be made regarding the resistance of the PWBA. The resistance that was measured in the degradation test does not coincide with the resistance that was measured in the unit-to-unit experiments. This is due to the extra resistance of a current limiter with a specification of 0,47  $\Omega$  that was measured in the unit-to-unit experiments. However, the resistance of the PWBA is expected to increase as a main result of connector degradation, while the current limiter is a resistor. Therefore the standard deviation of 12,9 m $\Omega$  is used for as the minimum for level setting in the first DOE.

Regarding the load the remark should be made that set variation during the degradation test (appendix A) was at one moment observed to be higher than the unit-to-unit variation (appendix G). This was caused by one of the shafts in the system that experienced friction. The rotation of

the shafts resolved this problem during the five measurements. This resulted in a decrease of the load and this caused the variation between sets. Moreover the degradation test does not show any indications of an increasing variation between sets over time. Therefore the standard deviation between units of 0,39 Ncm is used as minimum for level setting in the first DOE.

The values 12,9  $m\Omega$  and 0,39 Ncm are practically difficult values to use. Therefore the values of 20  $m\Omega$  and 0,40 Ncm are used in the experiments for DOE<sub>0</sub>.

Field data was necessary in order to use realistic settings for the second and third DOE (DOE<sub>1</sub> and DOE<sub>2</sub>). Although there was unit-to-unit data on field returned Finishers, this data did not contain the age of the measured units. Hence it is not possible to make a good statement about the unit-to-unit variation at a specific point in time (age). Because nor Flextronics nor its customer keeps track of the number of copies that a Finisher produces in the field, it can be said with certainty that there will not be any usable unit-to-unit data of field returned Finishers available in the short run regarding this dilemma.

Therefore the decision is made to assume that unit-to-unit variation does not change with time. What this assumption implies is that all units of the Finisher population deteriorate according to the same degradation path and degradation model as that was measured for the Finisher in the degradation test. This assumption is disputable but it is the best possible assumption to be made. First of all, it cannot be proven to be untrue. Second, badly founded assumptions on unit-to-unit variation of aged products would lead to high uncertainty of TTF predictions. However, the dilemma of changing unit-to-unit variation is one that the ROMDA concept could also face in the design stage of new products, as field data would neither be available for these products. This problem could naturally be resolved by degradation testing several units instead of the one unit that was used in this research.

Consequently the standard deviations between units are also used for the level settings of DOE<sub>1</sub> and DOE<sub>2</sub>. This leads to the following design grid of table 6.2.

*Table 6.2: Experimental design Main experiment*

	<b>X<sub>1</sub> (load in Ncm)</b>			<b>X<sub>2</sub> (resistance in <math>\Omega</math>)</b>		
	-	0	+	-	0	+
DOE 0	0	0,4	0,8	0	0,02	0,04
DOE 1	4,4	4,8	5,2	0,25	0,27	0,29
DOE 2	7,6	8	8,4	1,05	1,07	1,09

Note that the setting of the center point in DOE 0 is set at 0,4 Ncm and 0,02 Ohm instead of zero for both parameters. The degradation test, the limit setting experiment and the experiments by Van Hoorn [11], however all indicate that these deviations do not influence the value of the performance characteristic. Figure 6.5 presents a graphical representation of this experimental design. All three DOE's represent the expected degradation of the design parameters at a certain time.

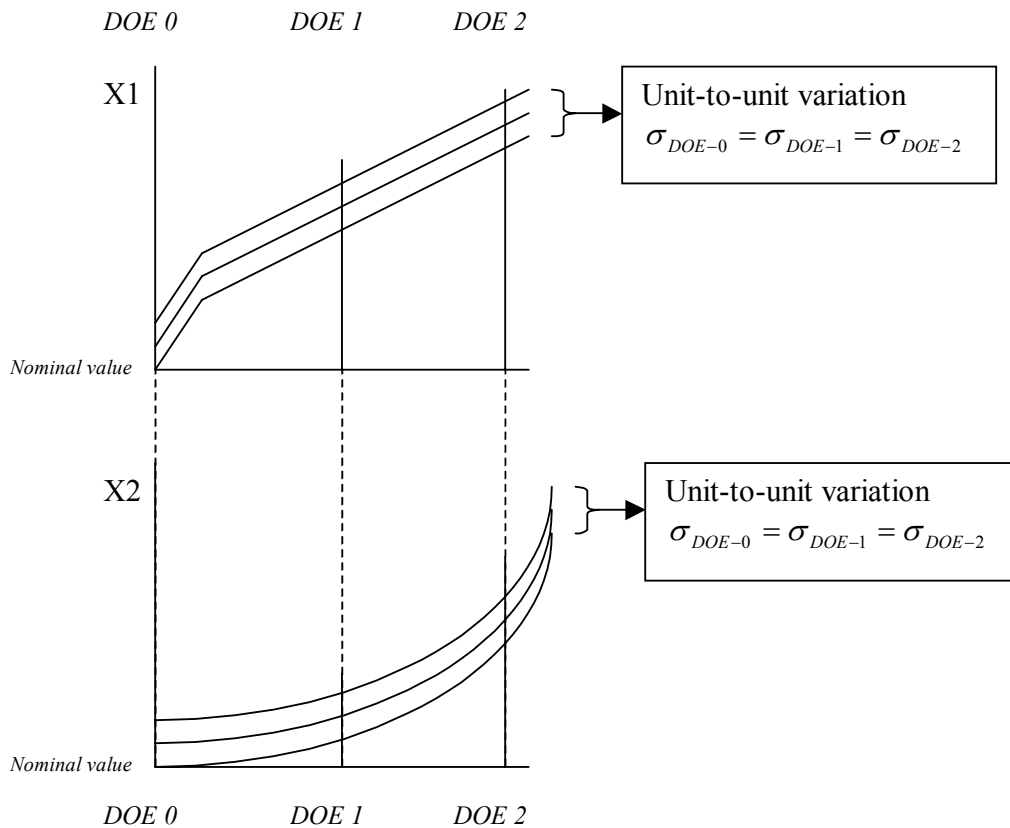


Figure 6.5: Graphical representation experimental design

The level settings per run are presented in Appendix F. For each combination of level settings five sets are produced. This is the same number of sets as that was used in the degradation test. Note that the combinations of runs are randomised in the experiments in order to prevent that conditions in a previous situation influence the results in the next situation.

### § 6.2.4 Measurement system analysis

Before the main experiment is started it is checked whether the measurements are reproducible and stable. Therefore the variation and averages between sets is compared for the various runs. This is done by means of a simple MSA that compares the +- and -+ setting of two measurements and three measurements of the 00 (centerpoints) setting. A measurement consists of five sets.

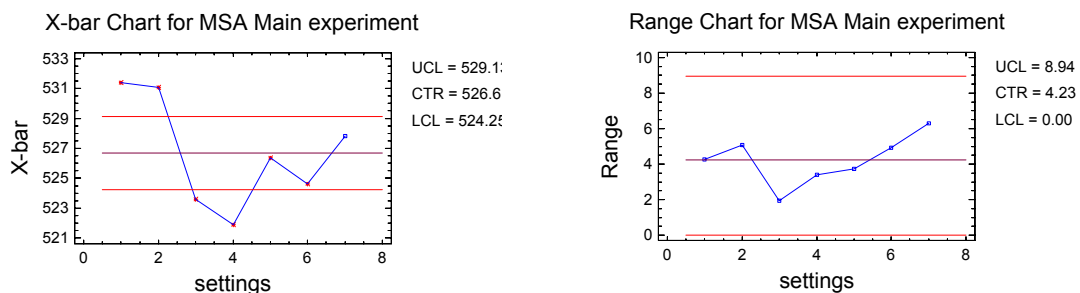


Figure 6.6: Control charts MSA Main experiment

The X-bar chart shows high and constant values for the -+ setting (measurement 1 and 2), low values for the +- setting (measurement 3 and 4) and average values for the 00 setting (measurement 5-7). The X-bar chart also shows an out of control situation for the -+ setting regarding the +- setting. In the usual types of DOE's this situation is wanted, because it enable the possibility to distinguish the influence of the settings. This way of performing DOE however has as a goal to generate measurements that represent a product population. As unit-to-unit variation is used for level setting this may result in out-of-control situations for the mean value of sets.

Most importantly the means of the sets with the same level settings are in control and so is the control chart. A remark should be made regarding the sequence of the sets. These were performed in random order. The two sets for the +- and -+ settings were conducted with a block of one day.

### § 6.3 Results Main experiment

The data that was generated in the experiment first needs to be analysed and checked on normality. This is done by means of Shewart control charts. For observations that cause an out-of-control situation in these charts it cannot be assumed that they belong to a normal probability distribution.

#### § 6.3.1 Analysis of the results

This sub-section analyses the results for each DOE separately. In order for the results to be used they need to be stable and predictable. This check is performed by means of control charts (figures 6.7, 6.9 and 6.11). The reason why each DOE is considered separately is because of the expected increase in range as the design parameters increase [11]. This contribution of the range of the performance characteristic in DOE 2 could then cover up a possible out-of-control situation in DOE 0 or DOE 1.

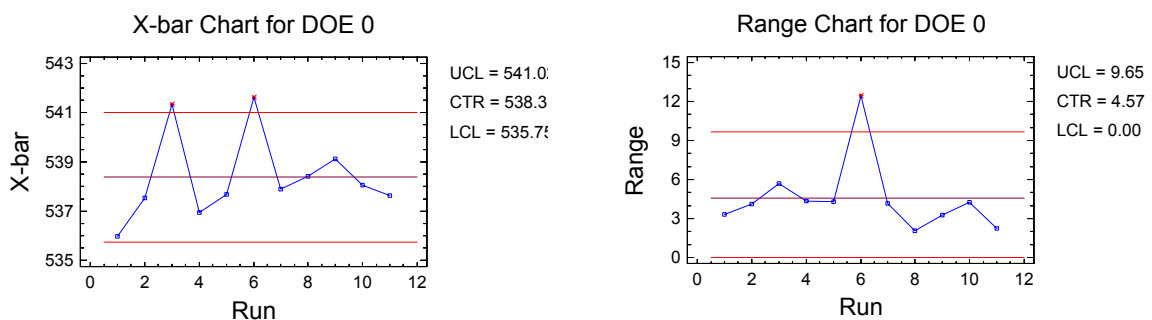


Figure 6.7: Control charts for DOE 0

The range chart for DOE 0 shows a clear out-of-control situation at run 6. This run has combination settings Load + and Resistance -. Therefore it is expected that this combination would lead to a mean value that is lower or equal to the mean value of DOE 0. The x-bart chart shows however a conspicuously high value for the mean value of this run. Appendix F shows that this high mean value and high range are caused by two of the five measurements in the set. Figure 6.8 presents two histograms with probability density plots that represent the data of DOE 0. One with the extremes of run six and one without. Removal of the two extreme values (547,63 and 548,11) brings the range back in control and leaves the observations of 535,64, 536,85 and 539,92 microseconds.

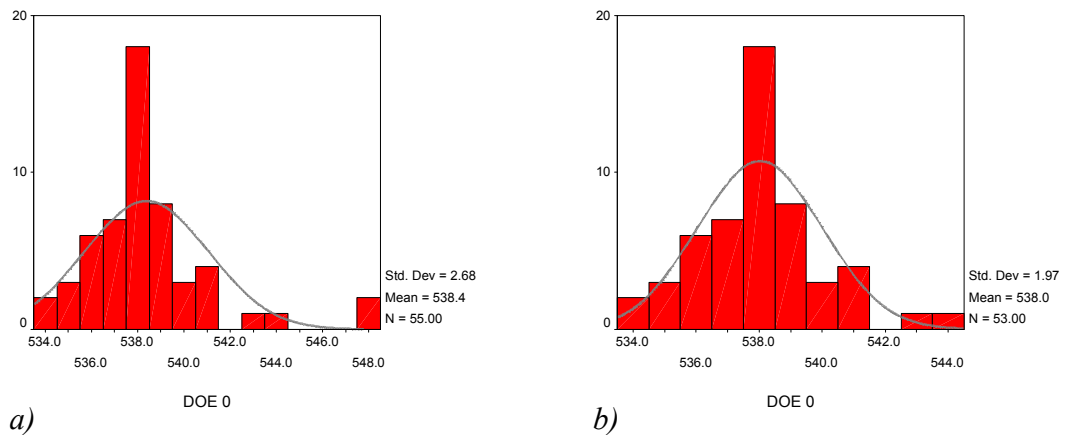


Figure 6.8: Histograms DOE 0  
a) with extremes of run 6  
b) without extremes of run 6

Removing these two values hardly influences the mean of the population. The mean decreases only 0,38 microseconds. The standard deviation however is affected stronger by this change and decreases from 2,68 to 1,97, which is a decrease of 36 percent. This in combination with the expectation that the values would be lower or equal to average has led to the decision to leave out these two values of run six further calculations.

The other out-of-control situation, for the x-bar chart, is the result of the level settings in the DOE. For this the standard deviations of the design parameters are used. Certain combinations of these settings may result in an observation that distinguishes itself from the rest of the measurements. This does however not imply that this observation is wrong, but that it represents a product that is significantly different from the mass.

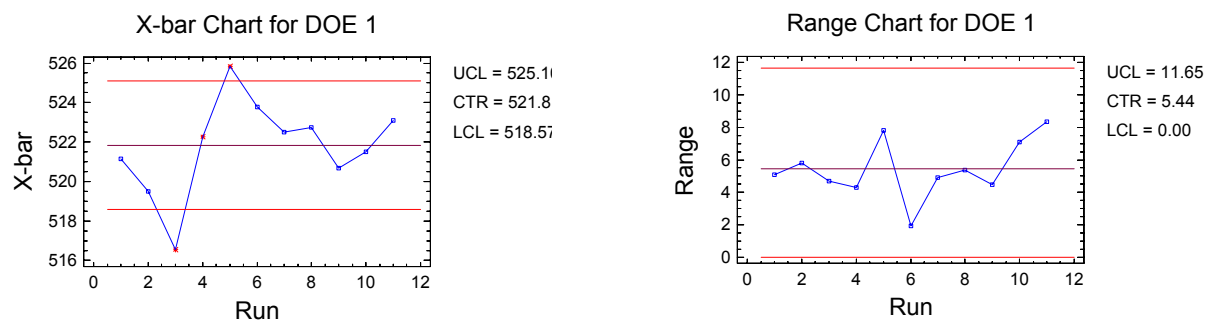


Figure 6.9: Control charts for DOE 1

The range chart for DOE 1 shows no out-of-control situations. The explanation for the out-of-control x-bar chart can be found above. This results in the following product population (figure 6.10)

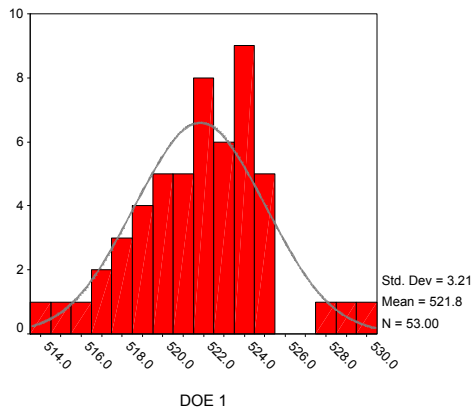


Figure 6.10: Histogram DOE 1

Note the lower average rise time and the higher variance of the current rise time. This shows that the performance characteristic also decreases with time in this experiment.

The control charts for the last DOE, DOE 2, are as follows.

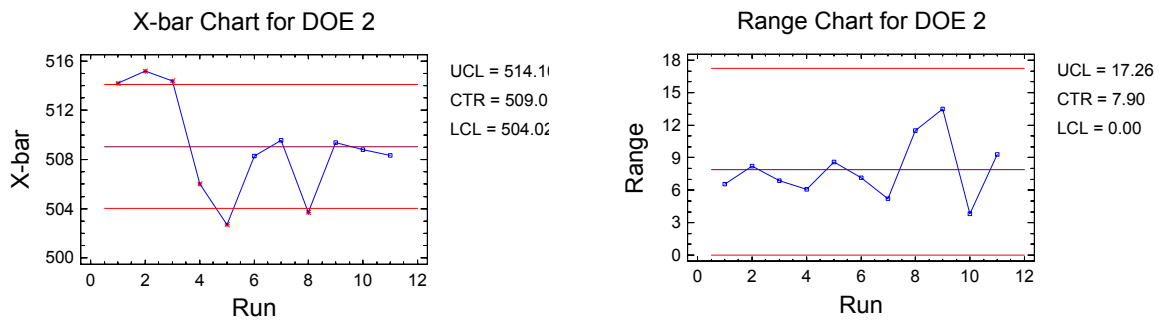


Figure 6.11: Control charts for DOE 2

The resulting distribution of the measured values for the current rise time is presented by the histogram in figure 6.12.

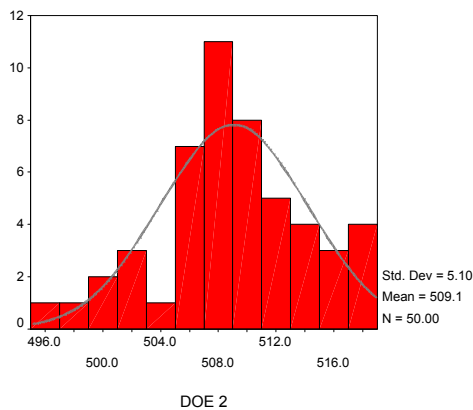


Figure 6.12: Histogram DOE 2

Subsequently it is checked if the means and ranges between the three DOE's are out-of-control (figure 6.13). If there is no statistical significance between the mean values of the three DOE's, the current rise time may not be modelled as a function of time and can therefore not be used as a performance characteristic. This analysis was done with the program SPSS because Statgraphics is not capable of producing control charts for sets larger than twenty-five samples.

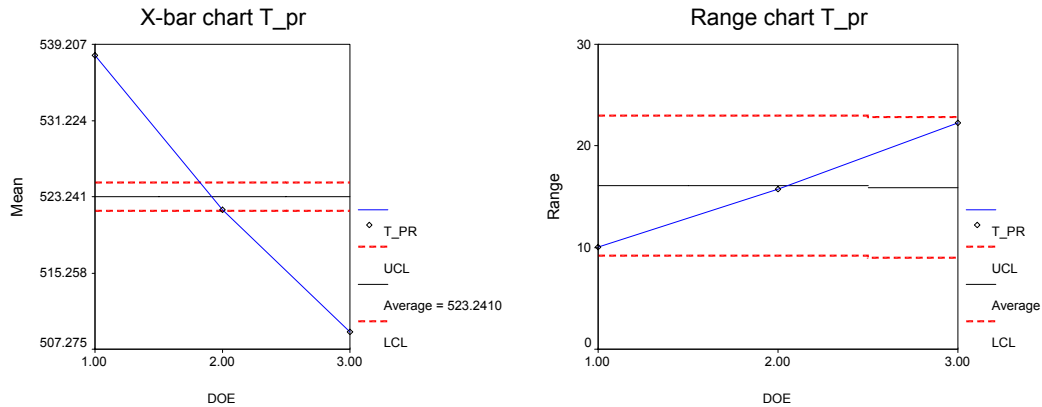


Figure 6.13: Control charts between DOE's

The x-bar chart for the three DOE's shows to be out of control as was expected [11]. Hence it is allowed to model the 'current rise time' as a function of time and thus it may be used as a performance characteristic. The x-bar chart also implies that the performance characteristic changes significantly as a function of its design parameters. Although the range chart shows to be in control it can be concluded that the mean range per DOE definitely increases by more than three sigma and thus changes with time. Next it needs to be determined how these design parameters affect the performance characteristic. Therefore Analysis Of Variance (ANOVA) is will be applied to determine which combinations of terms are significant and whether there are any interactions. Based on the findings by Van Hoorn [11] it is expected to have no interactions between terms. Moreover it is expected that the first and second order term for the load ( $X_1$ ) are significant and that for the resistance only the first order term is significant.

### § 6.3.2 Regression model

Performing the ANOVA was not a straightforward process. The three DOE's generated three datasets that were not joined by time and did thus not have consecutive values for their settings. These separate points in time made it impossible to perform ANOVA directly on the results. Therefore the degradation functions were used to generate a large dataset for every factor over time as in [46]. Subsequently ANOVA is performed to relate the design parameters to the performance characteristic.

First the degradation function of the performance characteristic needed to be identified. For this regression was performed on the data for the current rise time that was obtained in the DOE's. This resulted in the following function of the current rise time and its variance over time:

$$\mu_Y(t) = 538,024 - 3,942 \cdot 10^{-6} \cdot t + 8,289 \cdot 10^{-14} \cdot t^2 \quad (eq. 6.1)$$

$$\sigma^2_Y(t) = 3,88 + 3,928 \cdot 10^{-7} \cdot t + 2,252 \cdot 10^{-13} \cdot t^2 \quad (eq. 6.2)$$

This degradation function and the degradation functions of the design parameters were used to generate large datasets for these parameters over time. Subsequently ANOVA was used to determine how the design parameters influence the performance characteristic. The ANOVA table indicated that all terms that were tested were significant. Fitting this sort of model led to awkward degradation paths that contained twists. Small extrapolations also led to strange turns and twists in curvature that did correspond with expectations. The ANOVA could therefore not be trusted.

Therefore it was decided to use the model of the form that resulted from the DOE's that were conducted during Van Hoorn's master thesis project. These DOE's did have consecutive level settings and could therefore be easily analysed by means of ANOVA.

The main reason however for using these model terms is the fact that Van Hoorn's eventual model corresponded with the physics of failure that were observed. According to figure 6.2 the load should have a second order term with a negative coefficient. Moreover it was known from Van Hoorn's thesis that a higher resistance leads to a higher rise time.

Therefore the following form of the model was fitted [11].

$$\mu_Y = \alpha_0 + \alpha_1 \mu_{X_1} + \alpha_2 \mu_{X_2} + \alpha_{11} \mu_{X_1}^2 \quad (\text{eq. 6.3})$$

$$\sigma_Y^2 = \beta_0 + \beta_1 \mu_{X_1} + \beta_2 \mu_{X_2} + \beta_{11} \mu_{X_1}^2 \quad (\text{eq. 6.4})$$

Here  $\mu_Y$ ,  $\mu_{X_1}$  and  $\mu_{X_2}$  represent respectively the mean value of the performance characteristic and the mean values of the dominant design parameters, while  $\sigma_Y^2$ ,  $\sigma_{X_1}^2$  and  $\sigma_{X_2}^2$  represent respectively the variance of the performance characteristic, and the variance of design parameters  $X_1$  and  $X_2$ . The coefficients  $\alpha_0$ ,  $\alpha_1$ ,  $\alpha_2$ ,  $\alpha_{11}$ , and  $\beta_0$ ,  $\beta_1$ ,  $\beta_{11}$  and  $\beta_2$  will have to be determined by means of regression.

First the regression model for the mean is determined. This is done by means of nonlinear regression with least squares estimation (LSE). LSE minimizes the sum of the squared errors to obtain the coefficients in a degradation model. The estimation is made based on the data from the Main experiment (appendix F). For this not the added values are used, but the real values of the design parameters. This gives a real representation of the factors that influence the nip motor and more over facilitates the optimization step. The regression model is as follows.

$$\mu_Y = 504,964 + 6,292 \mu_{X_1} + 24,794 \mu_{X_2} - 0,692 \mu_{X_1}^2 \quad (\text{eq. 6.5})$$

The resulting  $R^2$  for this model is 94,75 percent.

This model represents the influence that the actual resistance and load have on the current rise time of the motor. Note that the design parameter factors are both functions of time that can be substituted into this model, making it time-dependent. Figure 6.14 represents the influences of both design parameters on the performance characteristic separately. Note that these influences are as expected.

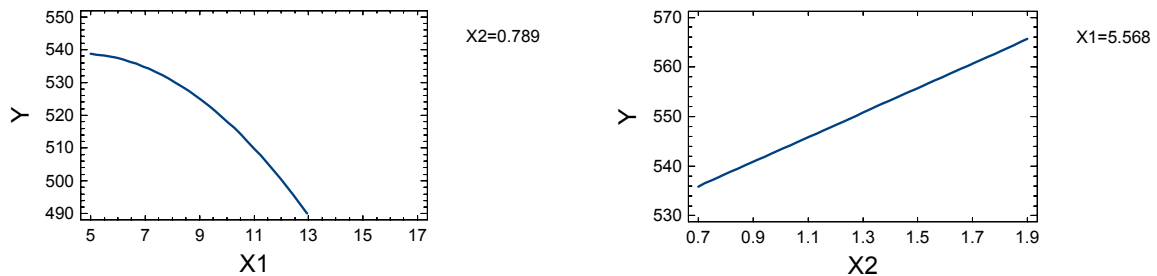


Figure 6.14: Influence of the actual DP values on the PC

The second regression model that should be determined concerns the expected variance of the performance characteristic as a function of the variances of the design parameters. This is however impossible due to a lack of information on time dependent unit-to-unit variation of the design parameters load and PWBA resistance.

### § 6.3.3 Specification limits

A product will only function properly as long as it satisfies its specifications. In order to determine the product's expected lifetime a specification limit needs to be set beyond which the product does no longer function properly and has thus failed. Setting the specification limits on the performance characteristic current rise time is somewhat more complicated than on other parameters, because there simply is no hard current rise time limit below which the paper transport function stalls and fails.

First of all it can be concluded that because of the dominant influence of the load on the rise time no upper specification limit needs to be set. The lower specification limit of the current rise time is reached when one of the degrading design parameters has reached its limit. Hence the expected TTF for both design parameters is calculated based on the degradation models that were obtained in the previous chapter.

#### USL load

The upper specification limit for the load does not only depend on the initial load on the system, but also on the motor that is used. Appendix G shows us that the mean initial load is equal to 5,33 Ncm and that the systems stalls at a mean load on the motor of 14,84 Ncm with a standard deviation of 0,33 Ncm. The mean expected load increase on the motor till failure will therefore be 9,51 Ncm. Hence the expected TTF will be:

$$\text{Load increase}(t_{USL}) = 2,0522 + 7,13689 \cdot 10^{-7} \cdot (t - 745.541,5) = USL = 9,51 \text{ Ncm}$$

This is at:

$$t_{USL} = 11.195.191 \text{ copies}$$

The upper specification limit of the PWBA resistance was determined on the module that was used in this main experiment, because this was the only new module present with this new PWBA. The maximum resistance that could be added until the failure of the system was observed to be 1,9  $\Omega$ . The standard deviation of the initial resistance of 12,9 m $\Omega$  will probably be a few negligible mili Ohms in comparison to the maximum added resistance of 1,9  $\Omega$ . This value of 1,9  $\Omega$  is assumed to be a hard limit that applies to all Finishers. Unfortunately no comparisons can be

made on this subject because there are no other parts that can be compared. Hence the expected TTF as a result of resistance increase of the PWBA will be:

$$R \text{ increase}(t_{USL}) = 1,293 \cdot 10^{-11} \cdot t^2 = 1900 \text{ m}\Omega$$

This is expected to be at:

$$t_{USL} = 12.122.091 \text{ copies}$$

According to these calculations the load is expected to be the first factor to fail. The expected value of the current rise time at this moment can be used as the lower specification limit for the rise time. Using equation 6.1 the LSL will consequently be:

$$LSL = \mu_y(t_{LSL}) = 538,024 - 3,942 \cdot 10^{-6} \cdot 11.195.191 + 8,289 \cdot 10^{-14} \cdot (11.195.191)^2 = 504.28 \mu\text{s}$$

Figure 6.15 shows the expected degradation of the performance characteristic over time with the lower specification level at which the paper transport function is expected to fail.

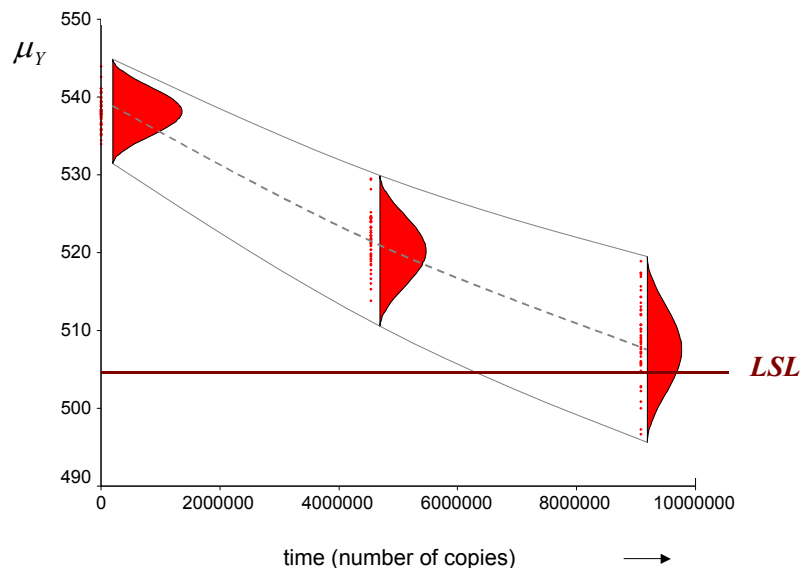


Figure 6.15: Performance characteristic as a function of time

The figure shows the decrease of the performance characteristic over time. Note that using the calculated specification limit would lead to the rejection of a part of the population even though the system was still functioning properly at this time. This is the unfortunate result of the fact that the degradation of the design parameters causes failure and not the degradation of the performance characteristic.

### § 6.4 Discussion

The Main experiment did not directly result to success. During the first attempt it was found out that the load on the system increased significantly with 3,11 Ncm. This was possibly due to the measurement routine. The paper transport system (including the shafts) was kept running and hot (motor between 62 and 63 degrees C) continuously before, during and between measurements.

Taking into account the slow degradation that was observed in the degradation test of the previous chapter, this increase of load was surprising and unexpected. This led to uncertainty about the nominal system load and total system load during the DOE's. Hence these DOE's could no longer be translated back to time. Consequently the experiment needed to be redone. Therefore the load of the Finisher was reduced by cleaning the shafts of the system. Appendix H shows the contribution to degradation of the shafts. This information may be used for further research on the load increase of the Finisher module.

The degradation models that were constructed in the previous chapter were used in this chapter to set up an experiment to predict the behaviour of the performance characteristic over life. Therefore the expected values of the design parameters were calculated at three points in time: when the product is new, halfway its life and as close as possible near its end of life. These expectations of degradation were manipulated in the system in order to model the change of the performance characteristic over time.

The experiment attempted to generate a probability distribution of the performance characteristic as a consequence of the variation in the design parameters between Finishers. Therefore unit-to-unit data on the design parameters of new Finishers were used for level setting in a design of experiments at the first time point. Unfortunately the lack of information on variation in degradation speeds between Finishers made it impossible to incorporate such variation in the other DOE's. Hence for these design parameter settings the same variation is used.

The experiment resulted in three normal distributions of the performance characteristic at each point in time. It was however not possible to perform ANOVA to determine the relevant terms in a model for the PC as function of its DP's with the standard statistical tools. Therefore a functional relationship was established between the performance characteristic and its design parameters based on the shape of the model by Van Hoorn [11]. Application of non-linear regression led to a model that corresponds to physics of failure expectations. This model in combination with the degradation models of the design parameters and the calculated specification limit makes it possible to predict and optimize reliability.

The Main experiment resulted in a model of the performance characteristic over time, which accurately represents the DOE settings. Some remarks must however be made to the question whether it accurately represents reality. The performance characteristic is a factor that represents the degradation of two factors. This implies that its accuracy and its uncertainties are also influenced by the accuracy and uncertainties in these two parameters. Recall, the remarks that were made in chapter 5 with respect to the degradation of the PWBA resistance. This model contained some uncertainties considering its accuracy. Extrapolating this model to time-to-failure increases the inaccuracy of the model, moreover because it is modelled as a second order function. The same can be said regarding the load even though this factor is modelled as a linear function of time.

A system or function fails when the performance characteristic exceeds its specification limit or when one of the design parameters exceeds its specification limit; whichever occurs first. In the case of the paper transport function the design parameter load will be the first parameter to exceed its specification limit. Therefore the specification limit of the current rise time was calculated based on the failure time of the load. Figure 6.15 shows that this leads to the possibility that Finishers with a lower current rise time than the lower specification limit still function properly. Hence the calculated lower specification limit for the performance characteristic current rise time is not a hard limit.

The final point of discussion applies to the unit-to-unit variation. It is very well possible that a different Finisher module would have degraded slower or faster than the unit that was used in the ADT. This would lead to a different behaviour of the performance characteristic over time and also to a change in variation. This makes it difficult to say if this function of the performance characteristic is representative for the entire Finisher population. The experiment that is described in this chapter however uses the initial unit-to-unit variation of new Finishers to model the performance characteristic for the Finisher population. Therefore the only variation that the model over time does not take into account is possible difference in degradation speeds between units [25]. For the time being there is no data that indicates that the two design parameters deteriorate significantly faster or slower for other Finisher units.

## Chapter 7 Design optimization

The mathematical functions that were derived in the previous two chapters make it possible to perform the last phase of the ROMDA concept. This implies an optimization step of the product's design with regard to robust reliability. First the performance of the present situation is determined. Subsequently the Desirability Technique by Derringer and Suich [32] is applied to find the settings for the design parameters that lead to the desired balance between Mean Time To Failure and the variance of the Mean Time To Failure. This optimized situation is then compared to the former, after which conclusions will be formulated.

### § 7.1 Performance present situation

Before calculating the optimal design parameter settings, the performance in the present situation should first be determined. In order to do this a simulation is run based on the obtained models with their variances. The degradation paths are presented in figure 7.1 and 7.2. The figure represents the simulation of a sample of 1000 Finisher modules.

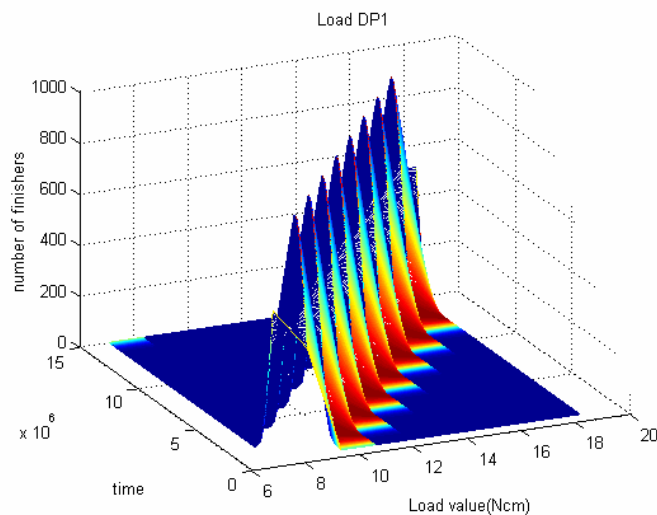


Figure 7.1: Simulated degradation path of the load for one thousand Finishers

The simulations are started at 745.541 copies. This is the lifetime from where on the load increases linear with time. These degradation paths are again superimposed on the rise time by means of equation 6.5. The resulting current rise time of the nip motor is presented in figure 7.3 a. For clarity this degradation function is presented in 2D. Application of the lower specification limit of  $504,28 \mu s$  leads to the failure rate curve in figure 7.3 b.

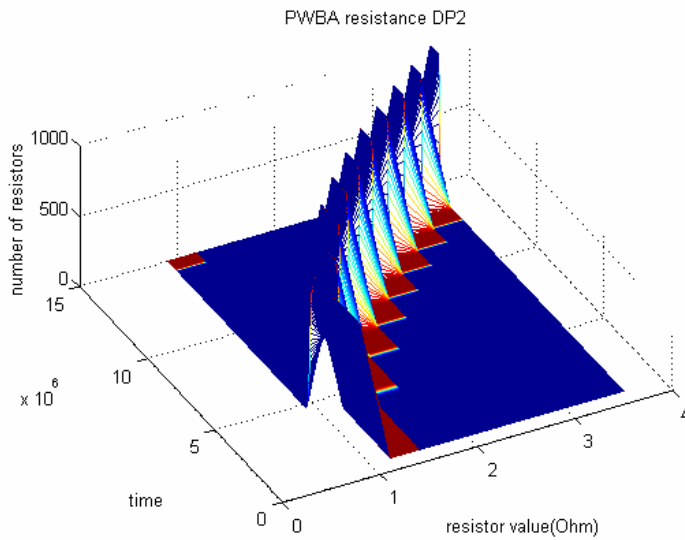


Figure 7.2: Simulated degradation path of the PWBA resistance for one thousand Finishers

The resulting degradation of the current rise time is represented in the following figure.

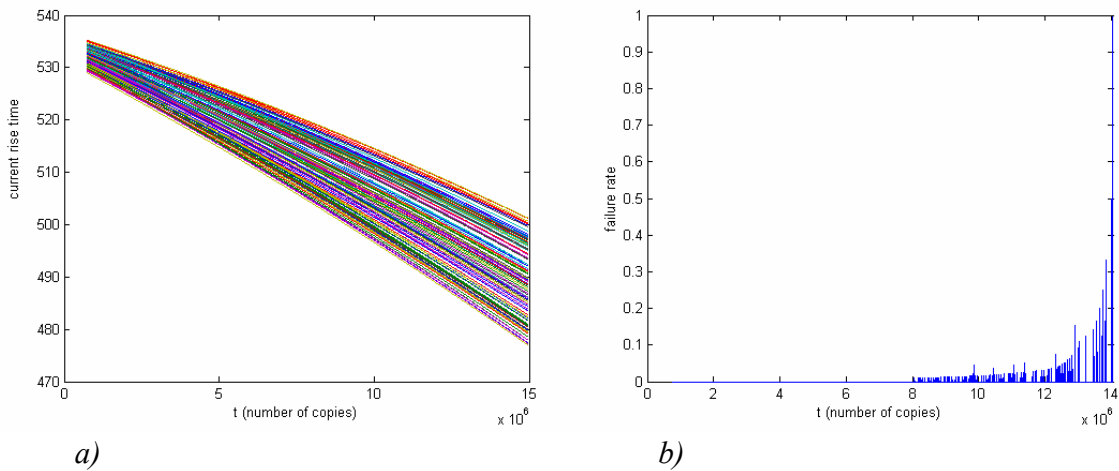


Figure 7.3:  
 a) The resulting current rise time  
 b) Failure rate curve for the Finisher population.

The resulting current rise time also shows the increasing variance as a result of the degradation of the design parameters as was observed during the Main experiment. It does however seem to have somewhat less curvature than figure 6.13. This may be the result of the deviations in fit of the model. On the other hand, figure 7.3 a) was constructed with a lot more samples. The model also shows that extrapolation of the rise time beyond the time of the last DOE leads to a faster decrease of this performance characteristic. This indicates an increasing dominance of the load over the resistance. The resulting failure rate curve for the Finisher population seems to start at

about eight million copies while all Finishers have failed at about 14 million copies. The failure rate curve shows a slow start after which it exponentially increases.

The expected MTTF that results from this simulation is 11.215.541 copies and the log of the Standard Deviation of the TTF,  $\log(\text{SDTTF})$ , is 14,48. Note that the MTTF is just negligibly higher than the in section 6.3.3 calculated TTF of 11.195.191. This difference can be dedicated to the fact that that TTF was calculated for the average Finisher while here the initial values of the Finisher from the Main experiment are used. The next section will attempt to optimize the design of the Finisher module. The performance indicators that are used to compare the new with the present situation are the MTTF and the SDTTF.

### § 7.2 Optimization of the Finisher module

In this section the Finisher module is optimized based on the performance indicators MTTF and SDTTF. The Desirability Technique by Derringer and Suich [32] is applied to determine the design parameter settings that lead to an optimal balance between MTTF and SDTTF. How this Desirability Technique works for the response variables MTTF and SDTTF is explained in appendix I. Before this method can be applied first the functions for the MTTF and SDTTF need to be established. This is done by means of a Design Of experiments on the simulation data.

First the function for the load is interpolated to time  $t=0$  in order to be able optimize the initial setting of the load. Therefore the load is interpolated to time  $t=0$  as if it were linear. The calculation is presented below. Figure 7.4 shows a graphical representation of this calculation.

$$\text{Load increase} = 7,13689 \cdot 10^{-7} \cdot 745.541 = 0,532 \text{ Ncm}$$

Therefore the initial load will be set  $2,052 - 0,532 = 1,52$  Ncm higher. This makes it possible to use the linear part of this degradation model from  $t=0$ .

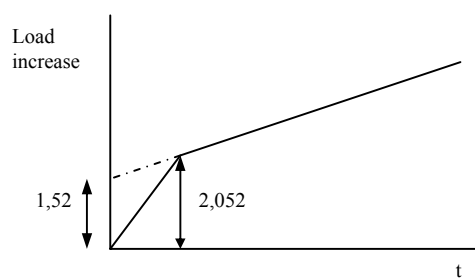


Figure 7.4: Interpolation of the degradation model

Subsequently the models for the MTTF and SDTTF are constructed based on a simulated DOE. Here the nominal values of the design parameters are used as center points and the standard deviations as applied in the Main experiment of 0,4 Ncm and 0,02  $\Omega$  are used as + and – settings. The DOE is constructed in order to make a model of the MTTF and SDTTF as a function of the DP's.

With this model the nominal design parameter settings can be optimized near the current settings as in [46]. The DOE results are as follows:

Table 7.1: DOE on the TTF

run	pattern	DP <sub>1</sub>	DP <sub>2</sub>	MTTF	Log(SDTTF)
1	--	6,688	0,689	12.105.541	14,60
2	-+	6,688	0,889	13.615.541	14,58
3	00	7,088	0,789	11.215.541	14,48
4	0-	7,088	0,689	10.165.541	14,31
5	+-	7,488	0,689	8.354.541	14,21
6	++	7,488	0,889	9.905.541	14,30
7	0+	7,088	0,889	11.815.541	14,49
8	+0	7,488	0,789	9.245.541	14,16
9	-0	6,688	0,789	12.505.541	14,58

The resulting functions do not directly contain these values, but correspond to places in the time matrix. This makes the calculations easier for the optimization program. The following functions are established:

$$MTTF = 1025.71 - 178,55 * DP_1 + 78,67 * DP_2 \quad (eq.7.1)$$

$$\log(SDTTF) = 5.201 - 0,182 * DP_1 + 0,041 * DP_2 \quad (eq.7.2)$$

The model of the PC as function of its DP's is only valid for the settings interval of the Main experiment and somewhat beyond. This puts limitations to the optimization range of the design parameters. Moreover optimization intervals need to be determined for the design parameter settings that are practically possible. Hence the following optimization intervals were defined:

$$DP1=[6.288; 7.888] \text{ and } DP2=[0.629; 0.989]$$

Subsequently, the optimal design parameter settings are calculated as described in appendix I. The target value for the MTTF is set to be twenty million and the target value for the log(SDTTF) is set near zero. The coefficient  $r$  is set to be 1.

This results in the following optimal values:

$$DP1 = 6.288 \text{ Ncm, which corresponds to a real setting of } DP1 = 6.288 - 1.52 = \mathbf{4.768 \text{ Ncm}} \text{ and } DP2 = \mathbf{0.989 \Omega}$$

This leads to a MTTF of 12.575.541 copies, which is 12,1 % longer than the expected 11.215.541 copies for the system that was used in the Main experiment. The log(SDTTF) is somewhat higher however. It has increased from 14,48 to 14,56, which is an actual increase from 1.943.498 copies to 2.105.366 copies. This is an increase in percentage of 8,3 %.

### § 7.3 Discussion

In conclusion it can be said that the simulated optimization step resulted in a considerable increase of the Mean Time To Failure of the Finisher module. This was accompanied by an also considerable loss in robustness of the reliability of the system's TTF. The person that performs the calculations can easily change the design parameter settings, MTTF and SDTTF that result from this optimization step. Depending on the wishes of the producer of the product, in this case

Flextronics, it can be decided to put more emphasis on one of the performance indicators MTTF or SDTTF. This can be achieved by adjusting the target values in the calculation to these wishes. This makes the Desirability Technique that was used a very flexible optimization method. With regard to outcome of the optimization step it needs to be said that it was not possible to verify the results in practice.

In this optimization step the design of the module was improved with regard to its performance characteristic. The lower specification limit of the PC was calculated based on the failure time of the design parameter load in combination with the initial settings of the Finisher module. This is described in sub-section 6.3.3. When the design is optimized (emphasis on MTTF) with regard to the performance characteristic this will lead to an initial value of the performance characteristic that results in an as large as possible time for the PC to reach its lower specification limit. However, in case the performance characteristic does not lead to failure, but one of its design parameters, the optimization method may calculate a setting for the non-dominant DP that moves the PC away from its failure limit. Therefore this may cause the false idea that the new MTTF is higher than it actually is. This can best be explained with an extreme example:

Imagine that we have the same design parameters load ( $DP_1$ ) and PWBA resistance ( $DP_2$ ) that influence the same current rise time (PC). But now the only parameter that can lead to failure is the load. Hence there exist no specification limits for  $DP_2$  or for the PC and the LSL for the rise time is calculated based on the expected failure time of the load. Subsequently the optimization algorithm is run. The initial value for the load turns out to be already the optimal value. The PC is however higher when the PWBA resistance is higher. And the higher the PC the longer it takes for the PC to reach its lower specification limit. Therefore the optimization algorithm will result in an extremely high setting for the PWBA resistance ( $DP_2$ ). The following figure illustrates this example.

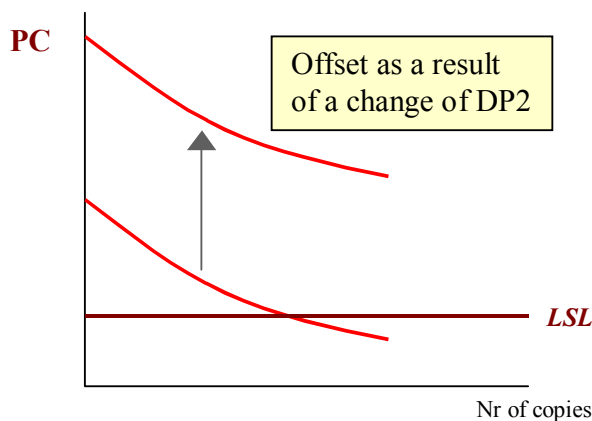


Figure 7.5: Example optimization issue

This figure indicates that it takes a huge amount of copies for the current rise time to reach its LSL and that the Finisher function would have an extremely longer MTTF than before.

However, because the nip motor will still stall at the same amount of load, which will be reached after the same expected amount of copies, the optimized situation in this example cannot be correct. With this in mind, it may be so that the MTTF in the optimized situation in section 7.2 is actually lower than that was calculated.

---

## Chapter 8 Conclusions & recommendations

### § 8.1 Research question

This final chapter discusses the conclusions of this work and provides recommendations to the ROMDA concept and to the possible implementation by Flextronics. The ROMDA concept by Van den Bogaard attempts to identify the dominant failure mechanism of a complex system and subsequently analyse and model the degradation of the design parameters that cause this failure mechanism. Degradation of these design parameters is then related to a performance characteristic that represents the failure mechanism. The concept finally aims to optimize the product's design by means of parameter design and tolerance design. This master thesis project investigates the possibility of practical application of ROMDA to the objectives of Flextronics Venray. Therefore the research question for this master thesis was formulated as follows:

*Is it possible to implement the ROMDA concept as proposed by Van den Bogaard into practice and apply it to design optimization, preventive maintenance and re-use?*

In the remainder of this chapter the conducted research will be reviewed. This will result in conclusions on this work, conclusions on the ROMDA concept and the answer to the research question. Subsequently recommendations will be made on further improvements on the ROMDA concept and for possible implementations for Flextronics International Europe.

### § 8.2 Review of this research

The first chapter provides an introduction to this thesis. It identifies the relation between today's business trends and the different business drivers that are important to companies. This advocates for involvement in the early stages of the product creation process. This leads to the introduction of the ROMDA concept, which is a concept for reliability prediction and optimization that can be applied in the early design stage. In this thesis it is investigated if it is possible to apply the ROMDA concept to the objectives of Flextronics International to optimize the design of its products and support re-use and preventive maintenance decisions based on one performance characteristic.

Chapter 2 discusses the literature that is relevant to the ROMDA concept and to this thesis. It starts, so to speak, with a broad view on reliability and then converges to ways to achieve robust reliability. First an introduction to reliability is provided. Subsequently reliability problems are categorized based on the dimensions time, specifications and statistics. Then section in three the topic reliability prediction is introduced followed by the Bathtub and Roller coaster curve. From there on the chapter moves on to literature on degradation testing, Robust Design and Tolerance Design, which are directly relevant to this work and to the concept.

In chapter 3 the basic idea behind the ROMDA concept is discussed. The chapter describes how the physical degradation of the design parameters affects the performance characteristic and shows the mathematical relationship between the parameters. It further shows how reliability can be calculated based on these functions in combination with specification levels. Analysis of the physical degradation of the design parameters provides for better understanding of the product's failure mechanism because it demonstrates how certain components actually degrade. Moreover, it provides for less uncertainty and higher credibility with regard to extrapolation to TTF. The establishment of a link between a performance characteristic and its degrading design parameters

provide for the opportunity to optimize the design with regard to the design parameters. Chapter three concludes with a definition of the application area of the ROMDA concept and the necessary elements for the concept in order to make predictions on reliability and to optimize the design of a product.

The fourth chapter starts with the roadmap that applies to the ROMDA concept. This roadmap is established in an order that provides for the best progress with regard to time and outcome. The chapter explains that the degradation profiles that are obtained in the degradation-testing phase should be applied in the set-up of the main experiment. The chapter further discusses the results that were achieved before the start of this master thesis. The results that were obtained in earlier experiments were conducted to see if it is possible to superimpose the degradation of the design parameters on the performance characteristic. The settings in this experiment were however not based on actual degradation data and could therefore not be related to real time. Moreover, the design parameters were assumed to have a linear degradation function. Therefore an accelerated degradation test was set-up in the next chapter in order to capture the actual physical degradation of the design parameters.

Chapter 5 contains the set-up, analysis and results of the accelerated degradation test that was performed on the Finisher module. The ADT accentuates that the failure mechanism that was selected before this thesis, is not the dominant mode of failure. Especially the rails in the module, which are used for movement of the Tamper and stapler M6, turn out to be weak points. The degradation test also pointed it out the difficulties of performing degradation analysis on large complex systems. This made the test time consuming. Testing only one Finisher unit took away the possibility of incorporating variation in degradation speeds between units in the next experiment. With regard to the operating conditions of the Finisher it must be emphasized that the assumption was made that not using paper during life acceleration would have a negligible effect on the degradation of the paper transport function. The same was assumed for the influence of actual time on the degradation of the PWBA. It is assumed that the shapes of the degradation models of the design parameters are representative for the degradation for these parameters of all Finishers. The results of this chapter are degradation models for the two design parameters and the conclusion that the factors current rise time, current peak A and current peak C may be used as performance characteristics.

In chapter 6, the degradation of the design parameters over life is related to the performance characteristic. The expected degradation of the design parameters is calculated at three points in time. One at  $t=0$ , one halfway its life and one near time-to-failure. This degradation is superimposed on the performance characteristic by means of Design Of Experiments. Here the unit-to-unit variation for new Finishers is used to generate a population of Finishers with different design parameter settings. It was assumed that the unit-to-unit variation of the design parameters stays constant over time as presented in figure 3.2 a). Therefore the experiment takes into account all sorts of unit-to-unit variation except for possible variation due to different degradation speeds [25]. This has resulted in a model of the performance characteristic as a function of its design parameters. In combination with the degradation models of the DP's and specification limit of the PC it is possible to estimate the product's quality and reliability at any moment in time. The use of more DOE's will probably lead to a more accurate model for the performance characteristic. However the three DOE's make it possible to determine if the PC's behaviour is linear, concave or convex with time. Because the DOE's are performed at great time distances with the last DOE just before failure this will probably lead to a good predictor for reliability over life. The specification limit for the paper transport function is in this case based on the time-to-failure of the DP that is expected to fail first. This is the load on the nip motor. Calculation of the lower specification limit of the performance characteristic based on this TTF leads to the unfortunate

fact that some products are rejected while they are still functioning properly. This is demonstrated by figure 6.15.

The combination of the two previously named functions enables the possibility of design optimization in chapter 7. Application of the Desirability Technique leads to the following design improvements.

The initial load should be set at 4,768 Ncm.

The initial PWBA resistance should be set at 989  $m\Omega$ .

This leads to an increase of 12,1 % for the MTTF and unfortunately also an increase of the SDTTF with 8,3%.

The Desirability Technique is a flexible method that has the possibility to put more or less emphasis on MTTF or SDTTF. This allows for the producer, Flextronics, to determine what balance between these two performance indicators it prefers for its products.

The optimization is performed on a performance characteristic with a lower specification limit that is the result of the expected failure time for the load. Section 7.3 provides a motivation how the PWBA resistance may affect the optimization of the MTTF and why the optimized MTTF may actually be lower than that was calculated.

### **§ 8.3 Final conclusions**

The final conclusion of this master thesis contains a statement on the research question. The following subsection starts by providing conclusions on the specific case of the Finisher module based on the observations that were made and the experience that was gained during the experiments of chapter five and six and the optimization in chapter seven. Subsequently the second subsection provides general conclusions on the ROMDA concept. The final section then provides a statement with motivation on the research question.

#### **§ 8.3.1 Finisher module**

The failure mode that was selected in a previous phase of the project proved not to be the dominant failure mode of the Finisher module. During the accelerated degradation test three rails in the Finisher module failed as a result of friction and contamination. Several other functions of the module also failed long before the paper transport function was expected to fail. These failures complicated the measurements and made them time consuming. But more importantly, the failure mode identification phase did not result in a parameter with which the quality and reliability of the entire module could be assessed. This also resulted in a degradation test that was more time consuming than necessary.

The performance characteristic that was evaluated in this thesis has a lower specification limit that is based on the failure of the paper transport function due to the design parameter load. Therefore the specification limit of the PC was set at its expected value when the load is expected to fail. This specification limit is not a hard technical failure limit and therefore a Finisher may still be functioning properly although its current rise time has exceeded the limit (figure 6.15). This may, in extreme cases, lead to underestimation of the reliability of used Finishers and therefore to the decision not to re-use reliable systems.

The discussion in section 7.3 shows that optimization with regard to the current rise time may result in a setting for the PWBA resistance that affects the calculation of the MTTF. The calculated MTTF in the optimized situation is possibly higher than this would be in reality. This is due to the fact that not the performance characteristic, current rise time, but the design parameter load causes failure of the paper transport function.

---

### **§ 8.3.2 ROMDA**

The previous subsection provides two reasons why it is preferred to have a dominant failure mechanism that fails as a result of a performance characteristic that exceeds its specification limit(s) and not failure due to a design parameter. Using a failure mechanism that is the result of the failure of one of the design parameters results in a soft specification limit for the performance characteristic and more difficulties with design optimization.

The total execution of all the phases of the ROMDA concept has taken several years to complete. Although this was a first trial, which mainly entailed a lot of learning, it can be said that the total execution took considerable time. In the design stage of new products this can have a substantial impact on the development time. The importance of time-to-market for many products therefore puts limitations on the application area of the ROMDA concept. It can be concluded that the ROMDA concept should be applied to products with a large development time. Relating this to the business processes that are distinguished in section 2.2, these will mainly be the business processes of professional (production) systems.

### **§ 8.3.2 Research question**

This research project has proven that the performance characteristic and its design parameters show significant change over time. The physical degradation of the design parameters was modelled based on relevant literature that was consistent with the degradation data. Subsequently the degradation of the design parameters was superimposed on the performance characteristic, which resulted in a model of the performance characteristic over time. This model makes it possible to monitor the system's performance and make estimations on its reliability. Finally an optimization was performed which resulted in design parameter settings, which extend the expected mean time-to-failure with 12,1 % while the standard deviation of the time-to-failure increases with 8,3%.

Finally it may be concluded that it is possible to implement the ROMDA concept into practice. The resulting time dependent model of the performance characteristic provides the possibility to monitor the performance of the system in the field. This provides the possibility to plan preventive maintenance at moments that lead to lower costs. The models also provide the possibility to estimate the reliability of the system based on the performance characteristic. Reliability predictions may be used to estimate the chance of the system's survival in the field during another economical life. Finally the last phase of the concept led to an improvement of the design with respect to its time-to-failure.

One of the objectives of Flextronics could however not be satisfied. The current rise time of the nip motor is not a performance characteristic that can be used to measure or predict the performance of the entire Finisher module because it does not represent the dominant failure mode. Therefore it can only be used for the paper transport function.

### **§ 8.4 Recommendations**

This is the final section of this master thesis and provides the recommendations that result from this research. The first subsection provides recommendations to ROMDA. The second subsection provides recommendations on verification and the final subsection of this thesis does this for further research by Flextronics on the Finisher module.

---

### **§ 8.4.1 ROMDA**

The first recommendation on ROMDA applies to the failure mode identification phase. It is strongly recommended that failure mode identification on large complex systems be performed with field data, when available. Field data can provide a very useful indication of which parts or components wear out first. Apart from this conclusion it is recommended to make some adjustments to the Failure Mode and Effects Analysis method that was used here. This thesis proposes to add three columns to the FMEA that questions, first whether a failure mechanism is time-dependent, second, if this is expected to occur gradual, rapid or instantaneous. And third the FMEA should question if the factors are well measurable.

The second recommendation to ROMDA regards optimization with regard to the performance characteristic. The previous section already concluded that it is preferred to apply ROMDA to a situation where the performance characteristic is the first parameter to fail. When this is not the case and failure is the result of a design parameter that exceeds a specification limit, this can lead to difficulties in the design optimization step. In this case, this thesis recommends linking the lower specification limit of the PC to the design parameter that is dominant for failure. In other words, the LSL of the PC is a function of the DP that fails first. This should lead to a more precise optimization step. Applying this link does however demand for caution with regard to possible failure of the other parameters. Also the application of this link when there are interactions between the design parameters should be examined.

### **§ 8.4.2 Verification**

This next recommendation regards the verification of the results by Flextronics. The degradation models that were obtained for the design parameters do not contain variations in degradation speeds between units. This leads to uncertainties for reliability prediction purposes. Flextronics can resolve this uncertainty in two ways. The first is by conducting more degradation tests on more units. This is however time-consuming and inefficient. The other, more effective and efficient way is by means of keeping track of the age of the Finishers in the field and using field data.

The ROMDA concept as it was performed here, was carried out in a laboratory environment. Although one tried to let the Finisher perform as it would in the field, it can never be said with certainty that this was actually the case. The results of the accelerated degradation test in particular may have been affected by laboratory conditions. An implementation into practice should therefore always be verified and updated with field data.

### **§ 8.4.3 Further research**

The final recommendations apply to further research by Flextronics on the Finisher module. The accelerated degradation test proved the weakness of the rails in the Finisher, which failed due to contamination and friction. Especially the resulted failure of the Tamper is critical to the functioning of the Finisher, because the Tamper makes sure that the paper is neatly stacked. In order for Flextronics to find a parameter with which it can measure and assess the performance of the entire Finisher it is recommended to conduct further research on these rails, especially with regard to the Tamper.

The degradation test also demonstrated the degradation of the current peaks A and C for both staplers. These two performance characteristics may be used for further research on the degradation of the stapler units in the module.

---

## References

- [1] Coppola, A.  
*Reliability engineering of electronic equipment: A historical perspective*,  
IEEE Transactions on Reliability, Vol. R-33, 1984 Apr, pp. 29-35
- [2] Denson, W.,  
*The history of reliability prediction*,  
IEEE Transactions on Reliability, Vol. 47, No. 3-SP, 1998 September
- [3] Blischke, R.W., and Prabhakar Murthy, D.N.,  
*Reliability Modeling, Prediction, and Optimization*,  
John Wiley & Sons, Inc., 2000
- [4] Brombacher, A.C., Sander, P.C., Sonnemans, P.J.M., Rouvroye, J.L.,  
*Managing product reliability in business processes "under pressure"*,  
Reliability engineering & system safety, to be published 2004
- [5] Brombacher, A.C.,  
*Designing reliable products in a cost and time driven market: a conflict or a challenge*,  
Technische Universiteit Eindhoven, 2000
- [6] Cost of non-quality, Business Week, April 30, 1990
- [7] Boersma, J., Loke, G., Loh, H.T., Lu, Y., Brombacher, A.C.,  
*Reducing product rejection via a High Contrast Consumer Test*,  
European Safety & Reliability (ESREL) Conference, 2003, Vol. 1: 191-193.
- [8] Stevens, F.,  
*Vele eersten zullen de laatste zijn*,  
Publication Frits Philips institute for quality management, 1993
- [9] Jiménez, J.  
*Laser diode reliability: crystal defects and degradation modes*,  
Comptes Rendus Physique, Vol. 4, No. 6, 663-673, 2003
- [10] Bogaard, J.A. van den, Shreehan s/o Jayaram, J., Brombacher, A.C.,  
*A method for reliability optimization through degradation analysis and robust design*,  
Annual reliability and maintainability symposium 2003, Proceedings Cat. No.03CH37415, pp.  
55-62, 2003
- [11] Hoorn, M.C.H. van,  
*An evaluation of a concept for reliability prediction and optimization through degradation  
analysis and robust design*,  
Master thesis Technische Universiteit Eindhoven, 2003
- [12] Lewis, E.E.,  
*Introduction to reliability engineering*,  
John Wiley & Sons, Inc., 1994

- [13] Wong, K.L., and Lindstrom, D.L.,  
*Off The Bathtub onto The Roller-Coaster Curve*,  
Proceedings Annual Reliability and Maintainability Symposium, IEEE, 1988
- [14] Brombacher, A.C.,  
*Reliability by Design*,  
John Wiley & Sons, Chichester, 1992
- [15] Phadke, M.S.,  
*Quality Engineering using Robust Design*,  
Prentice Hall International, London, 1989
- [16] Spence, R., Singh Soin, R.,  
*Tolerance design of electronic circuits*,  
Addison Wesley, 1988
- [17] Institute of Electrical and Electronics Engineers  
*IEEE Standard Computer Dictionary: A Compilation of IEEE Standard Computer Glossaries*.  
New York, NY: 1990.
- [18] Dinesh Kumar, U., Crocker, J., Knezevic, J., El-Haram, M.,  
*Reliability, Maintenance and Logistic Support – A Life Cycle Approach*  
Kluwer Academic Publishers, Boston, 2000
- [19] Brombacher A.C., Van Geest D.C.L., Herrmann, O.E.,  
*Simulation, a Tool for Designing-in Reliability*,  
Quality and Reliability Engineering International, special edition on ESREF, 1993
- [20] Lu Y., Loh, H.T., Brombacher A.C., Den Ouden, E.den.,  
*Accelerated stress testing in a time-driven product development process*,  
Elsevier, International Journal of Production Economics, Volume 67, Issue 1, 2000, Pages 17-26
- [21] Wendai Wang;  
*Improving the quality of field data reliability analysis*  
Reliability and Maintainability Symposium, 2001. Proceedings. Annual, 22-25 Jan, pp.285-289,  
2001
- [22] Meeker, W.Q., Hamada M.,  
*Statistical tools for the rapid development & evaluation of high-reliability products*,  
IEEE transactions on reliability, Vol. 44, No. 2, 187-198, 1995
- [23] Kececioglu, D.B.,  
*Reliability and Life Testing handbook Volume 2*,  
Prentice-Hall, Englewood Cliffs, 1994
- [24] Lu, C.J, Meeker, W.Q.,  
*Using degradation measures to estimate a Time-to-failure distribution*,  
Technometrics, Vol. 35, No. 2, 1993

- [25] Meeker, W.Q., Escobar, L.A.  
*Statistical methods for reliability data*,  
Wiley-Interscience, 1998
- [26] Meeker W.Q., Escobar, L.A., Lu, C.J.,  
*Accelerated degradation tests: Modeling and analysis*,  
Technometrics, Vol. 40, No. 2, 89-99, 1998
- [27] Chiao, C.H., Hamada, M.,  
*Analyzing experiments with degradation data for improving reliability and for achieving robust reliability*,  
Quality and engineering international, 17, 33-344, 2001
- [28] Hamada M.,  
*Using statistically designed experiments to improve reliability and to achieve robust reliability*,  
IEEE transactions on reliability, Vol. 44, No. 2, 206-215, 1995
- [29] Tseng, T.S., Hamada, M., and Chiao, C.H.,  
*Using Degradation Data to Improve Fluorescent Lamp Reliability*,  
Journal of Quality Technology, Vol. 27, No. 4, 363-369, 1995
- [30] Tseng, T.S., Hamada, M.S., Chiao, C.H.,  
*Using Degradation Data from a Fractional Factorial Experiment to Improve Fluorescent Lamp Reliability*,  
Research Report no. RR-94-95, University of Waterloo, Canada, 1994
- [31] Yang, G., Yang, K.,  
*Accelerated degradation-tests with tightened critical values*,  
IEEE Transactions on Reliability, Volume 51 , Issue: 4 , 463 – 468, 2002
- [32] Derringer, G., Suich, R.,  
*Simultaneous optimization of several response variables*,  
Journal of quality technology, Vol. 12, No. 4, 214-219, 1980
- [33] Condra, L.W.,  
*Reliability improvement with Design of Experiments*, second edition,  
Marcel Dekker, Inc., New York, 2001
- [34] Stamatis, D.H.,  
*Failure mode and effects analysis: FMEA from theory to execution*,  
Milwaukee: ASQC Quality Press, 1995
- [35] Van den Bogaard, J.A., Van Hoorn, M.H.C.,  
*A method for signature analysis*,  
Technische Universiteit Eindhoven, 2002
- [36] Hulsken, G., Brombacher, A.C., Bogaard, J.A. van den, Wynn, H.P., Di Bucchianico, A., Peeters, B., Theunissen, T., Shangquan, D.,  
*End-of-Life management of electronics products through functional signature analysis*,  
Proceedings of APEX, Anaheim, CA, 2004.

- [37] Eurandom,  
*Survival experiment nip rolls*,  
2002
- [38] Handbook of friction units of machines,  
Kragel'skii, I.V., Mikhin, M.N., Spektor, M., Dunaevsky, V.V.,  
ASME Press, New York, 1988
- [39] Flextronics International Europe,  
*Main Tray Experiments*,  
May 2002
- [40] Ohring, M.,  
*Reliability and failure of electronic materials and devices*,  
Academic Press, London, 1998
- [41] Malucci, R.D.,  
*Fretting corrosion degradation, threshold behavior and contact instability*,  
Electrical Contacts, 2003. Proceedings of the Forty-Ninth IEEE Holm Conference on , 8-10 Sept.  
2003
- [42] Flextronics International Europe,  
*Screening Experiments*,  
October 2002
- [43] Bothe, K.R., Bothe, A.K.,  
*World class quality: using design of experiments to make it happen*,  
Amacom, New York, 2000
- [44] Landheer, D., De Gee, A.W.J.,  
*Dynamische contactverschijnselen*,  
Technische Universiteit Eindhoven, 1993
- [45] Flextronics International Europe,  
*Part-to-Part Experiments*,  
December 2002
- [46] Bogaard, J.A. van den,  
*Simulation of the possibilities of the ROMDA concept*,  
Working paper
- [47] Pinheiro, J.C., Bates, D.M.,  
*Approximations to the log-likelihood function in the nonlinear mixed-effects model*,  
Journal of Computational and Graphical Statistics, Volume 4, Number 1, pp. 12-35, 1995.
- [48] Palmer, M.J., Phillips, B.F., Smith, G.T.,  
*Application of nonlinear models with random coefficients to growth data*,  
Biometrics 47, 623-635, June 1991



7	487010	1	21h0d4m1	23.99	5.00	9.21	40.00	23	23.40	338	7.780	316.07	319.76	27888.00	524.02	197.54	407.62	226.60	201.49	411.70	223.55	
7	85353	2	21h0d4m2	23.99	5.00	9.26	40.00	23	23.80	339	7.800	315.56	321.40	27926.00	526.62	204.21	396.66	224.29	204.29	418.24	233.41	
7		3	21h0d4m3	23.99	5.00	9.29	40.00	23	24.10	339	8.120	315.78	318.98	27920.00	526.79	204.89	413.41	226.20	202.85	425.15	224.34	
7		4	21h0d4m4	24.00	5.00	9.31	40.00	23	24.30	339	8.080	315.20	319.07	28062.00	525.74	202.36	401.96	222.74	202.36	410.80	224.19	
7		5	21h0d4m5	24.00	5.00	9.37	40.00	23	24.70	339	7.860	317.49	320.59	27995.00	526.55	205.57	417.21	226.84	203.41	421.10	225.49	
Datum=Tijsdip aanzetten acceleratie cyclus date 24.01 time 12.45 hours																						
8	503640	1	23h0d4m1	24.00	5.00	11.42	37.00	22	23.80	347	7.520	316.20	316.39	27446.00	521.74	198.20	401.84	223.51	200.93	365.20	223.24	Flux peak down after resistance measurement. Old values were: 355, 356, 354, 354, 354
8	81933	2	23h0d4m2	24.00	5.00	11.45	37.00	22	23.80	347	7.600	316.67	317.80	27584.00	524.65	201.33	400.92	221.94	205.12	368.71	224.16	
8		3	23h0d4m3	24.00	5.00	11.49	37.00	22	24.00	346	7.600	316.88	320.20	27586.00	524.02	202.16	417.82	225.16	200.48	406.26	225.77	
8		4	23h0d4m4	24.00	5.00	11.51	37.00	22	24.30	344	7.820	317.09	319.89	27953.00	526.94	203.36	416.98	222.42	202.49	413.04	224.65	
8		5	23h0d4m5	23.59	5.00	11.54	37.00	22	24.80	343	7.060	317.67	320.68	27980.00	523.85	201.44	391.07	220.16	203.01	419.25	228.39	nsMIF peak at this V instead of a full (no current at peak s)
Datum=Tijsdip aanzetten acceleratie cyclus date 22.01 time 14.00 hours																						
9	509710	1	23h0d4m1	24.00	5.00	15.15	37.00	22	24.9	351	6.340	316.07	317.89	27778.00	522.70	196.09	399.86	219.17	195.29	412.16	219.69	Resistance not measured by Erk, therefore possibly different values
9	80953	2	23h0d4m2	24.00	5.00	15.20	37.00	22	25.4	351	6.540	316.68	317.80	27730.00	520.52	195.73	404.98	219.12	196.50	386.14	224.16	
9		3	23h0d4m3	24.00	5.00	15.23	37.00	22	26.7	348	6.520	314.30	317.50	27791.00	524.79	195.85	399.01	221.86	198.02	403.20	220.73	
9		4	23h0d4m4	24.00	5.00	15.26	37.00	22	26.9	348	6.680	317.80	317.60	27794.00	528.09	196.80	396.56	220.61	196.91	407.69	221.49	
9		5	23h0d4m5	24.00	5.00	15.45	37.00	22	26.30	349	6.260	315.49	316.99	27939.00	527.91	195.97	410.83	223.19	195.53	406.24	223.10	
Datum=Tijsdip aanzetten acceleratie cyclus date 23.01 time 17.00 hours																						
10	529505	1	26h0d4m1	24.00	5.00	11.21	40.00	22	24.40	355	6.640	316.08	322.68	27543.00	524.50	197.29	419.54	226.25	200.26	428.47	227.62	Red wire PVBE soldered before measurement
10	117849	2	26h0d4m2	24.00	5.00	11.24	40.00	22	23.70	350	6.660	317.03	321.28	27699.00	522.90	198.47	428.41	226.55	198.63	423.75	228.11	
10		3	26h0d4m3	23.59	5.00	11.39	40.00	22	24.40	352	6.500	314.88	320.30	27766.00	524.65	195.98	423.17	224.89	199.73	427.11	229.62	Shielded with new steeper head because of failure of (usually used one
10		4	26h0d4m4	24.00	5.00	11.41	40.00	22	26.40	349	6.740	315.29	319.49	28039.00	527.63	200.31	423.86	229.51	198.88	441.03	227.37	
10		5	26h0d4m5	24.00	5.00	11.43	40.00	22	24.80	351	6.680	316.89	321.69	27873.00	527.67	199.87	419.20	226.24	200.20	439.98	229.92	Times obtained without staples in paper (failure steeper head)
											316.49	322.59										
											318.15	328.20										
Datum=Tijsdip aanzetten acceleratie cyclus date 26.01 time 14.20 hours																						
11	542362	1	28h0d4m1	23.59	5.00	10.50	39.00	22	24.20	359	6.840	309.96	313.89	27550.00	526.48	205.47	401.41	230.42	206.93	410.02	233.57	Orange wire PVBE soldered after first resistance measurement
11	130705	2	28h0d4m2	24.00	5.00	10.52	39.00	22	24.30	351	6.680	309.40	313.18	27706.00	525.02	206.28	404.38	234.71	204.03	411.06	232.88	
11		3	28h0d4m3	23.59	5.00	10.54	39.00	22	24.30	350	6.660	310.11	314.10	27331.00	525.94	204.68	409.82	229.80	205.84	411.95	232.16	
11		4	28h0d4m4	23.59	5.00	10.56	39.00	22	24.80	349	6.660	309.87	312.80	27500.00	525.72	206.70	409.35	230.91	206.35	406.73	237.00	
11		5	28h0d4m5	23.59	5.00	10.59	39.00	22	24.80	350	6.600	309.49	314.19	27566.00	527.44	204.02	408.11	234.06	204.99	422.15	233.07	
Datum=Tijsdip aanzetten acceleratie cyclus date 26.01 time 11.30 hours																						
12	555293	1	30h0d4m1	24.00	5.00	11.05	42.00	22	23.80	317	9.160	310.29	313.68	26711.00	519.35	205.31	406.37	233.16	206.24	419.26	229.69	Alignment ledge of edge soldered broken off during acc cycle
12		2	30h0d4m2	24.00	5.00	11.10	42.00	22	24.10	316	9.220	311.47	314.19	26196.00	528.54	205.41	412.25	234.38	205.60	412.06	229.98	Measurements made with new ledge
12		3	30h0d4m3	24.00	5.00	11.15	42.00	22	24.30	316	8.650	308.51	311.40	27943.00	519.64	204.52	407.78	230.12	206.42	407.51	231.40	Flux change PVBE
12		4	30h0d4m4	24.00	5.00	11.20	42.00	22	24.40	317	9.040	309.98	313.39	27636.00	522.90	206.2	416.87	229.72	211.21	426.70	231.49	Unplanned out of control of solderpad
12		5	30h0d4m5	24.00	5.00	11.23	42.00	22	24.80	319	8.990	306.26	312.88	27693.00	521.96	211.98	406.85	231.13	208.15	420.88	232.11	High value CRT
Datum=Tijsdip aanzetten acceleratie cyclus date 30.01 time 12.30 hours																						
13	572742	1	02h0d4m1	24.00	5.00	12.02	48.00	22	23.10	323	7.460	311.74	313.01	27983.00	518.95	206.67	406.48	235.63	207.07	407.11	254.93	Add 39.921 extra cycles (MP motor only device running)
13		2	02h0d4m2	24.00	5.00	12.05	48.00	22	23.60	328	7.400	309.99	312.69	28039.00	520.29	202.60	396.38	231.52	205.69	386.50	233.05	Failure of lamp due to the degradation of its run time
13		3	02h0d4m3	23.59	5.00	12.07	48.00	22	23.90	328	7.300	310.49	313.78	28178.00	522.61	204.42	406.50	230.34	206.95	413.96	237.20	
13		4	02h0d4m4	24.00	5.00	12.09	48.00	22	24.20	331	7.320	309.26	313.78	28061.00	522.48	206.48	413.31	233.56	208.34	419.29	234.69	
13		5	02h0d4m5	24.00	5.00	12.11	48.00	22	24.40	332	7.280	309.50	313.18	28075.00	521.93	205.65	415.40	229.79	208.67	413.89	230.87	
Datum=Tijsdip aanzetten acceleratie cyclus date 02.02 time 14.24 hours																						
14	577078	1	03h0d4m1								7.900											
14		2	03h0d4m2								7.780											
14		3	03h0d4m3								7.840											
14		4	03h0d4m4								7.500											
14		5	03h0d4m5								7.800											
Datum=Tijsdip aanzetten acceleratie cyclus date 03.02 time 10.30 hours																						
15	582473	1	04h0d4m1	24.00	5.00	9.32	48.00	23	23.90	327	7.320	310.70	315.39	28354.00	523.00	203.02	405.32	228.86	204.11	421.85	230.60	
15		2	04h0d4m2	24.00	5.00	9.34	48.00	23	24.30	329	7.380	310.50	314.38	28515.00	519.69	204.94	404.42	228.15	207.47	411.03	229.43	
15		3	04h0d4m3	23.59	5.00	9.37	48.00	23	24.80	330	7.380	309.39	314.12	28394.00	524.47	205.62	408.17	225.10	205.63	408.21	228.02	
15		4	04h0d4m4	23.59	5.00	9.39	48.00	23	24.80	331	7.400	310.82	314.60	28508.00	522.73	204.21	406.29	223.86	205.48	407.17	229.73	
15		5	04h0d4m5	24.00	5.00	9.41	48.00	23	24.90	327	7.260	309.66	313.76	28409.00	523.34	205.16	406.87	229.60	206.31	411.18	226.87	
Datum=Tijsdip aanzetten acceleratie cyclus date 04.02 time 10.30 hours																						

16	59648	1	06red0met1	24.00	4.99	11.02	49.00	22	24.90	354	6.200	316.42	320.49	28160.00	532.69	209.87	432.55	236.68	211.29	441.68	236.76	Unexplained out of control for extended
16		2	06red0met2	24.00	4.99	11.06	49.00	22	25.10	354	6.660	317.21	322.85	28357.00	526.43	209.6	435.58	231.84	210.96	446.01	235.52	Unexplained high value of CRT
16		3	06red0met3	24.00	4.99	11.09	49.00	22	25.20	352	6.680	316.69	321.99	28367.00	528.55	209.89	446.52	234.57	212.87	446.90	236.27	Possible cause: see below (power supply)
16		4	06red0met4	24.00	4.99	11.15	49.00	22	25.40	352	6.480	317.10	320.08	28061.00	523.83	209.85	447.42	234.95	209.33	431.15	236.04	
16		5	06red0met5	24.00	4.99	11.21	49.00	22	25.60	352	6.360	315.29	320.68	28463.00	524.50	208.5	429.95	233.37	212.54	438.93	232.66	
Datum-Tidsstip aanzetten acceleratie cyclus																						
17	616423	1	09red0met1	24.00	5.00	9.10	41.00	22	22.60	332	6.400	315.15	318.49	27797.00	521.80	215.7	434.43	239.43	218.57	440.15	241.68	This measurement found that SV power supply was running at a current
17		2	09red0met2	24.00	5.00	9.15	41.00	22	23.20	339	7.160	316.09	317.99	27988.00	519.93	218.9	449.26	246.60	217.42	444.67	241.04	Identical of U.S.A in stead of 1.A. These measurements were done
17		3	09red0met3	24.00	5.00	9.20	41.00	22	23.80	330	7.860	314.49	317.09	27870.00	522.09	215.72	447.13	243.20	216.76	447.47	241.04	with 1.A. Ampere
17		4	09red0met4	24.00	5.00	9.23	41.00	22	23.80	342	6.820	315.59	317.69	27870.00	520.28	217.62	450.87	242.17	215.57	446.09	240.22	These measurements at previous time could be influenced
17		5	09red0met5	24.00	5.00	9.26	41.00	22	23.80	342	6.840	315.49	318.10	27827.00	522.97	215.03	431.62	241.91	215.07	446.41	243.46	One of the measurement taken on purpose
Datum-Tidsstip aanzetten acceleratie cyclus																						
18	630368	1	11red0met1	24.00	5.00	9.42	45.00	22	23.60	347	7.860	311.40	314.97	28554.00	520.99	215.94	427.16	237.34	215.64	434.63	238.52	
18		2	11red0met2	24.00	5.00	9.44	45.00	22	24.00	346	7.340	311.11	314.39	28451.00	522.09	217.53	419.79	238.67	216.63	425.09	239.56	
18		3	11red0met3	24.00	5.00	9.46	45.00	22	24.30	343	7.380	310.49	314.59	28700.00	522.49	215.60	419.66	238.10	215.19	431.63	239.41	
18		4	11red0met4	24.00	5.00	9.48	45.00	22	24.60	342	7.160	311.01	314.47	28717.00	528.55	214.48	431.36	241.24	217.53	436.46	241.39	Only orange wire was taken here and reconnected instead of the entire
18		5	11red0met5	23.99	5.00	9.50	45.00	22	24.80	350	7.420	311.92	315.29	28619.00	524.69	215.74	439.11	239.79	216.43	438.05	245.31	set of wires
Datum-Tidsstip aanzetten acceleratie cyclus																						
19	643996	1	13red0met1	24.00	5.00	11.23	44.00	22	21.00	341	7.260	311.26	314.95	21357.00	527.47	210.30	414.47	236.52	214.06	416.29	236.10	Solenoid hood was loose
19		2	13red0met2	24.00	5.00	11.25	44.00	22	21.60	342	7.380	311.79	315.02	25555.00	528.01	210.93	419.48	231.96	213.66	423.65	237.54	CRT is strangely high when solenoid is out of control
19		3	13red0met3	24.00	5.00	11.26	44.00	22	22.20	345	7.400	311.29	314.49	24901.00	528.84	212.97	418.14	235.91	214.87	427.39	237.77	
19		4	13red0met4	24.00	5.00	11.30	44.00	22	22.80	345	7.140	310.38	313.85	24965.00	538.72	215.6	417.52	234.38	214.80	427.79	238.25	Variation caused by orange wire
19		5	13red0met5	24.00	5.00	11.32	44.00	22	23.00	359	7.460	310.69	313.80	24950.00	530.13	214.95	424.15	236.63	213.12	412.06	238.55	
Datum-Tidsstip aanzetten acceleratie cyclus																						
20	650467	1	16red0met1	24.00	5.00	11.03	42.00	22	23.00	367	7.960	316.47	319.19	31626.00	525.84	216.0	419.67	240.09	219.32	430.22	243.52	Resistance main connector was already unplugged
20		2	16red0met2	24.00	5.00	11.05	42.00	22	23.20	366	7.840	316.30	321.67	31363.00	524.03	222.62	421.92	243.00	224.77	437.06	247.38	
20		3	16red0met3	24.00	5.00	11.07	42.00	22	23.50	360	7.800	316.49	322.10	30875.00	525.63	223.99	431.56	245.98	224.12	443.90	246.60	Solenoid hood was loose
20		4	16red0met4	24.00	5.00	11.09	42.00	22	23.60	370	7.600	317.66	320.98	31403.00	528.85	222.36	434.45	243.62	222.23	428.10	247.09	CRT is strangely high when solenoid is out of control
20		5	16red0met5	24.00	5.00	11.10	42.00	22	23.90	360	7.700	316.78	321.09	31227.00	526.51	223.68	433.11	246.36	225.39	435.40	245.97	
Datum-Tidsstip aanzetten acceleratie cyclus																						
21	677793	1	19red0met1	23.99	4.99	13.23	39.00	23	24.70	368	9.600	305.75	310.47	31451.00	524.56	216.62	407.03	230.41	219.66	411.64	235.47	Measurement tool has been set-up from scratch, because of movement to
21		2	19red0met2	23.99	4.99	13.26	39.00	23	25.00	368	9.260	306.41	311.18	31254.00	524.19	221.79	405.86	233.21	217.40	423.76	237.78	DTI measure the last couple of days
21		3	19red0met3	23.97	4.99	13.28	39.00	23	25.50	363	9.360	305.69	310.59	31216.00	526.32	220.38	406.43	236.63	216.72	415.86	235.45	Difficulties with edge solenoid
21		4	19red0met4	23.96	4.99	13.30	39.00	23	25.70	375	9.320	306.63	310.75	31155.00	521.99	222.5	396.28	234.35	221.80	411.94	236.60	Solenoid hood was loose
21		5	19red0met5	23.99	4.99	13.32	39.00	23	25.90	374	9.500	306.90	310.68	30901.00	525.29	222.02	406.51	236.38	221.03	402.46	238.66	CRT is strangely high when solenoid is out of control
Datum-Tidsstip aanzetten acceleratie cyclus																						
22	694539	1	20red0met1	24.00	5.00	14.57	33.00	24	24.70	333	7.200	307.69	313.32	30790.00	521.81	212.72	387.81	223.33	211.00	406.74	227.42	Solenoid hood was thought to be loose
22		2	20red0met2	24.00	5.00	15.00	33.00	24	25.30	341	7.120	306.69	313.80	30465.00	522.21	211.85	400.85	225.48	212.38	406.65	230.05	CRT is strangely high when solenoid is out of control
22		3	20red0met3	24.00	5.00	15.05	33.00	24	25.90	336	7.100	309.29	313.29	30451.00	520.42	209.22	402.30	223.80	211.29	406.55	225.76	
22		4	20red0met4	24.00	5.00	15.07	33.00	24	26.30	332	6.820	308.17	312.86	30502.00	526.77	209.57	397.15	227.76	209.09	405.09	226.19	Lab put a sheet back in the stack of paper before measurement initiation
22		5	20red0met5	24.00	5.00	15.09	33.00	24	26.50	334	7.020	308.19	313.28	30313.00	525.70	209.33	387.49	229.49	209.20	402.76	228.54	
Datum-Tidsstip aanzetten acceleratie cyclus																						
23	702978	1	25red0met1	24.00	5.00	12.23	39.00	22	23.10	374	8.420	307.10	311.83	27971.00	517.69	213.5	394.28	225.49	213.48	416.94	228.93	
23		2	25red0met2	24.00	5.00	12.26	39.00	22	23.60	374	7.700	306.96	311.32	27896.00	521.30	212.26	395.74	222.76	212.64	398.46	227.78	
23		3	25red0met3	24.00	5.00	12.28	39.00	22	23.80	362	7.660	306.80	310.59	27817.00	517.27	210.36	398.87	224.35	213.13	396.31	228.05	
23		4	25red0met4	24.00	5.00	12.30	39.00	22	24.10	359	7.380	306.10	309.90	27892.00	519.79	212.89	390.40	228.54	212.26	396.24	226.36	
23		5	25red0met5	24.00	5.00	12.32	39.00	22	24.30	359	7.600	307.12	311.40	28697.00	520.37	209.99	391.23	223.92	212.26	399.30	227.94	
Datum-Tidsstip aanzetten acceleratie cyclus																						
24	715210	1	27red0met1	23.99	5.00	9.26	35.00	22	22.10	347	8.420	311.60	315.63	27734.00	520.53	213.94	409.13	237.44	216.86	414.14	236.59	Resistance results has extreme range
24		2	27red0met2	23.99	5.00	9.30	35.00	22	22.60	346	8.060	311.26	315.69	27748.00	518.14	218.6	403.68	234.12	220.59	403.34	238.04	Problems with BG. Without 339, 335, 333, 333
24		3	27red0met3	23.99	5.00	9.33	35.00	22	23.00	339	8.180	310.69	316.68	27688.00	519.24	218.96	397.83	236.27	216.43	412.51	233.77	
24		4	27red0met4	23.99	5.00	9.36	35.00	22	23.30	413	8.320	310.01	316.47	27495.00	527.50	217.7	403.36	233.02	215.38	416.27	233.27	
24		5	27red0met5	23.99	5.00	9.38	35.00	22	23.90	445	8.460	311.76	315.17	27622.00	523.59	216.6	410.39	236.63	216.46	406.33	238.45	

## Appendix B: Used data degradation test

	Removed value	Removed for modeling	Not used value	Conspicuous value										
L3 copies	M7 copies	M6 copies	MIP copies	Solenoid T_CRT	PWBA R_Loc	Slip T1	Slip T2	M7	ipeaka M7	ipeakb M7	ipeack M7	ipeakb M6	ipeakb M6	ipeakb M6
1	0	0	26926.00	520.76	336	4.7	317.12	318.96	211.07	344.23	218.71	207.8	352.06	217.43
1	0	0	27042.00	521.42	337	4.92	317.8	318.29	209.89	355.57	218.36	212.24	361.49	220.37
1	0	0	27084.00	523.55	336	4.96	316.47	320.07	213.16	357.28	217.93	212.3	369.4	224.29
1	0	0	26844.00	524.46	336	4.86	316.89	318.6	209.24	359.7	219.79	208.43	357.67	223.02
1	0	0	26942.00	525.03	339	4.78	315.59	318.6	207.74	356.01	222.03	209.72	352.75	225.75
2	13120	86280	27351.00	528.48	342	4.58	314.79	319.69	190.5	383.72	192.74	190.62	391.78	196.44
2	13120	86280	27343.00	527.26	342	4.44	316.8	320.03	190.16	386.63	194.16	189.42	399.85	193.81
2	13120	86280	27462.00	526.57	343	4.16	315.42	319.09	188.54	387.09	189.9	192.23	393.91	195.36
2	13120	86280	27442.00	529.19	342	4.36	314.28	318.7	191.88	379.56	190.08	189.02	383.37	194.96
2	13120	86280	27317.00	529.18	341	4.36	314.82	318.5	189.49	396.92	185.5	186.03	395.56	190.54
3	39616	0	25750.4	526.57	338	5.42	320.695	323.995	177.83	364.73	201.53	180.39	365.9	202.62
3	39616	0	25750.4	524.81	339	5.6	319.896	324.595	176.56	363.46	193.44	177.75	364.44	204.55
3	39616	0	25750.4	525.49	339	5.66	320.085	323.189	182.95	369.16	203.43	187.73	364.95	201.75
3	39616	0	25750.4	526.53	338	5.7	317.982	321.034	179.51	368.75	200.08	177.75	375.06	198.86
3	39616	0	25750.4	528.16	339	5.74	317.083	319.494	178.24	374.53	199.16	177.3	368.43	200.2
4	52108	3831	332202	27463.00	338	5.675	315.083	317.58	194.6	410.89	225.75	197.73	392.87	226.67
4	52108	3831	332202	27519.00	339	5.515	312.7	317.5	197.6	388.8	220.94	196.93	401.12	219.94
4	52108	3831	332202	27604.00	339	5.735	313.91	316.98	195.26	399.81	219.49	194.41	394.74	220.53
4	52108	3831	332202	27553.00	338	5.445	313.16	316.94	192.91	400.59	221.42	192.82	402.96	219.55
4	52108	3831	332202	528.64	339	5.125	313.4	317.39	195.88	400.35	219.7	200.23	404.55	224.54
5	65915	8766	17532	433243.5	345	6.780	315.88	319.78	200.88	413.40	234.39	203.45	423.78	235.25
5	65915	8766	17532	433243.5	345	6.340	316.29	318.49	200.81	423.20	233.19	201.61	413.96	233.88
5	65915	8766	17532	433243.5	344	6.620	315.49	319.08	202.92	416.90	225.70	200.66	423.33	228.35
5	65915	8766	17532	433243.5	344	6.200	316.29	318.79	200.22	427.78	227.91	198.97	422.88	230.02
5	65915	8766	17532	433243.5	337	6.000	315.61	317.98	197.55	430.85	227.59	198.37	418.68	228.47
6	72257	10880	21760	577867.5	338	6.180	319.68	320.78	190.11	424.27	217.14	191.53	409.19	216.93
6	72257	10880	21760	577867.5	338	6.080	316.10	321.14	192.16	401.49	217.16	192.17	410.71	221.76
6	72257	10880	21760	577867.5	338	6.060	316.89	320.58	191.17	412.12	218.50	191.01	419.46	219.34
6	72257	10880	21760	577867.5	338	6.000	316.28	319.39	190.26	410.73	215.22	190.27	411.81	217.56
6	72257	10880	21760	577867.5	338	6.060	316.30	320.29	190.86	410.23	216.67	191.23	422.10	218.66
7	86353	15246	30492	662991.5	339	7.780	315.67	319.76	197.54	407.82	226.60	201.49	411.70	223.55
7	86353	15246	30492	662991.5	339	7.900	315.66	321.40	204.21	396.66	225.32	204.29	418.24	233.41
7	86353	15246	30492	662991.5	339	8.120	315.78	318.98	204.89	413.41	226.20	202.66	425.15	224.34
7	86353	15246	30492	662991.5	339	8.060	315.20	319.07	200.24	401.96	222.74	202.36	410.60	224.19
7	86353	15246	30492	662991.5	339	7.680	316.28	320.59	205.57	417.21	226.64	203.41	421.10	225.49
8	91983	17456	34912	706086.5	347	7.520	316.20	319.39	198.20	401.84	223.51	200.93	395.20	223.24
8	91983	17456	34912	706086.5	347	7.600	316.67	320.07	201.33	400.92	221.94	205.12	398.71	227.64
8	91983	17456	34912	706086.5	346	7.400	317.88	320.20	202.16	417.82	226.16	200.49	408.26	225.77
8	91983	17456	34912	706086.5	344	7.280	317.09	319.89	200.96	418.99	224.82	202.49	413.04	224.65
9	98053	19479	38958	745541.5	343	7.060	317.67	320.68	196.09	399.86	219.17	203.01	419.25	228.39
9	98053	19479	38958	745541.5	343	6.340	314.07	317.89	196.09	399.86	219.17	195.29	412.16	219.69
9	98053	19479	38958	745541.5	348	6.540	314.68	317.80	195.73	404.98	219.12	196.50	396.14	224.16
9	98053	19479	38958	745541.5	348	6.520	314.30	317.50	195.95	399.01	221.86	198.02	403.20	220.73
9	98053	19479	38958	745541.5	348	6.480	312.80	317.60	196.90	386.56	220.61	196.91	407.69	221.49
9	98053	19479	38958	745541.5	349	6.260	313.49	316.99	195.97	410.83	223.19	195.53	406.24	223.10
10	117849	26078.00	52156	874215.50	355	6.640	316.08	322.68	197.29	419.54	226.25	200.26	429.47	227.62
10	117849	26078.00	52156	874215.50	350	6.660	317.03	321.28	198.47	428.41	226.65	199.63	423.75	228.11
10	117849	26078.00	52156	874215.50	352	6.500	314.89	320.30	195.98	423.17	224.99	199.73	427.11	229.82
10	117849	26078.00	52156	874215.50	349	6.740	315.29	319.49	200.31	423.66	229.51	198.88	431.03	227.37
11	130705	30363.00	60726	957779.50	351	6.680	314.89	321.69	199.87	418.20	226.24	200.20	438.98	229.92
11	130705	30363.00	60726	957779.50	351	6.84	309.96	313.89	205.47	401.41	230.42	206.93	410.02	233.67
11	130705	30363.00	60726	957779.50	351	6.68	309.40	313.18	206.28	404.38	234.71	204.03	411.06	233.88
11	130705	30363.00	60726	957779.50	350	6.66	310.11	314.10	204.88	409.82	229.90	205.84	411.95	232.16
11	130705	30363.00	60726	957779.50	349	6.66	309.87	313.80	206.70	409.35	230.91	206.35	409.73	237.00
11	130705	30363.00	60726	957779.50	350	6.60	309.48	314.19	204.02	408.11	234.06	204.98	422.15	233.07

12	143626.00	34670.00	69340	1041766.00	28711.00	519.95	317.00	9.18	310.29	313.68	205.31	408.37	233.16	206.24	419.26	229.89
12	143626.00	34670.00	69340	1041766.00	28196.00	528.54	316.00	9.22	311.47	314.19	205.41	412.25	230.28	205.60	412.06	229.98
12	143626.00	34670.00	69340	1041766.00	27943.00	519.64	316.00	8.66	308.51	311.40	204.53	407.79	230.12	206.42	407.51	231.49
12	143626.00	34670.00	69340	1041766.00	27626.00	522.90	317.00	9.04	308.98	313.39	206.12	416.87	229.72	211.21	426.70	231.49
12	143626.00	34670.00	69340	1041766.00	27883.00	521.56	319.00	8.56	308.28	312.98	211.98	406.65	231.13	209.15	420.88	232.11
13	161085.00	40489.67	80979.33	1188170.50	27983.00	518.56	323.00	7.460	311.74	313.01	206.67	406.48	236.63	207.07	407.11	234.93
13	161085.00	40489.67	80979.33	1188170.50	28039.00	520.29	328.00	7.400	309.99	312.69	202.60	396.38	231.52	205.68	396.50	233.05
13	161085.00	40489.67	80979.33	1188170.50	28178.00	522.48	328.00	7.300	310.49	313.89	204.32	406.94	230.34	206.95	413.96	237.20
13	161085.00	40489.67	80979.33	1188170.50	28061.00	522.48	331.00	7.320	309.26	313.78	206.48	413.31	233.56	208.34	419.29	234.68
13	161085.00	40489.67	80979.33	1188170.50	28075.00	521.93	332.00	7.280	309.50	313.18	205.56	415.40	229.79	208.67	413.89	230.87
14	165421.00	41935.00	83870	1216354.50			7.90									
14	165421.00	41935.00	83870	1216354.50			7.78									
14	165421.00	41935.00	83870	1216354.50			7.84									
14	165421.00	41935.00	83870	1216354.50			7.50									
14	165421.00	41935.00	83870	1216354.50			7.50									
15	170756	43713.33	87426.67	1251032.00	28354.00	523.00	327	7.320	310.70	315.39	203.82	409.32	228.86	204.11	421.85	230.60
15	170756	43713.33	87426.67	1251032.00	28515.00	519.89	329	7.360	310.50	314.38	204.34	404.42	228.15	207.47	411.03	229.43
15	170756	43713.33	87426.67	1251032.00	28304.00	524.47	330	7.360	309.39	314.12	205.82	408.17	225.10	205.63	408.21	226.02
15	170756	43713.33	87426.67	1251032.00	28508.00	522.73	331	7.400	310.82	314.60	204.21	406.29	223.86	205.48	407.17	229.73
15	170756	43713.33	87426.67	1251032.00	28409.00	523.34	327	7.260	309.66	313.76	205.16	406.87	229.60	206.31	411.18	226.87
16	184891.00	48425.00	96850	1342909.50	28180.00		320.49	6.200	318.42	320.49	209.87	432.55	236.68	211.29	441.68	236.76
16	184891.00	48425.00	96850	1342909.50	28387.00		322.85	6.560	317.21	322.85	209.16	435.58	231.94	210.96	446.01	235.52
16	184891.00	48425.00	96850	1342909.50	28387.00		321.99	6.680	318.68	321.99	209.89	446.52	234.57	212.87	448.90	236.27
16	184891.00	48425.00	96850	1342909.50	29061.00		320.09	6.480	317.10	320.09	209.85	447.42	234.56	209.33	431.15	236.04
16	184891.00	48425.00	96850	1342909.50	28468.00		320.69	6.360	315.29	320.69	208.15	429.95	233.37	212.54	438.93	232.66
17	204771	50051.67	110103.3	1472129.50	27797.00	521.80	318.49	6.400	315.15	318.49	215.17	434.43	239.43	218.57	440.15	241.88
17	204771	50051.67	110103.3	1472129.50	27908.00	519.93	318.57	7.060	315.09	318.57	218.19	449.26	246.60	217.42	449.66	244.08
17	204771	50051.67	110103.3	1472129.50	27870.00	522.09	317.09	7.160	314.49	317.09	215.72	447.13	243.20	216.76	447.47	241.04
17	204771	50051.67	110103.3	1472129.50	27870.00	520.28	317.89	6.920	313.59	317.89	217.62	450.87	242.17	215.57	441.09	240.22
18	218711	59698.33	119396.7	1562739.5	26554.00	520.90	318.10	6.840	312.49	318.10	215.03	431.62	241.91	215.07	456.41	243.46
18	218711	59698.33	119396.7	1562739.5	26554.00	520.90	347	7.580	311.40	314.97	215.94	427.16	237.34	215.84	434.63	238.52
18	218711	59698.33	119396.7	1562739.5	28451.00	522.09	346	7.340	311.11	314.39	217.53	419.79	238.87	216.63	425.09	239.56
18	218711	59698.33	119396.7	1562739.5	28780.00	528.55	343	7.360	310.49	314.59	215.80	419.86	238.10	215.19	431.63	239.41
18	218711	59698.33	119396.7	1562739.5	28717.00	528.55	342	7.160	311.01	314.47	214.48	431.36	241.24	217.53	436.46	241.39
18	218711	59698.33	119396.7	1562739.5	28619.00	524.68	350	7.420	311.92	315.29	215.74	439.11	238.79	216.43	438.05	245.31
19	232339	64241.00	128482	1651321.5	31357.00	527.47	341	7.260	311.28	314.95	210.30	414.47	236.52	214.06	416.29	236.10
19	232339	64241.00	128482	1651321.5	30555.00	528.01	342	7.360	311.79	315.02	210.93	419.48	231.96	213.66	423.65	237.54
19	232339	64241.00	128482	1651321.5	30490.00	528.84	345	7.240	311.29	314.49	212.57	418.14	236.91	214.87	427.39	237.77
19	232339	64241.00	128482	1651321.5	30406.00	528.72	345	7.140	310.38	313.85	215.16	417.52	234.38	214.80	427.79	236.25
19	232339	64241.00	128482	1651321.5	31626.00	525.84	339	7.460	310.89	313.80	214.95	424.15	236.63	213.12	412.08	236.55
20	248830	69738.00	139476	1758513	31383.00	524.03	367	7.940	316.47	319.19	216.10	419.67	240.09	219.32	430.22	243.52
20	248830	69738.00	139476	1758513	30875.00	525.63	366	7.940	318.49	322.10	223.99	431.56	245.98	224.12	443.90	246.60
20	248830	69738.00	139476	1758513	31403.00	528.85	370	7.800	318.49	322.10	223.99	431.56	245.98	224.12	443.90	246.60
20	248830	69738.00	139476	1758513	31227.00	526.51	360	7.600	317.86	320.36	222.36	434.45	243.82	222.23	428.10	247.09
20	248830	69738.00	139476	1758513	31227.00	526.51	370	7.700	318.78	321.09	223.68	433.11	246.36	225.39	435.40	245.97
21	266136	75507.00	151014	1871002	31451.00	524.56	366	9.600	305.75	310.47	216.62	407.03	230.41	219.66	411.64	235.47
21	266136	75507.00	151014	1871002	31254.00	524.19	368	9.280	306.41	311.18	221.79	405.86	233.21	217.40	423.76	237.78
21	266136	75507.00	151014	1871002	31218.00	526.32	363	9.390	305.89	310.39	220.38	406.43	235.83	216.72	415.66	235.45
21	266136	75507.00	151014	1871002	31155.00	521.98	375	9.320	306.63	310.75	222.15	396.29	234.35	221.80	411.94	236.60
21	266136	75507.00	151014	1871002	30801.00	525.29	374	9.500	306.80	310.88	223.02	406.51	236.38	221.03	420.46	238.86
22	272882	77755	155510	1914851	30790.00	521.81	333.00	7.20	307.68	313.32	212.72	387.81	223.33	211.00	406.74	227.42
22	272882	77755	155510	1914851	30468.00	520.21	341.00	7.12	309.68	313.80	211.58	400.85	225.48	212.38	408.65	230.05
22	272882	77755	155510	1914851	30468.00	522.40	338.00	7.10	309.29	313.29	209.22	402.30	223.80	211.29	406.55	225.76
22	272882	77755	155510	1914851	30502.00	526.77	332.00	6.82	309.17	312.86	209.57	397.15	227.76	209.09	405.09	226.19
22	272882	77755	155510	1914851	30312.00	525.70	334.00	7.02	308.18	313.28	209.33	387.49	229.49	209.20	402.76	228.54

23	291221	83868	167736	2034054.5	27971.00	517.68	374.00	8.00	307.10	311.83	213.15	394.28	225.49	213.48	418.94	228.93
23	291221	83868	167736	2034054.5	27896.00	521.30	374.00	7.70	306.98	311.32	212.26	395.74	222.76	212.64	398.46	227.78
23	291221	83868	167736	2034054.5	27817.00	517.27	362.00	7.68	306.80	310.59	210.99	388.87	224.35	213.13	398.31	228.05
23	291221	83868	167736	2034054.5	27892.00	519.79	359.00	7.38	306.10	309.90	212.99	390.40	228.54	212.26	396.24	226.36
23	291221	83868	167736	2034054.5	28097.00	520.37	359.00	7.60	307.12	311.40	209.99	391.23	223.92	212.26	399.30	227.94
24	303553	87979	175968	2114212.5	27734.00	520.53		8.42	311.80	315.83	213.84	409.13	237.44	216.86	414.14	236.59
24	303553	87979	175968	2114212.5	27748.00	518.14		8.08	311.28	315.69	218.16	403.68	234.12	220.59	403.34	238.04
24	303553	87979	175968	2114212.5	27698.00	519.24		8.18	310.99	316.98	218.96	397.93	236.27	216.43	412.51	239.97
24	303553	87979	175968	2114212.5	27495.00	527.50		8.32	312.01	316.47	217.17	403.36	233.92	215.39	418.27	239.27
24	303553	87979	175968	2114212.5	27652.00	523.59	345.00	8.46	311.76	315.17	216.46	410.39	236.83	216.46	408.33	238.45
25	324660	95015	190030	2251408	27615.00	516.69		7.84	308.52	311.90	226.32	415.21	243.88	228.55	424.78	241.32
25	324660	95015	190030	2251408	27613.00	516.62	346.00	7.40	307.39	310.88	224.60	419.68	241.14	227.68	422.44	242.43
25	324660	95015	190030	2251408	27735.00	519.78	348.00	7.38	305.85	310.80	222.49	415.59	238.69	223.04	426.26	245.21
25	324660	95015	190030	2251408	27905.00	522.86	346.00	7.34	305.16	308.91	221.35	426.10	241.76	223.90	418.59	242.42
25	324660	95015	190030	2251408	27467.00	521.08	340.00	7.18	306.06	309.30	222.22	411.38	243.30	225.73	415.53	245.35
26	358918	106434	212868	2474085	27134	517.3967		7.76	305.799	303.813	198.42	375.92	210.1	196.33	389.14	210.23
26	358918	106434	212868	2474085	27360	520.7633		7.86	303.179	300.288	192.63	340.09	210.06	191.52	366.83	208.12
26	358918	106434	212868	2474085	27426	519.34		7.36	295.494	300.097	189.97	280.62	206.79	190.58	279.3	208.02
26	358918	106434	212868	2474085	27469	519.51		7.6	295.593	299.863	191.58	263.64	207.54	193.04	275.05	211.41
26	358918	106434	212868	2474085	27349	524.0033		7.58	295.166	299.637	192.16	258.26	209.59	191.74	271.96	205.3
27	378273	112885.7	225771.3	2599892.5	27609	515.37		8.06	309.58	314.292	207.01	411.87	226.09	210.45	421.85	229.04
27	378273	112885.7	225771.3	2599892.5	27496	518.5233		7.38	309.795	313.084	210.33	411.4	230.4	212.73	411.85	233.88
27	378273	112885.7	225771.3	2599892.5	27844	519.9467		8.02	309.488	313.392	208.11	406.13	229.24	209.82	419.36	228.88
27	378273	112885.7	225771.3	2599892.5	27844	513.07		7.58	309.787	314.281	209.39	409.52	227.6	211.78	416.15	229
27	378273	112885.7	225771.3	2599892.5	27649	519.8133		7.7	310.30	314.689	207	407.14	229.2	209.34	422.17	229.44
28	400281	120221.7	240443.3	2799349.5	27491.00	508.83		9.08	306.554	309.181	219.19	432.82	235.29	221.53	434.65	240.67
28	400281	120221.7	240443.3	2799349.5	27464.00	512.0433		8.66	304.37	308.047	221.27	418.67	240.85	221.57	424.44	244.55
28	400281	120221.7	240443.3	2799349.5	27561.00	512.7467		9.16	304.297	308.505	218.25	420.02	240.17	223.68	429.79	238.64
28	400281	120221.7	240443.3	2799349.5	27461.00	512.7467		7.98	306.283	308.047	221.02	430.12	241.08	223.59	423.28	242.91
28	400281	120221.7	240443.3	2799349.5	27336.00	517.43		8.1	305.716	309.192	222.36	435.44	245.19	225.72	429.23	249.1
29	420969	127117.7	254235.3	2933821.5	27479.00	514.22		8.66	312.078	315.764	224.73	452.79	247.46	223.01	446.5	251.18
29	420969	127117.7	254235.3	2933821.5	27709.00	522.3433		8.74	309.932	313.289	227.62	423.91	246.22	228.37	419.95	249.73
29	420969	127117.7	254235.3	2933821.5	27534.00	514.5167		8.64	309.513	314.1	227.24	430.27	249.95	226.36	429.77	250.81
29	420969	127117.7	254235.3	2933821.5	27557.00	515.6367		8.82	310.895	313.005	224.33	432.78	244.04	223.59	420.56	244.13
29	420969	127117.7	254235.3	2933821.5	27412.00	515.1567		8.58	308.386	311.405	223.14	427.18	246.44	222.67	418.19	248.75
30	447294	135892.7	271785.3	3104934	27213.00	516.0233		8.46	308.88	314.742	234.05	441.38	241.87	236.08	459.98	246.53
30	447294	135892.7	271785.3	3104934	27163.00	516.0333		8.58	309.473	313.561	231.32	444.55	244.84	233.54	454.47	248.33
30	447294	135892.7	271785.3	3104934	27237.00	518.8167		8.54	310.861	314.467	230.84	452.05	244.1	232.32	457.15	245.05
30	447294	135892.7	271785.3	3104934	27093.00	520.4233		8.72	310.587	313.997	229.19	455.74	245.07	231.65	452.53	248.89
30	447294	135892.7	271785.3	3104934	27237.00	522.59		8.82	310.499	314.591	230.3	461.32	243.72	227.48	474.23	248.03
31	468008	142797.3	285594.7	3239575	27284.00	511.35		8.24	309.181	313.7	217.15	391.49	224.91	218.45	400.11	227.1
31	468008	142797.3	285594.7	3239575	27315.00	516.87		8.18	309.297	315.764	212.03	390.49	219.45	216.15	393.68	223.7
31	468008	142797.3	285594.7	3239575	27340.00	517.5767		8.32	310.589	314.484	210.21	383.04	216	214.13	382.55	221.04
31	468008	142797.3	285594.7	3239575	27196.00	520.4467		8.76	309.169	314.3	208.3	378.22	217.66	209.09	383.97	217.17
31	468008	142797.3	285594.7	3239575	27217.00	519.9733		8.28	308.896	315.405	206.05	369.59	212.02	204.88	379.44	214.65
32	495739	152041	304082	3419826.5	27424.00	512.9167		8.58	306.39	311.606	227.59	417.96	236.87	231.52	420.64	238.91
32	495739	152041	304082	3419826.5	27066.00	516.3167		8.46	306.142	312.07	230.89	413.47	240.42	234.46	432.91	244.6
32	495739	152041	304082	3419826.5	27411.00	513.8633		8.82	306.378	312.091	228.59	437.88	241.12	228.71	434.48	240.89
32	495739	152041	304082	3419826.5	27311.00	511.1167		8.58	307.097	311.728	228.99	423.12	238.87	233.21	417.62	242.72
32	495739	152041	304082	3419826.5	27273.00	519.14		8.14	307.475	311.205	231.62	429.34	241.31	230.84	432.17	243.58
33	504241	154875	309750	3475089.5	27062.00	514.3167		8.12	300.595	304.284	228.28	403.52	237.1	233.82	409.45	240.21
33	504241	154875	309750	3475089.5	27209.00	513.3067		8.1	301.486	305.492	226.64	410.12	239.12	231.26	422.41	236.1
33	504241	154875	309750	3475089.5	27068.00	514.89		8.14	301.425	304.8	228.88	418.23	233.72	229.36	413.57	238.09
33	504241	154875	309750	3475089.5	27203.00	518.45		8.2	300.693	304.872	227.22	405.38	237.7	229.73	424.39	241.81
33	504241	154875	309750	3475089.5	27099.00	516.9767		7.76	301.288	305.995	226.47	412.26	238.8	228.29	431.3	236.23

## Appendix C: Degradation Data PWBA resistance

measurement	NIP copies	Resistance	Resistance + offset	measurement	NIP copies	Resistance	Resistance + offset	measurement	NIP copies	Resistance	Resistance + offset
1	0	336	336	12	1041766	317	350	23	2034054.5	374	407
1	0	337	337	12	1041766	316	349	23	2034054.5	374	407
1	0	336	336	12	1041766	316	349	23	2034054.5	362	395
1	0	336	336	12	1041766	317	350	23	2034054.5	359	392
1	0	339	339	12	1041766	319	352	23	2034054.5	359	392
2	85280	342	342	13	1188170.5	323	356	24	2114212.5	347	379
2	85280	342	342	13	1188170.5	328	361	24	2114212.5	346	378
2	85280	343	343	13	1188170.5	328	361	24	2114212.5	339	371
2	85280	342	342	13	1216354.5	331	364	24	2114212.5	443	475
2	85280	341	341	13	1216354.5	332	365	24	2114212.5	443	475
3	257504	338	338	14				25	2251408	345	378
3	257504	339	339	14				25	2251408	346	379
3	257504	339	339	14				25	2251408	348	381
3	257504	338	338	14				25	2251408	346	379
3	257504	339	339	14				25	2251408	340	373
4	332202	338	338	15	1251032	327	360	26	2474085	382	415
4	332202	339	339	15	1251032	329	362	26	2474085	383	416
4	332202	339	339	15	1251032	330	363	26	2474085	382	415
4	332202	338	338	15	1251032	331	364	26	2474085	382	415
4	332202	339	339	15	1251032	327	360	26	2474085	382	415
5	433243.5	345	345	16	1342909.5	354	387	27	2599892.5	404	437
5	433243.5			16	1342909.5	354	387	27	2599892.5	404	437
5	433243.5	346	346	16	1342909.5	352	385	27	2599892.5	404	437
5	433243.5	344	344	16	1342909.5	352	385	27	2599892.5	403	436
5	433243.5	345	345	16	1342909.5	352	385	27	2599892.5	404	437
6	577867.5	337	337	17	1472129.5	332	365	28	2799349.5	401	434
6	577867.5	338	338	17	1472129.5	328	361	28	2799349.5	401	434
6	577867.5	338	338	17	1472129.5	330	363	28	2799349.5	401	434
6	577867.5	338	338	17	1472129.5	342	365	28	2799349.5	401	434
6	577867.5	338	338	17	1472129.5	332	365	28	2799349.5	401	434
7	662991.5	338	338	18	1562739.5	347	380	29			
7	662991.5	339	339	18	1562739.5	346	379	29			
7	662991.5	339	339	18	1562739.5	343	376	29			
7	662991.5	339	339	18	1562739.5	342	375	29			
7	662991.5	339	339	18	1562739.5	350	383	29			
8	706086.5	347	347	19	1651321.5	341	374	30	2933821.5	419	452
8	706086.5	347	347	19	1651321.5	342	375	30	2933821.5	419	452
8	706086.5	346	346	19	1651321.5	345	378	30	2933821.5	419	452
8	706086.5	344	344	19	1651321.5	345	378	30	2933821.5	420	453
8	706086.5	343	343	19	1651321.5	339	374	30	2933821.5	420	453
9	745541.5	351	351	20	1758513	367	393	31	3104934	431	464
9	745541.5	351	351	20	1758513	356	393	31	3104934	431	464
9	745541.5	348	348	20	1758513	360	393	31	3104934	431	464
9	745541.5	348	348	20	1758513	370	403	31	3104934	431	464
9	745541.5	349	349	20	1758513	360	393	31	3104934	431	464
10	874215.50	355	355	21	1871002	386	419	32	3239575	426	461
10	874215.50	350	350	21	1871002	388	421	32	3239575	427	460
10	874215.50	352	352	21	1871002	383	416	32	3239575	426	459
10	874215.50	349	349	21	1871002	375	408	32	3239575	426	459
10	874215.50	351	351	21	1871002	374	407	32	3239575	427	460
11	957779.50	359	359	22	1914851	333	366	33	3419826.5	489	522
11	957779.50	351	351	22	1914851	341	374	33	3419826.5	489	522
11	957779.50	350	350	22	1914851	338	371	33	3419826.5	489	522
11	957779.50	349	349	22	1914851	332	365	33	3419826.5	489	522
11	957779.50	350	350	22	1914851	334	367	33	3419826.5	493	526

Colors are related to Appendix A

## Appendix D: Verification experiments

<b>Solenoid hood experiment</b>											
Objective: To determine whether a loose solenoid hood has influence on the measurement value of the factors that are stated below											
Two situations are compared: Normal situation (hood is fixated) and Defective situation (hood is not fixated)											
Good					Bad						
Initial values	Solenoid time	CR time	Stapling time 1	Stapling time 2	Solenoid time	CR time	Stapling time 1	Stapling time 2			
Run 1	measurement 1	24929	511.87	305.286	308.289	Run 2	25413	508.09	303.195	306.995	
			508.87					510.32			
			508.29					508.46			
	measurement 2	24737	509.02	304.291	306.994		25247	510.64	303.892	308.092	
		509.41				512.1					
		508.71				509.45					
<b>Average</b>		<b>24833</b>	<b>509.3616667</b>	<b>304.7885</b>	<b>307.6415</b>	<b>25330</b>	<b>509.8433333</b>	<b>303.5435</b>	<b>307.5435</b>		
<b>Repetition 1</b>											
Run 3	measurement 1	25047	510.61	302.57	305.908	Run 4	25220	509.47	302.791	308.095	
			509.23					509.21			
			508.15					512.8			
	measurement 2	24976	503.28	302.79	305.889		25359	510.14	303.389	306.892	
		514.41				506.56					
		510.23				512.08					
<b>Average</b>		<b>25011.5</b>	<b>509.3183333</b>	<b>302.68</b>	<b>305.8985</b>	<b>25289.5</b>	<b>510.0433333</b>	<b>303.09</b>	<b>307.4935</b>		
<b>Repetition 2</b>											
Run 5	measurement 1	25061	510.17	301.493	306.387	Run 6	25316	508.32	305.119	307.427	
			515.29					511.12			
			504.8					508.44			
	measurement 2	24962	509.67	302.93	306.689		25450	511.1	303.091	306.994	
		509.89				512.85					
		509.5				513.02					
<b>Average</b>		<b>25011.5</b>	<b>509.8066667</b>	<b>302.2115</b>	<b>306.538</b>	<b>25383</b>	<b>510.8083333</b>	<b>304.105</b>	<b>307.2105</b>		
<b>Medians per factor</b>		25011.5	509.3617	302.68	305.8985	25330	510.04333	303.5435	307.4935		
<b>Ranges per factor</b>		178.5	0.568333333	2.577	1.743	93.5	0.965	1.015	0.333		
<b>Differences means (D)</b>		318.5	0.68163	0.8635	1.595						
<b>Range average (d)</b>		136	0.766666667	1.796	1.038						
<b>Ratio(D/d)</b>		2.34	0.89	0.48	1.54						

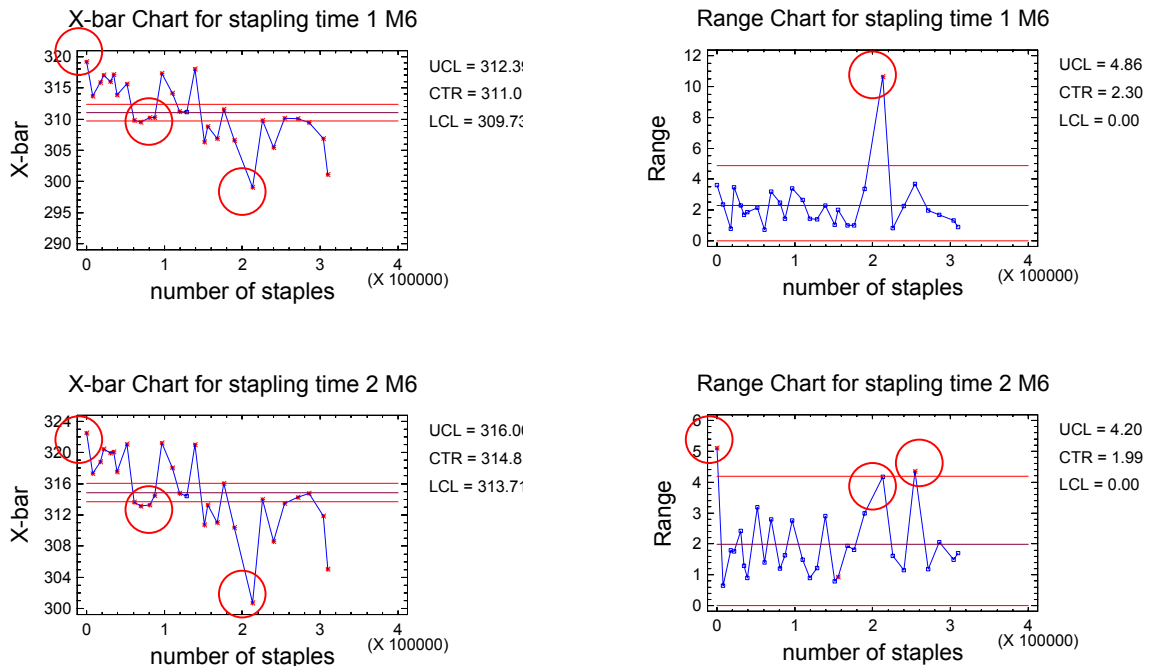
A minimal ratio of 1.25:1 for D/d indicates that there is significant difference between the good and the bad situation.

<b>Power source experiment</b>												
Objective: To determine whether a change in power configuration as observed during the degradation test has influence on the measurement value of the factors that are stated below												
Two situations are compared: Normal situation (source is completely open) and Defective situation (source is half open)												
Good					Bad							
	Solenoid time	CR time			Solenoid time	CR time						
Run 1	measurement 1	26358	511.57	Run 2	26274	507.18	Run 3	26345	510.26	510.9		
			510.08			511.49						516.4
			506.99			510.49						512.78
	measurement 2	26415	504.35		26327	516.4					509.05	517.69
		517.69				516.31						
		516.31				511.165						
<b>Average</b>		<b>26386.5</b>	<b>511.165</b>	<b>26300.5</b>	<b>511.2316667</b>							
<b>Repetition 1</b>												
Run 3	measurement 1	26464	518.9	Run 4	26512	515.97	Run 5	26768	513.88	518.29		
			513.9			516.09						519.74
			507.36			509.48						520.76
	measurement 2	26578	513.72		26345	512.93					510.26	519.74
		515.07				510.9						
		519				512.605						
<b>Average</b>		<b>26521</b>	<b>514.6566667</b>	<b>26428.5</b>	<b>512.605</b>							
<b>Repetition 2</b>												
Run 5	measurement 1	26512	512.19	Run 6	26507	508.61	Run 5	26768	513.88	518.29		
			513.63			508.61						520.76
			516.83			519.74						513.88
	measurement 2	26485	508.78		26768	519.74					510.26	519.74
		520.46				513.88						
		505.89				518.29						
<b>Average</b>		<b>26498.5</b>	<b>512.9633333</b>	<b>26637.5</b>	<b>514.9816667</b>							
<b>Medians per factor</b>		26498.5	512.96	26428.5	512.61							
<b>Ranges per factor</b>		134.5	3.491666667	337	3.75							
<b>Differences means (D)</b>		70	0.35									
<b>Range average (d)</b>		235.75	3.620833333									
<b>Ratio(D/d)</b>		0.30	0.10									

A minimal ratio of 1.25:1 for D/d indicates that there is significant difference between the good and the bad situation.

## Appendix E: Degradation analysis back-up parameters

### Stapling time 1 and 2 for stapler M6:

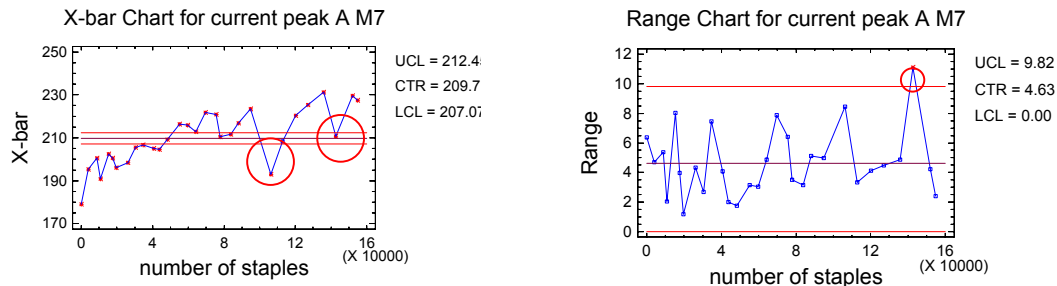


#### X-bar chart and Range charts for stapling time 1 and 2 of M6

The figures show two practically the same X-bar charts for both stapling positions of the moving stapler (M6). These two should look alike because the staples are stitched with the same stapler. Note the many out-of-control situations for stapling time two. At first glance this factor seems to be decreasing with time. However, this factor suffers from many uncertainties, which make it hazardous to model it. The out-of-controls for the range chart of stapling time 2 are explained from left to right. The initial measurement shows to be already out-of-control. Remember that the measurements for the stapler function are for a field returned stapler that was installed after the initial stapler broke down. Therefore this measurement is directly performed after the installation of this field returned stapler. Therefore it may be so that the first measurements are influenced by stuck and hardened lubricant in the stapler. After this first measurement the following measurements seem to be stable. Next note the out-of-control of measurement 26. This measurement also shows to be out-of-control for the first stapling time. At this measurement the rail along which the moving stapler moves was contaminated which resulted in friction. This affected movement and also the current consumption of the stapling function. The third situation that is out-of-control is caused by a plastic cover that shields the stapler when it performs its job. This cover was somewhat stuck, which resulted in the out-of-control situation. This set of five measurements however does not lead to odd mean values. The last remarkable situation is the second red circle from the right in the x-bar charts. Here the stapling time shows a very clear drop. This situation can be explained by the replacement of the stapler cartridge, which did no longer provide for good staples and hence needed to be replaced by a new cartridge. For more details on the stapler time see the dataset for the stapling time in appendix A.

## Current peaks of stapler M6

The x-bar and range charts for M6 show the following for its three current peaks.

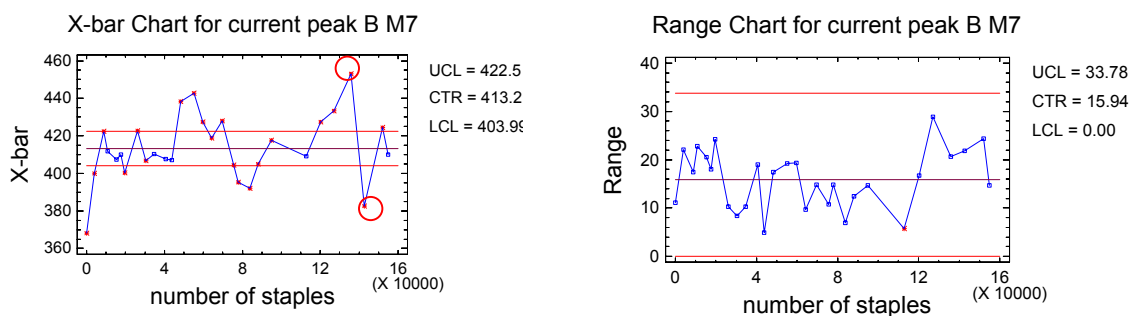


X-bar chart and Range chart for current intensity peak A of M7

The range chart shows to be out of control at one point (measurement 31). This led to a current intensity that was lower than what was expected. This was caused by a problem with a plastic cover that hangs in front of the stapler.

In the x-bar chart two other observations stand out. These are measurements 26 and 27. At measurement 26 the rail of the stapler motor M6 was contaminated, which led to friction. This influenced the value of the current peak for both staplers. This was also visualized in the current profile by a flattened current peak B that consisted of two bumps/peaks instead of one. The relatively low value of measurement 27 may well be the result of the repair of the stapler rail. For this the stapler had to be taken out. However this has not been proven and therefore measurement 27 is left in. It may be concluded that the x-bar chart is clearly out-of-control and shows a clear trend of degradation.

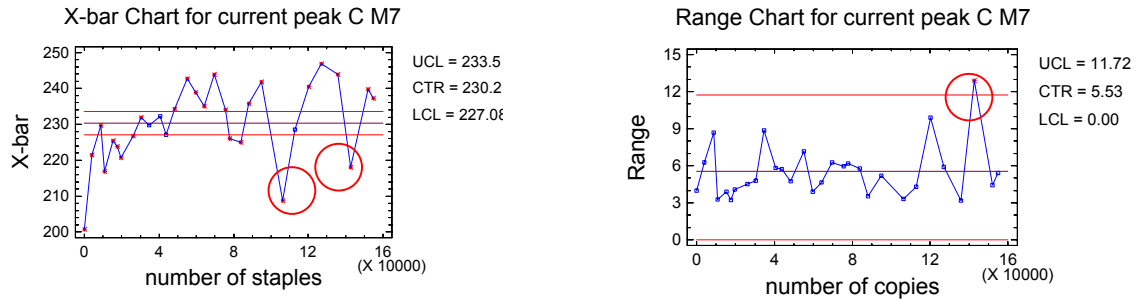
The measurements for peak B of the fixed stapler are as follows.



X-bar chart and Range chart for current intensity peak B of M7

In this figure measurement number 26 (rail friction) is already taken out because it had an enormous range of 120 that caused an extremely low value for peak B. As mentioned this peak consisted of two bumps/peaks instead of just one. The remaining range chart is in control while the x-bar chart is out-of-control and extremely variable. A possible reason for this variety is the fact that this factor is measured while stitching fifty sheets of paper. As not all sheets of paper will be equally thick, this may cause the variation in the measurements. The two extremes that are

marked with a red circle are caused by the influence of the plastic cover that was already mentioned for peak A. In short it cannot be concluded that peak B of the fixed stapler (M7) shows measurable degradation.



X-bar chart and Range chart for current intensity peak C of M7

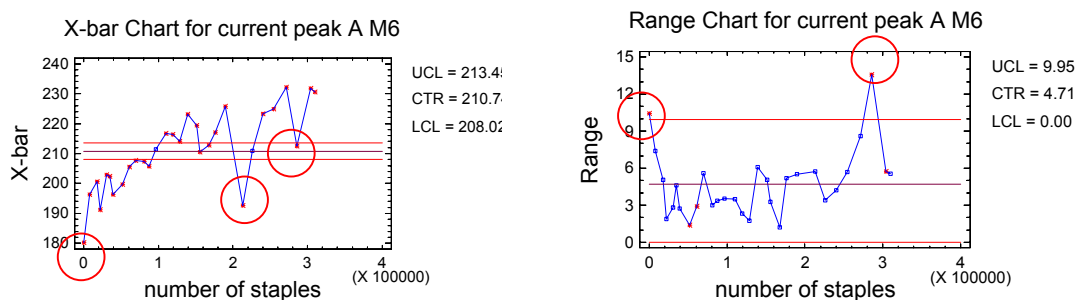
For this factor the same can be concluded as for factor peak A. The range chart shows an out-of-control situation at measurement 31. This is caused by the earlier mentioned plastic cover. The left extreme in the x-bar chart is again caused by the contaminated rail. These values are hence removed from the dataset.

The x-bar chart is clearly out-of-control and shows an increasing current consumption of the C peak. Therefore it may be concluded that current peak C of stapler M7 shows degradation.

Eye-catching are the very low values of the first measurements for the current peaks. In case the stapler were a brand new product that just had been produced, the very fast increase of current consumption could have been due to a run in effect. But these are measurements on a stapler from a field returned Finisher that was installed after the initial stapler failed. Therefore it may be so that the first measurements are influenced by stuck and hardened lubricant in the stapler.

### Current peaks of stapler M6

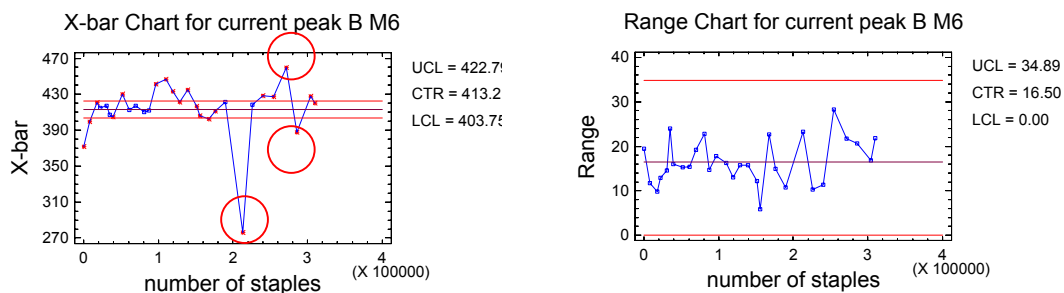
For the moving stapler (M6) holds the same as for the fixed stapler. This stapler however made twice the number of staples as the fixed stapler made during the degradation test. The x-bar charts and range charts for the three measured factors are as follows.



X-bar chart and Range chart for current intensity peak A of M6

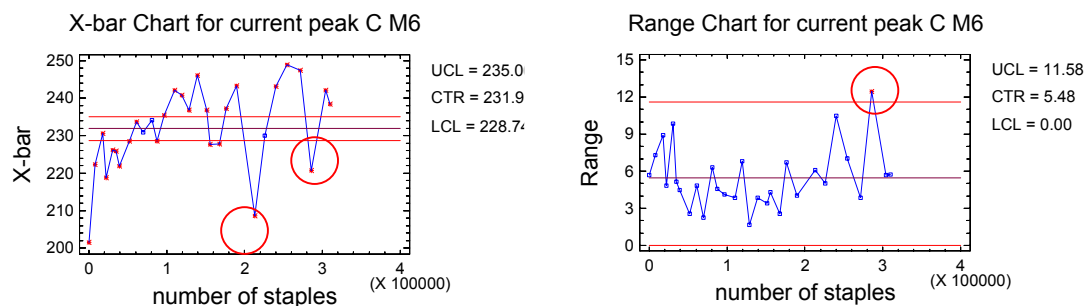
Again it can be noted that the range chart is out-of-control at measurement 31. This led to an unexpected lower measured value in the x-bar chart, which was due to the problem with the plastic cover. Also measurement 26 shows an extreme drop in the x-bar chart. This was due to the friction in the contaminated rail of stapler M6 that prevented it from moving, as it should. This obviously affected its current consumption for peak A. This measurement was therefore removed from the dataset.

It is conspicuous that the first measurement for the field returned stapler is out-of-control. This may be caused by hardening and sticking of the lubricant within the stapler as a result of its inactivity. Therefore it is decided to remove the first measurement from the data set. Finally, it can be concluded that current peak of the moving stapler (M6) significantly shows degradation.



X-bar chart and Range chart for current intensity peak B of M6

For the discussion on the B peak for this stapler we want to refer to the discussion on peak B for the fixed stapler (M7). Therefore it cannot be concluded that this factor may be modeled as a function of time.

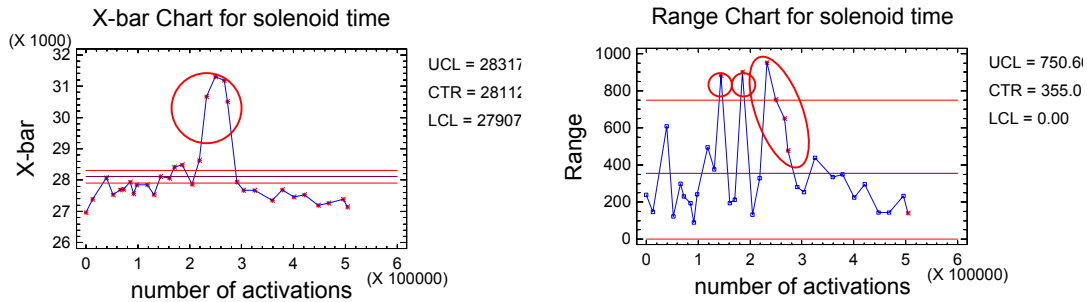


X-bar chart and Range chart for current intensity peak C of M6

For this factor the same holds as for current peak C of the fixed stapler. The same difficulties cause the out-of-control situation and the deviations from the expected value for the mean. Therefore these data points are removed and it may be concluded as a result of its out-of-control x-bar chart that this factor shows degradation.

## Tray election function

The tray election function that is performed by the diverter solenoid L3 ages with its number of activations. As described in section 5.2 the solenoid is expected to deteriorate as a result of internal friction and friction of its attached system. As a consequence of this friction the time that is needed for its activation is expected to increase. The X-charts and R-charts are as follows.



### X-bar chart and Range chart Solenoid time

The range chart shows some notable out-of-control situations. Starting from left to right the first out-of-control situation is a mysterious one. It was not possible to trace back a direct reason for this high range. This leads to a relatively high value in the x-bar chart. At this moment it was decided to wait until the following measurements to see if this out-of-control situation would persist. The next two measurements were in control and their means were at the same high level as the out-of-control situation. Therefore no action was undertaken.

The next out-of-control situation was at the same moment of a very high and unexpected current rise time for the nip motor. At this moment a problem with the power source was observed. It turned out to be running on only half power. This situation was later on imitated in a separate experiment to see whether this could actually be of influence. Appendix D shows that it could not be proven that this was of influence on neither both factors.

The last out-of-control situation concerns four measurements that also led to very high observations in the x-bar chart. Here it was discovered that the cover on the solenoid was not fixed to the rest of the system. Also this situation was reproduced in a separate experiment (appendix D). Here it was proven that the loose cover influenced the measurements for the solenoid and hence these measurements were removed from the set. This brought the measurement situation back to normal.

Oddly enough the measurements were somewhat lower and show a slightly downward trend after this problem was dealt with. One explanation could be an alteration in the set-up of the measurement tool after an exposition. The second possibility could be that the iron plunger within the solenoid had become permanently magnetic, which could affect the speed with which it activates. Therefore the solenoid was checked on magnetism. This was measured to be 5,5 Gauss (or 5,5 E-4 Tesla), which is a negligible amount.

Although it was expected that the solenoid time would increase with time, it cannot be said that this is supported by the data. The x-bar chart is out-of control, but the solenoid first shows an increase and later a decrease. Therefore it is decided not to model the solenoid time as a function of time.

## Appendix F: Main experiment

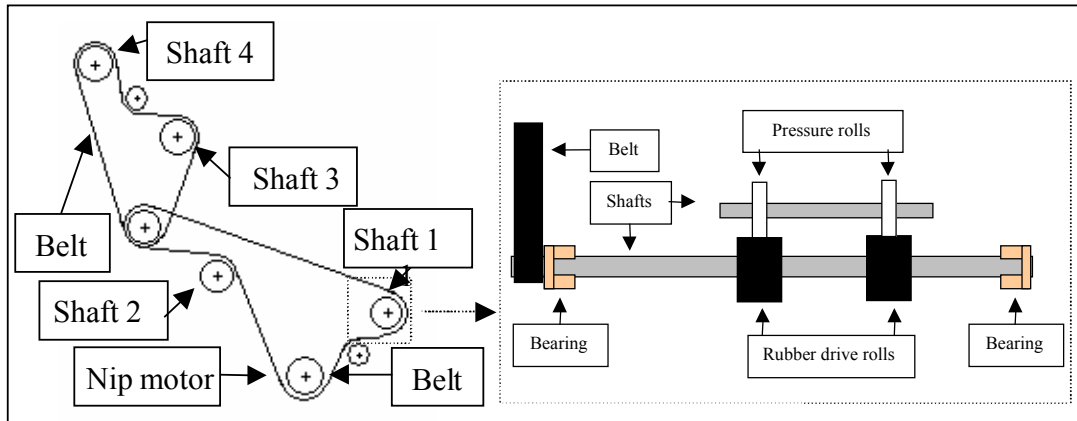
D.O.E. 0	File number	RUN	Step	Pattern	Extra load (Ncm)	Extra resistance	T amb	Humidity	Supply 24V	Supply 5V	Current Rise 10ms	Current Rise 1ms	Current Rise 1ms	Mean rise 1ms
0	1	1		--	0 Ncm	0 Ω	23	48	24	5	531.2	541	533.41	535.203
1	1	2					23	48	24	5	539.48	535.17	538.62	537.757
2	1	3					23	48	24	5	535.78	534.61	532.95	534.447
3	1	4					23	48	24	5	535.16	533.38	541.25	536.597
4	1	5					23	48	24	5	540.15	536.35	531.29	535.93
5	2	1		+	0 Ncm	0,04 Ω	23	48	24	5	534.76	539.59	539.36	537.903
6	2	2					23	48	24	5	542.89	535.86	537.37	538.707
7	2	3					23	48	24	5	534.23	544.99	538.95	539.39
8	2	4					23	48	24	5	542.22	525.17	538.36	535.25
9	2	5					23	48	24	5	532.88	538.98	537.55	536.47
10	3	1		00	0,4Ncm	0,02 Ω	23	48	24	5	543.96	544.32	543.63	543.97
11	3	2					23	48	24	5	541.75	535.39	545.11	540.75
12	3	3					23	48	24	5	541.8	542.91	543	542.57
13	3	4					23	48	24	5	541.93	537.27	535.61	538.27
14	3	5					23	48	24	5	546.18	540.17	537.03	541.127
15	4	1		0-	0,4Ncm	0 Ω	23	48	24	5	541.46	531.39	540.59	537.813
16	4	2					23	48	24	5	540.92	536.95	536.97	538.28
17	4	3					23	48	24	5	544.2	532.97	532.34	536.503
18	4	4					23	48	24	5	537.76	539.57	537.24	538.19
19	4	5					23	48	24	5	530.81	537.34	533.65	533.933
20	5	1		00	0,4Ncm	0,02 Ω	23	48	24	5	539.91	533.62	533.71	535.747
21	5	2					23	48	24	5	535.23	538.38	544.14	539.25
22	5	3					23	48	24	5	541.23	537.06	539.78	539.357
23	5	4					23	48	24	5	532.37	540.82	532.05	535.08
24	5	5					23	48	24	5	537.62	541.91	537.35	538.96
25	6	1		+	0,8Ncm	0 Ω	23	48	24	5	537.85	533.11	535.96	535.64
26	6	2					23	48	24	5	539.07	534.28	537.2	536.85
27	6	3					23	48	24	5	538.93	541.91	538.91	539.917
28	6	4					23	48	24	5	547.36	544.5	551.02	547.627
29	6	5					23	48	24	5	544.25	551.97	548.1	548.107
30	7	1		++	0,8Ncm	0,04 Ω	23	48	24	5	539.3	542.27	533.62	538.397
31	7	2					23	48	24	5	537.74	543.06	539.24	540.013
32	7	3					23	48	24	5	538.43	543.4	531.69	537.84
33	7	4					23	48	24	5	536.14	537.07	538.72	537.31
34	7	5					23	48	24	5	536.74	532.75	538.02	535.837
35	8	1		0+	0,4Ncm	0,04 Ω	23	48	24	5	538.39	540.19	535.91	538.163
36	8	2					23	48	24	5	538.45	538.85	537.05	538.117
37	8	3					23	48	24	5	541.04	535.36	540.1	538.833
38	8	4					23	48	24	5	541.04	540.25	537.19	539.493
39	8	5					23	48	24	5	532.05	540.98	539.27	537.433
40	9	1		00	0,4Ncm	0,02 Ω	23	48	24	5	538.27	537.68	537.91	537.953
41	9	2					23	48	24	5	541.3	543.3	536.8	540.467
48	9	3					23	48	24	5	541.46	542.62	539.1	541.06
49	9	4					23	48	24	5	534.72	541.71	538.68	538.37
50	9	5					23	48	24	5	532.86	541.96	538.53	537.783
51	10	1		+	0,8Ncm	0,02 Ω	23	48	24	5	540.89	535.53	537.44	537.953
52	10	2					23	48	24	5	537.86	539.48	534.05	537.13
53	10	3					23	48	24	5	535.13	538.28	535.83	536.413
54	10	4					23	48	24	5	544.48	536.06	541.44	540.66
55	10	5					23	48	24	5	534.91	542.19	537.15	538.083
56	11	1		-0	0 Ncm	0,02 Ω	23	48	24	5	537.42	537.53	534.74	536.563
57	11	2					23	48	24	5	543.43	538.4	534.51	538.78
58	11	3					23	48	24	5	536.99	539.85	535.95	537.597
59	11	4					23	48	24	5	538.25	535.5	539.03	537.593
60	11	5					23	48	24	5	536.78	535.19	540.77	537.58

D.O.E. 1	File number	RUN	Stat	Pattern	Extra load (Ncm)	Extra resistance	T emp	Humidity	Supply 24V	Supply 5V	Current R0a 6ma	Current R0a 6ma	Current R0a 6ma	Max. R0a 6ma
0	1	1	--		4,4 Ncm	0,25 Ω	22	48	24	5	526.31	526.2	519.41	523.9867
1	1	2					22	48	24	5				no trigger
2	1	3					22	48	24	5	524.12	515.3	517.28	518.8933
3	1	4					22	48	24	5	519.24	516.4	522.85	519.4967
4	1	5					22	48	24	5	523.01	522	521.71	522.2233
5	2	1	0-		4,8 Ncm	0,25 Ω	22	48	24	5	518.07	511.6	518.37	516.0067
6	2	2					22	48	24	5	530.46	515.9	519.13	521.8233
7	2	3					22	48	24	5	516.24	521.7	519.31	519.0767
8	2	4					22	48	24	5	521	523.8	518.49	521.11
9	2	5					22	48	24	5				no trigger
10	3	1	+-		5,2 Ncm	0,25 Ω	22	48	24	5	516.20	516.63	512.97	515.27
11	3	2					22	48	24	5	518.00	518.75	518.71	518.49
12	3	3					22	48	24	5	520.55	519.06	515.75	518.45
13	3	4					22	48	24	5	518.56	518.53	512.89	516.66
14	3	5					22	48	24	5	515.29	510.33	515.72	513.78
15	4	1	0+		4,8 Ncm	0,29 Ω	22	48	24	5	522.18	525.35	526.36	524.63
16	4	2					22	48	24	5	521.23	523.93	526.52	523.89
17	4	3					22	48	24	5	520.38	512.77	527.82	520.32
18	4	4					22	48	24	5	526.41	522.64	515.86	521.64
19	4	5					22	48	24	5	516.89	521.18	524.46	520.84
20	5	1	-+		4,4 Ncm	0,29 Ω	22	48	24	5	532.00	525.76	530.56	529.44
21	5	2					22	48	24	5	518.14	528.74	525.01	523.96
22	5	3					22	48	24	5	529.38	519.29	525.06	524.58
23	5	4					22	48	24	5	518.33	529.31	517.47	521.70
24	5	5					22	48	24	5	521.96	538.75	527.81	529.51
25	6	1	-0		4,4 Ncm	0,27 Ω	22	48	24	5	518.72	530.55	523.13	524.13
26	6	2					22	48	24	5	523.79	519.19	530.21	524.40
27	6	3					22	48	24	5	531.78	518.13	519.55	523.15
28	6	4					22	48	24	5	524.44	524.29	519.22	522.65
29	6	5					22	48	24	5	521.83	531.17	520.70	524.57
30	7	1	00		4,8 Ncm	0,27 Ω	22	48	24	5	519.61	528.01	521.00	522.87
31	7	2					22	48	24	5	525.90	526.09	521.32	524.44
32	7	3					22	48	24	5	526.13	526.15	521.15	524.48
33	7	4					22	48	24	5	525.28	518.26	519.78	521.11
34	7	5					22	48	24	5	518.66	519.40	520.69	519.58
35	8	1	00		4,8 Ncm	0,27 Ω	22	48	24	5	523.90	523.35	520.51	522.59
36	8	2					22	48	24	5	524.15	528.52	521.20	524.62
37	8	3					22	48	24	5	518.38	527.71	523.57	523.22
38	8	4					22	48	24	5	523.41	524.53	524.01	523.98
39	8	5					22	48	24	5	513.03	527.50	517.26	519.26
40	9	1	+0		5,2 Ncm	0,27 Ω	22	48	24	5	528.08	525.44	513.26	522.26
41	9	2					22	48	24	5	524.72	520.85	519.53	521.70
42	9	3					22	48	24	5	521.90	518.57	524.86	521.78
43	9	4					22	48	24	5	508.80	514.81	529.69	517.77
44	9	5					22	48	24	5	516.27	515.56	527.82	519.88
45	10	1	++		5,2 Ncm	0,29 Ω	22	48	24	5	522.68	524.61	522.83	523.37
46	10	2					22	48	24	5	518.80	518.60	526.52	521.31
47	10	3					22	48	24	5	525.71	520.59	517.41	521.24
48	10	4					22	48	24	5	527.86	517.98	527.12	524.32
49	10	5					22	48	24	5	513.75	523.90	514.08	517.24
50	11	1	00		4,8 Ncm	0,27 Ω	22	48	24	5	518.94	519.87	520.40	519.74
51	11	2					22	48	24	5	524.95	515.81	520.37	520.38
52	11	3					22	48	24	5	529.99	523.83	530.45	528.09
53	11	4					22	48	24	5	521.71	530.65	523.26	525.21
54	11	5					22	48	24	5	520.05	526.66	519.61	522.11

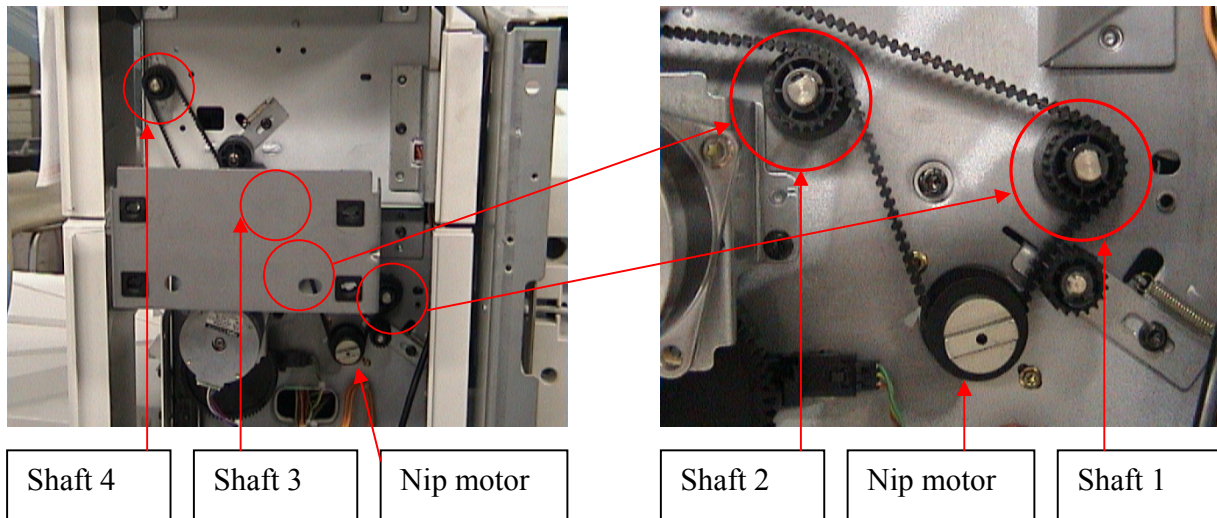
D.O.E.-2	File number	RUN	Stat	Pattern	Extra load (Ncm)	Extra resistance	T amb	Humidity	Supply 2kV	Supply 5V	Current Rise time	Current Rise time	Current Rise time	Mean rise time
0	1	1	--		7,6 Ncm	1,05 Ω	23	49	24	5				no trigger
1	1	2					23	49	24	5	508.33	515.59	519.23	514.38
2	1	3					23	49	24	5				no trigger
3	1	4					23	49	24	5	501.96	515.14	515.29	510.80
4	1	5					23	49	24	5	520.92	514.34	516.84	517.37
5	2	1	++		7,6 Ncm	1,09 Ω	23	49	24	5	511.03	516.21	504.86	510.70
6	2	2					23	49	24	5	517.33	524.37	515.11	518.94
7	2	3					23	49	24	5	516.64	521.86	506.88	515.13
8	2	4					23	49	24	5	511.68	521.39	507.81	513.63
9	2	5					23	49	24	5	522.64	513.93	515.77	517.45
10	3	1	-0		7,6 Ncm	1,07 Ω	23	49	24	5	509.46	517.48	520.04	515.66
11	3	2					23	49	24	5	513.41	525.83	512.10	517.11
12	3	3					23	49	24	5	516.84	510.19	503.60	510.21
13	3	4					23	49	24	5	516.83	511.77	522.20	516.93
14	3	5					23	49	24	5	512.93	516.96	506.22	512.04
15	4	1	0-		8 Ncm	1,05 Ω	23	49	24	5	505.81	508.40	512.21	508.81
16	4	2					23	49	24	5	503.58	503.02	501.60	502.73
17	4	3					23	49	24	5	495.36	514.64	509.99	506.66
18	4	4					23	49	24	5	507.05	517.80	493.48	506.11
19	4	5					23	49	24	5	499.40	513.21	504.83	505.81
20	5	1	+0		8,4 Ncm	1,07 Ω	23	49	24	5	502.87	509.00	502.64	504.84
21	5	2					23	49	24	5	505.17	495.70	515.69	505.52
22	5	3					23	49	24	5	499.47	500.21	492.33	497.34
23	5	4					23	49	24	5	489.94	513.79	496.16	499.96
24	5	5					23	49	24	5	509.42	498.96	509.48	505.95
25	6	1	00		8 Ncm	1,07 Ω	23	49	24	5	506.38	509.83	505.47	507.23
26	6	2					23	49	24	5	497.86	511.29	508.23	505.79
27	6	3					23	49	24	5	514.27	506.12	496.37	505.59
28	6	4					23	49	24	5	518.98	512.69	498.75	510.14
29	6	5					23	49	24	5	512.35	512.62	513.17	512.71
30	7	1	0+		8 Ncm	1,09 Ω	23	49	24	5	515.84	526.86	496.65	513.12
31	7	2					23	49	24	5	517.65	497.65	513.00	509.43
32	7	3					23	49	24	5	517.65	501.11	506.64	508.47
33	7	4					23	49	24	5	512.18	508.52	502.99	507.90
34	7	5					23	49	24	5	516.91	501.82	508.19	508.97
35	8	1	+-		8,4 Ncm	1,05 Ω	23	49	24	5	503.75	510.83	508.48	507.69
36	8	2					23	49	24	5	501.11	507.19	498.36	502.22
37	8	3					23	49	24	5	500.86	487.96	501.30	496.71
38	8	4					23	49	24	5	505.29	509.37	509.97	508.21
39	8	5					23	49	24	5				no trigger
40	9	1	00		8 Ncm	1,07 Ω	23	49	24	5	516.80	524.09	502.09	514.33
41	9	2					23	49	24	5	502.30	500.77	499.39	500.82
42	9	3					23	49	24	5	516.82	510.73	510.38	512.64
43	9	4					23	49	24	5	509.89	499.01	512.69	507.20
44	9	5					23	49	24	5	510.27	513.19	512.43	511.96
45	10	1	++		8,4 Ncm	1,09 Ω	23	49	24	5				no trigger
46	10	2					23	49	24	5	514.95	515.05	502.39	510.80
47	10	3					23	49	24	5				no trigger
48	10	4					23	49	24	5	514.64	515.31	495.68	508.54
49	10	5					23	49	24	5	509.01	502.68	509.30	507.00
50	11	1	00		8 Ncm	1,07 Ω	23	49	24	5	505.68	499.31	503.35	502.78
51	11	2					23	49	24	5	517.65	511.50	507.08	512.08
52	11	3					23	49	24	5	502.37	517.68	507.21	509.09
53	11	4					23	49	24	5	504.56	515.13	509.97	509.89
54	11	5					23	49	24	5	503.83	514.66	504.60	507.70



## Appendix H: Restoration of the shafts



*Rolls mechanism driven by NIP motor*



The increase in load that was caused during the Main experiment was  $8,788 - 5,676 = 3,112$  Ncm.

The order in which the shafts were cleaned was:  
Shaft 4, shaft 1+shaft 2, shaft 3

The reduction of the load that was observed per cleaned shaft was:  
Shaft 4: - 0,916 Ncm  
Shaft 1+2: - 1,364 Ncm  
Shaft 3: - 0,332 Ncm

## Appendix I: The Desirability Technique

A technique that can be used to achieve robust reliability is the “Desirability Technique” by Derringer and Suich [32].

This is a method for approximating optimality for a combination of multiple response variables. In order to achieve robust reliability the response variables in this thesis are the equations 7.1 and 7.2 for the MTTF and SDTTF in section 7.2

For translating the value of MTTF (or  $\hat{Y}$ ) to a desirability index the following transformation equation is needed:

$$d_i = \begin{cases} 0 & \hat{Y} \leq Y_* \\ \left[ \frac{\hat{Y} - Y_*}{Y^* - Y_*} \right]^r & Y_* < \hat{Y} < Y^* \\ 1 & \hat{Y} \geq Y^* \end{cases}$$

In order to get results it is necessary to define the minimal value of desirability for  $Y$ ,  $Y_*$ .

Further also the target value of  $Y$ ,  $Y^*$  needs to be defined. Further a value of  $r$  should be decided in concordance with the producer of the product. A small value of  $r$  (e.g. 0,1) would mean that any value of  $\hat{Y}_i$  above  $Y_{i*}$  was just about as desirable as any other value of  $\hat{Y}_i$  above  $Y_{i*}$ . A large value of  $r$  means that  $\hat{Y}_i$  should be considerably above  $Y_{i*}$  to be desirable. Setting a minimal value, a target value and the  $r$  coefficient make it possible to define the preferred balance of importance between the two response variables.

The same should be done with regard to the standard deviation of the TTF. Except now one wants to minimize this response variable. The objective is to make the SDTTF as small as possible. Therefore a SDTTF as closer to zero has a higher desirability  $d$ . In order to have a higher desirability for a smaller standard deviation, we need to rewrite the equation a little.

First we define an upper limit on the SDTTF, say  $\sigma_Y^*$ . In order to get a high value of  $d$  when  $\sigma_Y$  is small, and vice versa, we need to have a positive value of the equation before it is converted by  $r$ . The most desired value is  $c$ , which is zero in this case. Hence the equation will be:

$$d_i = \begin{cases} 0 & \hat{\sigma}_Y \geq \sigma_Y^* \\ \left[ \frac{\hat{\sigma}_Y - \sigma_Y^*}{c - \sigma_Y^*} \right]^r & 0 < \hat{\sigma}_Y < \sigma_Y^* \\ 1 & \hat{\sigma}_Y = 0 \end{cases}$$

As in the previous case it will be necessary to define a value for  $r$ .

Overall desirability can then be calculated by means of the following formula.

$$D = (d_Y \times d_{\sigma_Y})^{1/2}$$

A computer model should be run to calculate the overall desirabilities with the possible combinations of the design parameters that lead to an as high as possible the desired combination of MTTF and SDTTF.

---

## Appendix J: Side study

---

### ML estimation of parameters in growth models by means of Laplacian approximation

*A supplement to the ROMDA concept*

**Mark Damen**

Department of Technology Management  
Technische Universiteit Eindhoven  
June, 2004

---

#### Abstract

Growth models can be applied to a large variety of problem areas, such as biology, product engineering and even astronomy. This paper was originally written for the area of product engineering, though an example from biology is used. The ROMDA concept by Van den Bogaard [10] uses degradation data of design parameters to model product degradation. This paper serves as a supplement to ROMDA. It provides an explanation and elaboration in Matlab of a method to estimate parameters in the nonlinear mixed effect model as described by Pinheiro and Bates [47]. It was chosen to approximate this estimation by means of the Laplacian approximation, because this leads to the best mix of efficiency and accuracy without having to define abscissas. The outcome of this study can be used for further development into a method that supports non-parametric estimation of growth data.

#### Background

The ROMDA concept [10] is a method for reliability prediction and optimization that can be applied in the design stage. It tries to analyze and model the degradation of certain design parameters and link this to a performance characteristic, which can be used for reliability prediction purposes. Relating the performance characteristic to its design parameters provides the additional possibility to optimize the design of the product. This is done by means of the Robust Design method [15].

When products have a long technical life span it is difficult to obtain degradation data until time to failure. This requires for extrapolation. The further degradation models are extrapolated with respect to time, the higher the uncertainty of their accuracy becomes. In this situation it is important to model the degradation data that we do have as accurately as possible.

Lu and Meeker [24] estimate parameters in a degradation model for fatigue cracks by means of calculating the least squares difference between the degradation data and a physical degradation model. Chiao and Hamada [27] use an extension to MLE to calculate the parameters in their degradation models for Light Emitting Diodes. Palmer, Phillips and Smith use [48] Gauss-Hermite integration to maximize a likelihood function with random effects for growth data of animals. Meeker and Escobar [25, 26] provide a general maximum likelihood estimation function for estimating parameters in nonlinear mixed effects degradation functions. Their function is

based on the work of Pinheiro and Bates [47] who describe four approximations to the loglikelihood. In this study the Laplacian approximation is used. According to their article this leads to the best mix of efficiency and accuracy without having to define abscissas.

### Estimation function

This section introduces the estimation function and defines all the variables. From now on the terms degradation model and degradation data are used, because they apply to the area of interest.

The subscript  $i$  indicates the product for which an observation was made  
The subscript  $j$  indicates the  $j$ th observation of the degradation path

Then  $y_{ij}$  is the  $j$ th observation for the performance of product  $i$  and  $f_{ij}$  is the expected performance (degradation) for product  $i$  at the  $j$ th time/observation.

$$\text{Then } y_{ij} = f_{ij} + \varepsilon_{ij} = f(\varphi_{ij}, t_{ij}) + \varepsilon_{ij} \quad \text{where } i = 1, \dots, M, j = 1 \dots n_i \quad (\text{eq. 1})$$

Note that different products can have a different amount of observations (denoted by  $n_i$ ).

The variable  $\varphi_{ij}$  is a function of the fixed effects  $\boldsymbol{\beta}$  and the random effects  $\mathbf{b}_i$ .

$$\varphi_{ij} = \mathbf{A}_{ij}\boldsymbol{\beta} + \mathbf{B}_{ij}\mathbf{b}_i \quad \text{where } \mathbf{b}_i \sim N(0, \sigma^2 \mathbf{D}) \quad (\text{eq. 2})$$

where  $\mathbf{D}$  is the covariance matrix of the random effects.

Substituting equation 2 into equation 1 shows that the degradation function is a function of its fixed effects, its random effects and time. Pinheiro and Bates from here on do no longer state the factor time in their functions, and therefore neither does this paper. They use MLE to find the most likely values for the fixed effects, vector  $\boldsymbol{\beta}$ . Therefore they maximize the following function:

$$p(\mathbf{y} | \boldsymbol{\beta}, \mathbf{D}, \sigma^2) = \int p(\mathbf{y} | \mathbf{b}, \boldsymbol{\beta}, \mathbf{D}, \sigma^2) p(\mathbf{b}) d\mathbf{b} \quad (\text{eq. 3})$$

The first probability function is a univariate probability density function. The second is a multivariate probability density function. The type of probability function here can be any of the known continuous probability density functions. The article from here on uses the normal probability density function, which makes the estimation process parametric.

### Laplacian Approximation

Laplacian approximations are frequently used in Bayesian inference to estimate marginal posterior densities and predictive distributions. These techniques can also be used for the integration considered here.

For product  $i$  the normally distributed likelihood probability function is as follows:

$$p(\mathbf{y}_i | \boldsymbol{\beta}, \mathbf{D}, \sigma^2) = \int (2\pi\sigma^2)^{-(n_i+q)/2} |\mathbf{D}|^{-1/2} \exp[-g(\boldsymbol{\beta}, \mathbf{D}, \mathbf{y}_i, \mathbf{b}_i) / 2\sigma^2] d\mathbf{b}_i \quad (\text{eq. 4})$$

Here the two probability functions (univariate and multivariate) are combined into one function. Note the exponent, which contains  $n_i$  and  $q$ . Here  $n_i$  is the number of observations in degradation path  $i$  and  $q$  is the number of random effects. The function  $g(\boldsymbol{\beta}, \mathbf{D}, \mathbf{y}_i, \mathbf{b}_i)$  is also a combination of the univariate and multivariate normal distributions.

$$g(\boldsymbol{\beta}, \mathbf{D}, \mathbf{y}_i, \mathbf{b}_i) = \|\mathbf{y}_i - \mathbf{f}_i(\boldsymbol{\beta}, \mathbf{b}_i)\|^2 + \mathbf{b}_i \mathbf{D}^{-1} \mathbf{b}_i \quad (\text{eq. 5})$$

The double brackets term is called the *Euclidean Distance* term and is equal to the square root of the sum of squares. Mathematically this is expressed by

$$\|\mathbf{y}_i - \mathbf{f}_i(\boldsymbol{\beta}, \mathbf{b}_i)\|^2 = \sqrt{\sum_{j=1}^{n_i} |y_{ij} - \mathbf{f}_{ij}(\boldsymbol{\beta}, \mathbf{b}_i)|^2} \quad (\text{eq. 6})$$

Consequently equation five results in a number and not a vector.

An estimation of the vector  $\mathbf{b}_i$  is calculated for each degradation path by minimizing equation five with respect to  $\mathbf{b}_i$ . Here the  $\boldsymbol{\beta}$  remains a vector of fixed effects that needs to be estimated.

$$\hat{\mathbf{b}}_i = \hat{\mathbf{b}}_i(\boldsymbol{\beta}, \mathbf{D}, \mathbf{y}_i) = \arg \min_{\mathbf{b}_i} g(\boldsymbol{\beta}, \mathbf{D}, \mathbf{y}_i, \mathbf{b}_i) \quad (\text{eq. 7})$$

The outcome of equation 7 is a vector of length  $q$  (number of random effects) for every degradation path  $i$ .

A second order Taylor expansion of  $g$  around  $\hat{\mathbf{b}}_i$  results in the following approximation:

$$g(\boldsymbol{\beta}, \mathbf{D}, \mathbf{y}_i, \mathbf{b}_i) \cong g(\boldsymbol{\beta}, \mathbf{D}, \mathbf{y}_i, \hat{\mathbf{b}}_i) + \frac{1}{2} [\mathbf{b}_i - \hat{\mathbf{b}}_i]^T g''(\boldsymbol{\beta}, \mathbf{D}, \mathbf{y}_i, \hat{\mathbf{b}}_i) [\mathbf{b}_i - \hat{\mathbf{b}}_i] \quad (\text{eq. 8})$$

Equation 8 can be substituted into equation 4. The article then directly presents the Laplacian approximation of the probability (or likelihood) function for all  $M$  products (eq. 9).

$$p(\mathbf{y} | \boldsymbol{\beta}, \mathbf{D}, \sigma^2) \cong (2\pi\sigma^2)^{-N/2} |\mathbf{D}|^{-M/2} \exp\left[-\frac{1}{2\sigma^2} \sum_{i=1}^M g(\boldsymbol{\beta}, \mathbf{D}, \mathbf{y}_i, \hat{\mathbf{b}}_i)\right] \times \int (2\pi\sigma^2)^{q/2} \exp\left\{-\frac{1}{2\sigma^2} \sum_{i=1}^M [\mathbf{b}_i - \hat{\mathbf{b}}_i]^T g''(\boldsymbol{\beta}, \mathbf{D}, \mathbf{y}_i, \hat{\mathbf{b}}_i) [\mathbf{b}_i - \hat{\mathbf{b}}_i]\right\} d\mathbf{b}_i \quad (\text{eq. 9})$$

Elaboration of the second part of equation 9, namely the integral, results in the function

$$\prod_{i=1}^M |g''(\boldsymbol{\beta}, \mathbf{D}, \mathbf{y}_i, \hat{\mathbf{b}}_i)|^{-1/2} \quad (\text{eq. 10})$$

The two stripes imply taking the *determinant*.

Substituting equation 10 for the integral in equation 9 results in the following likelihood function.

$$p(\mathbf{y}|\boldsymbol{\beta}, \mathbf{D}, \sigma^2) = (2\pi\sigma^2)^{-N/2} |\mathbf{D}|^{-M/2} \prod_{i=1}^M \left| g''(\boldsymbol{\beta}, \mathbf{D}, \mathbf{y}_i, \hat{\mathbf{b}}_i) \right|^{-1/2} \exp\left[-g(\boldsymbol{\beta}, \mathbf{D}, \mathbf{y}_i, \hat{\mathbf{b}}_i) / 2\sigma^2\right]$$

where  $N = \sum_{i=1}^M n_i$  (eq. 11)

Subsequently the function  $g''$  is approximated. A more detailed elaboration of how this function is approximated can be found in [47].

$$g''(\boldsymbol{\beta}, \mathbf{D}, \mathbf{y}_i, \mathbf{b}_i) \cong \mathbf{G}(\boldsymbol{\beta}, \mathbf{D}, \mathbf{y}_i) = \frac{\partial \mathbf{f}(\boldsymbol{\beta}, \mathbf{b}_i)}{\partial \mathbf{b}_i^T} \bigg|_{\mathbf{b}_i = \hat{\mathbf{b}}_i} \frac{\partial \mathbf{f}(\boldsymbol{\beta}, \mathbf{b}_i)}{\partial \mathbf{b}_i} \bigg|_{\mathbf{b}_i = \hat{\mathbf{b}}_i} + \mathbf{D}^{-1} \quad (\text{eq. 12})$$

Where  $\frac{\partial \mathbf{f}(\boldsymbol{\beta}, \mathbf{b}_i)}{\partial \mathbf{b}_i} \bigg|_{\mathbf{b}_i = \hat{\mathbf{b}}_i} = [\nabla f_{i1}(\mathbf{b}_i) \quad \nabla f_{i2}(\mathbf{b}_i) \dots \nabla f_{in_i}(\mathbf{b}_i)]$  (eq. 13)

Here the  $\nabla$ , which is called Nabla, is the vector derivative with respect to  $\mathbf{b}_i$ . Therefore equation 13 results in a matrix of  $q$  rows and  $n_i$  columns.

The multiplication of a matrix of size  $n \times q$  with a matrix of size  $q \times n$  results in a matrix of  $q \times q$ . As the covariance matrix  $\mathbf{D}$  in equation 12 is also a  $q \times q$  matrix, these two matrices can be added.

In order to make the computations more efficient Pinheiro and Bates use the log of the likelihood function, which leads to the same outcomes of the estimation.

The loglikelihood is defined as follows:

$$l_{LA}(\boldsymbol{\beta}, \mathbf{D}, \sigma^2 | \mathbf{y}) = -\frac{1}{2} \left\{ N \log(2\pi\sigma^2) + M \log|\mathbf{D}| + \sum_{i=1}^M \log|\mathbf{G}(\boldsymbol{\beta}, \mathbf{D}, \mathbf{y}_i)| + \sigma^{-2} \sum_{i=1}^M g(\boldsymbol{\beta}, \mathbf{D}, \mathbf{y}_i, \hat{\mathbf{b}}_i) \right\}$$

(eq. 14)

Here  $N = \sum_i^M n_i$

Equation 14 shows that the vector  $\hat{\mathbf{b}}_i$  does not depend on  $\sigma^2$ . Therefore for given  $\boldsymbol{\beta}$  and  $\mathbf{D}$  the maximum likelihood estimate of  $\sigma^2$  (based on equation 14) is:

$$\hat{\sigma}^2 = \hat{\sigma}^2(\boldsymbol{\beta}, \mathbf{D}, \mathbf{y}) = \sum_{i=1}^M g(\boldsymbol{\beta}, \mathbf{D}, \mathbf{y}_i, \hat{\mathbf{b}}_i) / N \quad (\text{eq. 15})$$

In order to calculate the estimated variance the estimated vector of the random effects,  $\hat{\mathbf{b}}_i$ , is substituted into equation 5 for  $\mathbf{b}_i$ .

Note that the final term in equation 14, which is  $\sigma^{-2} \sum_{i=1}^M g(\boldsymbol{\beta}, \mathbf{D}, \mathbf{y}_i, \hat{\mathbf{b}}_i)$ , consists of  $N$  times the estimated variance divided by the variance. The resulting term will therefore be  $N$ .

Substituting equation 15 back into equation 14 will therefore lead to the following final loglikelihood function.

$$l_{LA} = l_{LA}(\boldsymbol{\beta}, \mathbf{D} | \mathbf{y}) = -\frac{1}{2} \left\{ N \left[ 1 + \log(2\pi) + \log(\hat{\sigma}^2) \right] + M \log |\mathbf{D}| + \sum_{i=1}^M \log |\mathbf{G}(\boldsymbol{\beta}, \mathbf{D}, \mathbf{y}_i)| \right\} \quad (eq. 16)$$

This function needs as inputs the observed degradation data matrix  $\mathbf{y}$ , an estimate for the covariance matrix  $\mathbf{D}$  and a vector of starting values for the fixed effects,  $\boldsymbol{\beta}$ . The loglikelihood is maximized by calculating the vector  $\boldsymbol{\beta}$  that maximizes equation 16.

In Matlab this is achieved by minimizing the function  $-l_{LA}$  by means of the function *fminsearch*.

### Application and results

The Laplacian approximation was applied to a data set and growth function for orange trees. The degradation or growth function has only one random effect and is as follows:

$$y_{ij} = \frac{\beta_1 + b_{i1}}{1 + \exp\left[-(t_{ij} - \beta_2) / \beta_3\right]} + \varepsilon_{ij} \quad (eq. 17)$$

The article does not present the solution of the Laplacian approximation for this problem. This can therefore be seen as an addition.

The total estimation process takes place in two steps. First the starting values are estimated. This can be done by means of the Least Squares Estimation method. Subsequently the algorithm is used to estimate the values of the fixed effects. During the application of this algorithm it is assumed that the first step was already executed and that this lead to an estimation of the exact value for the covariance matrix.

The results are presented in table 1. As starting values we used  $\beta_1 = 100$ ,  $\beta_2 = 100$ ,  $\beta_3 = 100$  and for  $\mathbf{D}$  the value that was obtained by Pinheiro and Bates as the exact solution was used. This is  $\mathbf{D} = 16.281$ . It must however be noted, that using a different estimate for the covariance matrix also leads to distinct estimation results.

Table 1: Estimation results for Orange trees data

Approximation	Log(sqrt( $\mathbf{D}$ ))	Beta 1	Beta 2	Beta 3	Log(variance)	$l$
Alternating	1.389	191.049	722.556	344.164	4.120	- 131.585
Gaussian <sub>10</sub>	1.123	194.325	727.490	348.065	4.102	- 130.497
Gaussian <sub>200</sub>	1.396	192.293	727.074	348.074	4.119	- 131.571
Laplacian		191.9361	727.8279	727.8279	4.1192	- 131.5712
Exact	1.395	192.053	727.906	348.073	4.119	- 131.572

From this table it may be concluded that the programmed Laplacian approximation to the loglikelihood gives an almost exact solution to the estimation problem. It is the most effective approximation algorithm without having to define abscissas.

The program also showed that it is important to provide a good estimate for the covariance matrix. The starting values for the fixed effects are of minor influence to the outcome of their estimation.

### **Comparison to LSE**

The results will now be compared to estimations that are made by means of Least Squares Estimation. In each situation the same starting values of  $\beta_1 = 100$ ,  $\beta_2 = 100$ ,  $\beta_3 = 100$  and the same covariance matrix  $\mathbf{D} = 16.281$  are used.

#### *Fixed effects model*

The first situation assumes no random effects, but just fixed effects. This leads to the following estimation results:

$$\hat{\beta}_1 = 192.9105, \hat{\beta}_2 = 726.8779 \text{ and } \hat{\beta}_3 = 355.8220 \text{ and } \log(\sigma^2) = 6.2137$$

The variance is clearly larger than in the case of the Laplacian approximation of the Maximum Likelihood function in the mixed effects model. Assuming that the exact estimations in [47] are correct it can also be said that the LSE estimations are quite good for the first two fixed effects. However, the estimation of the third fixed parameter  $\hat{\beta}_3$  is quite distinct.

#### *Mixed effects model*

In the second situation we compare the programmed algorithm with the estimations by LSE for the mixed effects model in equation 17. This is in essence the same as optimizing the estimated variance in equation 15 with respect to the vector  $\boldsymbol{\beta}$ . This results in the following estimations:

$$\hat{\beta}_1 = 191.0591, \hat{\beta}_2 = 722.6107 \text{ and } \hat{\beta}_3 = 344.2015 \text{ and } \log(\sigma^2) = 4.1185$$

Note the striking resemblance of the outcome to the Alternating approximation. Naturally the estimated variance for this solution is smaller than that of the variance in the Laplace approximation.

### **Conclusion**

The programmed Laplacian approximation in Matlab performs excellently in comparison to the other approximations. Its performance does however depend on the initial value of the covariance matrix. This makes a good estimation of the starting values very important for the rest of the estimation process.

Also compared to LSE in the fixed effects model and LSE in the mixed effects model it results to better estimation of  $\boldsymbol{\beta}$ . Nevertheless it must be noted that especially with regard to the fixed effects model the computational time is considerably longer.

Before using this algorithm one must make sure to have an accurate estimation of the covariance matrix. Deviations of the covariance matrix lead to less accurate estimates for the vector  $\boldsymbol{\beta}$ .

---

Summarizing, this algorithm may well serve as a supplement to the ROMDA reliability concept. Better estimations of the coefficients in a model can produce more reliable degradation models. When these models need to be extrapolated to time-to-failure this may result in better estimations of this failure moment. A next step for optimization of the written program may lie in making the estimation algorithm non-parametric instead of parametric. This results in estimations with less bias, because they are less influenced by the assumptions of a probability distribution.

---

**Programme: Matlab files**

**Filename: nlmemain.m**

% This is the main file which executes a Maximum Likelihood Parameter Estimation  
% for a Non Linear Mixed Effects model as proposed by Pinheiro and Bates (1995, 2001).  
% This same approximation algorithm is used by the nlme function in S-plus.

```
clear all
clc
warning off
```

```
N=input('How many parameters would you like to estimate? ');
disp(' ')
```

```
B=zeros(N,1);
```

```
for n=1:1:N
%Input starting values by the user in the form [B1;B2;B3]
B(n,1)=input('Provide the starting value: ');
```

```
end
q=input('How many random effects does the degradation function contain? ');
disp(' ')
```

```
D=input('Specify an estimation of the covariance matrix of the random effects: ');
```

```
disp(' ')
disp('Estimating the parameters in a Nonlinear Mixed Effects Model')
disp('by means of Laplace approximation of the log-likelihood function')
disp('as described by Jose C. Pinheiro and Douglas M. Bates')
```

```
Options = optimset('TolX', 1E-5, 'TolFun', 1E-5, 'MaxFunEvals', 1E10);
disp('Calculating.....')
```

```
[Beta_hat,FVAL,EXITFLAG,OUTPUT] =
FMINSEARCH('nlmelikelihoodfunction',B,Options,D,q);
```

```
disp(' ')
disp(' ')
% Check if the algorithm has converged
if EXITFLAG>=1
disp('The estimated values are as follows: ')
disp(' ')
Beta1=Beta_hat(1)
Beta2=Beta_hat(2)
Beta3=Beta_hat(3)
disp(' ')
Number_of_function_evaluations=FVAL
```

```
else disp('Unfortunately the algorithm did not converge to a solution.')
end
```

```
disp(' ')
disp(' ')
disp('by Mark Damen')
disp('Technische Universiteit Eindhoven')
disp('Department of Technology Management')
disp('The Netherlands')
```

---

**Filename: nmelikelihoodfunction.m**

```
function loglikelihood=nmelikelihoodfunction(B,D,q)
degradationdata;
timedata;
Options = optimset('TolX', 1E-8, 'TolFun', 1E-8,'MaxFunEvals', 1E10);

h=[1e-10];
s=0;
G=0;

for i=1:1:M

b=ones(q,1);
[b_hat(:,i),exit,flag]=fminsearch('nlmeadd1',b,Options,B,Y(i,:),D);

end

for i=1:M

% First derivative of the degradation function with regard to b(i)
afgeleide_f=((nlmeadd3(B,i,(b_hat(:,i)+h))-nlmeadd3(B,i,b_hat(:,i))))./h;

%second order derivative approximation of g.
g_dubbel_accnt=(afgeleide_f)*transp(afgeleide_f)+inv(D);
G=G+log(det(g_dubbel_accnt));

s=s+(nlmeadd2(B,i,b_hat(:,i),D)/N);

end

sigma_squared_hat=s;
loglikelihood=0.5*(N*(1+log(2*pi))+log(sigma_squared_hat))+M*log(det(D))+(G));
```

---

**Filename: nlmeadd1.m**

```
function g=nlmeadd1(b,B,Y,D)

timedata;
degradation_function=zeros(1,J);
f=zeros(1,J);

for j=1:J

% The degradation function
degradationfunction

if isreal(degradation_function)>=1
    f=degradation_function;
else f=NaN;
end

g=(sqrt(sum((abs(Y-f).^2))).^2+transp(b)*inv(D)*b;

end
```

---

**Filename: nlmeadd2.m**

```
function g=nlmeadd2(B,i,b,D)

degradationdata;
timedata;
degradation_function=zeros(1,J);
f=zeros(1,J);
for j=1:J

% The degradation function
degradationfunction
end

if isreal(degradation_function)>=1
    f=degradation_function;
else f=NaN;
end

g=(sqrt(sum((abs(Y(i,:)-f).^2))).^2+transp(b)*inv(D)*b;
```

---

**Filename: nlmeadd3.m**

```
function g=nlmeadd2(B,i,b,D)

degradationdata;
timedata;
degradation_function=zeros(1,J);
f=zeros(1,J);
for j=1:J

% The degradation function
degradationfunction
end

if isreal(degradation_function)>=1
    f=degradation_function;
else f=NaN;
end

g=(sqrt(sum((abs(Y(i,:)-f).^2))).^2+transp(b)*inv(D)*b;
```

**Filename: degradationfunction.m**

```
degradation_function(j)=(B(1)+b(1))./(1+exp(-(t(j)-B(2))/B(3)));
```

**Filename: timedata.m**

```
% This file contains the timevector for the moments at which the observations took place
% Replace the data with your own time matrix
t=[118 484 664 1004 1231 1372 1582];

% Do not change!!!!
matrixsize_t=size(t);
J=matrixsize_t(2);
```

***Filename: degradationdata.m***

% This file standard contains degradation data for the growth of orange trees as used in the article  
% An approximation to the log-likelihood function in the Non-Linear Mixed Effects model  
% by Pinheiro & Bates (1995,2001)

% Every row contains the degradation or growth observations for one unit/product/object/system  
% Replace the data with your own observations

```
Y=[30 58 87 115 120 142 145; 33 69 111 156 172 203 203; 30 51 75 108 115 139 140;  
   32 62 112 167 179 209 214; 30 49 81 125 142 174 177];
```

```
% Do not change!!!!  
matrixsize_Y=size(Y);  
M=matrixsize_Y(1);  
N=matrixsize_Y(1)*matrixsize_Y(2);
```